AD-A143 266 ANTENNA PERFORMANCE VERIFICATION AT LAUNCH SITE A FEASIBILITY STUDY ON PR..(U) NEW MEXICO STATE UNIV LAS CRUCES PHYSICAL SCIENCE LAB H D WEINSCHEL ET AL. 1/1

UNCLASSIFIED JAN 84 SCIENTIFIC-2 AFGL-TR-84-0069 F/G 9/5 NL

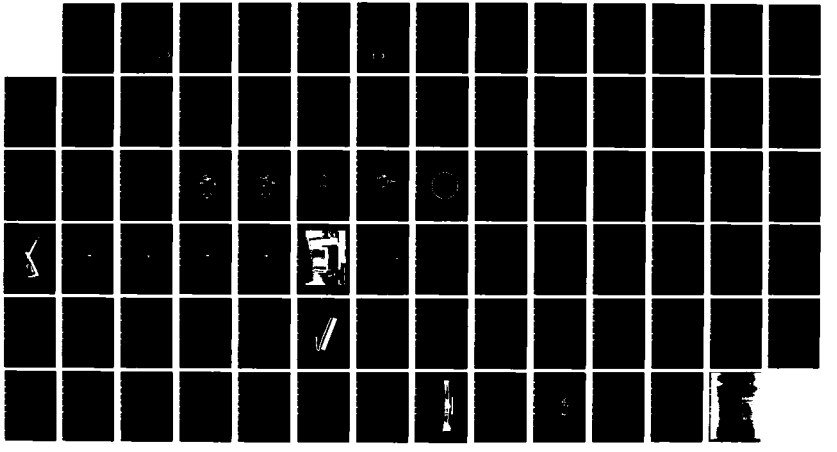

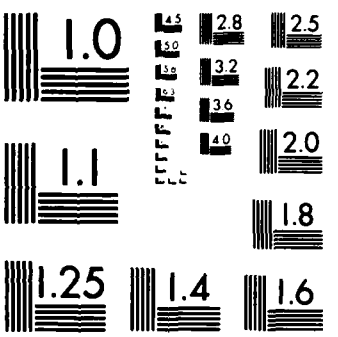

(12)

AFGL-TR-84-0069

ANTENNA PERFORMANCE VERIFICATION AT LAUNCH SITE

A Feasibility Study on Preflight Performance Testing of Stripline Slot Arrays Mounted on a Rocket

H. Dieter Weinschel
Al Waterman

Physical Science Laboratory
New Mexico State University
Box 3548
Las Cruces, New Mexico 88003-3548

January 1984

Scientific Report No. 2

Prepared for

Air Force Geophysics Laboratory
Air Force Systems Command
United States Air Force
Hanscom AFB, Massachusetts 01731

This report has been reviewed by the ESD Public Affairs Office (PA) and is releasable to the National Technical Information Service (NTIS).

This technical report has been reviewed and is approved for publication

Willard F. Thorn
WILLARD F. THORN
Contract Manager

Edward F. McKenna
EDWARD F. McKENNA
Branch Chief

FOR THE COMMANDER

C. N. Stark
C. N. STARK
Division Director

Qualified requestors may obtain additional copies from the Defense Technical Information Center. All others should apply to the National Technical Information Service.

If your address has changed, or if you wish to be removed from the mailing list, or if the addressee is no longer employed by your organization, please notify AFGL/DAA, Hanscom AFB, MA 01731. This will assist us in maintaining a current mailing list.

Do not return copies of this report unless contractual obligations or notices on a specific document requires that it be returned.

REPORT DOCUMENTATION PAGE

1a. REPORT SECURITY CLASSIFICATION Unclassified	1b. RESTRICTIVE MARKINGS
2a. SECURITY CLASSIFICATION AUTHORITY	3. DISTRIBUTION/AVAILABILITY OF REPORT Approved for public release: distribution unlimited
2b. DECLASSIFICATION/DOWNGRADING SCHEDULE	
4. PERFORMING ORGANIZATION REPORT NUMBER(S)	5. MONITORING ORGANIZATION REPORT NUMBER(S) AFGL-TR-84-0069
6a. NAME OF PERFORMING ORGANIZATION Physical Science Laboratory New Mexico State University 6b. OFFICE SYMBOL (If applicable)	7a. NAME OF MONITORING ORGANIZATION Air Force Geophysics Laboratory
6c. ADDRESS (City, State and ZIP Code) Box 3548 Las Cruces, New Mexico 88003-3548	7b. ADDRESS (City, State and ZIP Code) Hanscom AFB, Massachusetts 01731 Monitor/Willard Thorn/LCR
8a. NAME OF FUNDING/SPONSORING ORGANIZATION 8b. OFFICE SYMBOL (If applicable)	9. PROCUREMENT INSTRUMENT IDENTIFICATION NUMBER F19628-81-C-0004
8c. ADDRESS (City, State and ZIP Code)	10. SOURCE OF FUNDING NOS.

PROGRAM ELEMENT NO.	PROJECT NO.	TASK NO.	WORK UNIT NO.
62101F	6759	04	BA

11. TITLE (Include Security Classification)
(Over)

12. PERSONAL AUTHOR(S)
Weinschel, H.Dieter, and Waterman, Al

13a. TYPE OF REPORT	13b. TIME COVERED	14. DATE OF REPORT (Yr., Mo., Day)	15. PAGE COUNT
Scientific Rpt No.2	FROM _____ TO _____	1984 January	80

16. SUPPLEMENTARY NOTATION

17. COSATI CODES		
FIELD	GROUP	SUB. GR.

18. SUBJECT TERMS (Continue on reverse if necessary and identify by block number)
Antenna, S-Band, Preflight Verification, Stripline, Field Tests, Radiation Hazards, Array, Near-field Probing

19. ABSTRACT (Continue on reverse if necessary and identify by block number)

The Physical Science Laboratory/NMSU made a feasibility study for preflight testing of cylindrical stripline arrays at the launch site. Far-field radiation patterns were compared to near-field probe measurements. Various array damages were simulated. The results showed a good correlation between the near-field probe measurements and the far-field patterns. The conclusion drawn from the study was that damaged arrays could be detected by near-field probing in the field. However, intermittent problems such as pinched coaxial cables and loose connectors may go undetected.

20. DISTRIBUTION/AVAILABILITY OF ABSTRACT	21. ABSTRACT SECURITY CLASSIFICATION
UNCLASSIFIED/UNLIMITED ☐ SAME AS RPT. ☒ DTIC USERS ☐	Unclassified

22a. NAME OF RESPONSIBLE INDIVIDUAL	22b. TELEPHONE NUMBER (Include Area Code)	22c. OFFICE SYMBOL
Willard Thorn	617-861-3149	LCR

DD FORM 1473, 83 APR EDITION OF 1 JAN 73 IS OBSOLETE

Block 11 (Contd)

ANTENNA PERFORMANCE VERIFICATION AT LAUNCH SITE

Feasibility Study on Preflight Performance Testing of Stripline Slot Arrays Mounted on a Rocket

TABLE OF CONTENTS

LIST OF TABLES

LIST OF FIGURES

LIST OF FIGURES (Continued)

LIST OF FIGURES (Continued)

1.0 INTRODUCTION

The purpose of the report is to present the results of a study on the feasibility of preflight antenna performance tests at a launch facility. The report includes a description of the measurement setup, the measured data, the conclusions drawn from the measurements, and recommendations for the field test equipment. The appendix contains the documentation of the test antenna.

The objectives of the tests were twofold: first, to establish what type of antenna damage would be detected by far-field pattern measurements; second, to determine if the far-field pattern measurements could be correlated to near-field probe measurements. To keep the measurements within reasonable bounds only a few probable types of damage were selected. Any damage that could be detected by visual inspection of the outside surface of the antenna was excluded. The type of damage investigated was having one or two subarrays disabled by a fault in the coaxial feed harness or having one of the elements disabled by a break in the printed circuit harness. The third type concerned faulty antenna mounting. It is felt that these are the more probable types of damage that would be encountered.

Three different probes were used to obtain information on the probe response. It was also an opportunity to see if a particular probe would be preferable. Included in the probe measurements were probe position tests.

On the basis of the above tests it appears feasible to use a near-field probe to detect antenna problems of the nature discussed above.

A short discussion on RF radiation hazards is included, but no hard guidelines are given. The subject is only introduced to make the operator aware of the problem. For detailed discussion on RF radiation hazards, the references and other publications should be consulted.

All figures follow the text, beginning on page 20.

2.0 EQUIPMENT USED AND TEST SETUP

All the measurements were made on the model range leg of the PSL outdoor antenna range complex. The far-field measurements were made with standard equipment and need no discussion. The setup for the near-field measurement is shown in Figure 1. The signal was transmitted from the Model 55.385 stripline slot array and detected with a probe mounted on a stand. The detected signal was transmitted through a coaxial line to the receiver in the control room. The output was recorded in polar format with a recorder whose rotation was synchronized with the rotation of the Mod 55.385 antenna. The equipment used is listed in Table 1.

TABLE 1

EQUIPMENT LIST

RR #2819	-	Test Equipment Used
Testing Range	-	Model Range
Isolator	-	2 - 4 GHz
Mixer	-	14 - 3
Receiver	-	SA Model 1752
Recorder	-	SA Model 1553
Transmitter	-	SA Model 2163
Dish	-	Dipole in 5' Dish
Antenna	-	Model 55.385 AE265, AE297, AE270, AE011, AE012, AE301
Power Meter	-	Boonton Electronics Model 42B
		41 - 4E Sensor
Counter	-	5248
Probe	-	1.7 Coaxial to Waveguide Adaptor
Probe	-	Disk Dipole
Probe	-	Small Dipole

3.0 MEASUREMENTS

3.1 Impedance

Before the tests at the antenna range were started, impedance measurements were made at the laboratory. Since radiation tests were planned for the intact antenna and also for a simulated damaged array, the impedances were measured for those antenna conditions. The results are shown in Figures 2 through 5. A comparison of the impedance curves shows that it would not be possible to detect a damaged subarray by impedance measurements if the array is as large as the one being tested. The impedance changes are of approximately the same order of magnitude as the variation one obtains measuring different intact arrays.

3.2 Far-Field Radiation Measurements

A set of far-field patterns were measured to compare the intact antenna with conditions simulating a damaged harness. The vehicle coordinates for the measurements are such that the nose of the vehicle is at $\theta=0^\circ$ and the subarray with the serial number AE265 is at $\phi=0^\circ$; $\theta=90^\circ$. The coaxial harness configuration and the location of the subarray is shown in Figure 6. The $\phi=0^\circ$ and $\theta=90^\circ$ of the radiation patterns are shown in Figures 7 through 12. The effect of disconnecting one or two subarrays is very pronounced and very much as expected. The patterns form a baseline for the subsequent tests.

4.0 THE NEAR-FIELD PROBES

Three different probes were used during the measurements. The probes are shown in Figure 13. One is a disk dipole Model 44.001; the other is a coaxial to waveguide adaptor. The waveguide will probably be the preferred choice since it is easily mounted. The third probe is an electrically small dipole which is useful because it can measure the output from individual slots. Its disadvantage is that in some situations it may receive insufficient power for the measurement. Its use will be discussed in more detail in the section about antenna mounting. Probe radiation patterns were measured for the dipole and the waveguide. Both probes were backed by RF absorbent plates to reduce the back radiation. The patterns are shown in Figures 14 through 17.

After the completion of the documentation type measurements, the Model 55.385 antenna and the waveguide probe were set up for near-field measurements. The setup is shown in Figure 18. The first series of measurements was made using an intact array and varying the probe position. The sketch in Figure 19 shows the various displacements of the probe. The distance from the surface of the cylinder was varied from 4 to 8 inches. The probe was also displaced from the centerline of the antenna along the axis of the cylinder. The results are shown in Figures 20 through 24. At 4 inches the peaks of the individual subarrays are more pronounced compared to the far-field pattern. A comparison between Figure 8 and Figure 21 shows that the probe pattern even at a 6 inch distance from the antenna approaches that of the far-field pattern. There is little difference between the 8 and 6 inch probe positions. The ripples in the pattern (Figure 22) are due to vibrations caused by the wind and can be ignored. The effect of displacing the probe along the vehicle axis, shown in

Figures 23 and 24, is negligible. The conclusions drawn from this series of tests are that placing the probe 6 inches from the antenna is reasonable and that the placement of the probe is not critical.

The electrically small dipole is placed very close to the antenna. It will show peaks for the individual slots and small minima for the gaps between the subarrays. The pattern generated with this probe is shown in Figure 25.

5.0 CORRELATION TESTS

The main purpose of the investigation is to detect, by near-field probing of the antenna, faults in the antenna system that would deteriorate the far-field pattern. In other words, is there a good correlation between the near-field and the far-field measurements with respect to antenna system damage? The tests described in the previous sections of the report were made to establish a baseline showing how the system damage affects the radiation pattern; the probe tests were made to help in the selection of the probe and to establish the sensitivity of the test to probe position.

Radiation patterns shown in Figures 26 through 31 and Figures 33 through 44 were obtained using the near-field probes. Only two probes were used. One of them is the short dipole for testing the field approximately 0.1λ from the antenna. The other probe was the coaxial to waveguide adaptor, which was located approximately 1λ from the antenna. The disk dipole was not used since it had already been established that the results do not significantly differ from those of the waveguide.

The patterns in Figures 26 through 29 show the result of simulated cable damages. A line break in the printed circuit harness was simulated by covering one of the slots with aluminum foil. The result was a sharp null which could be easily detected by either probe. Similarly a break of the coaxial cable was simulated by disconnecting the cables that feed one or two subarrays. The corresponding far-field patterns are shown in Figures 10 and 12. The data shows that there would be no problem detecting a nonfunctioning element or subarray.

A defect that would not be detected by either far-field or near-field probe measurements is illustrated in Figures 30 and 31. Connectors in the feed harness were loosened without obtaining any distinctive change in the radiation pattern. In flight the condition would probably produce RF noise due to mechanical vibration.

Another condition that may go undetected is illustrated by the patterns in Figures 33 through 44. The coaxial harness cables were deliberately bent and pinched as shown in Figure 32. This produced an intermittent problem which made detection uncertain. The implication is that great care needs to be exercised during the installation of the harness since a preflight probe is not a reliable method for detecting loose connectors or damaged cables.

6.0 ANTENNA MOUNTING

Additional tests were made to determine how a faulty antenna mounting affects the radiation pattern. The antenna used was a Model 55.205 stripline slot array mounted on a 17 inch diameter vehicle. The antenna was mounted so that it did not make good contact with the vehicle skin; in one place there was a gap of about 0.050 inches between the antenna and the vehicle skin. The result is a deep minimum in the pattern. The far-field pattern was recorded at the antenna range and is shown in Figure 45.

Near-field probe tests were made in the laboratory but were not recorded. These tests illustrate the usefulness of the small dipole probe and its limitations. The results from the dipole probe showed that all elements were radiating, indicating that there were no damaged lines. But the tests gave no indication that the far-field pattern would be unsatisfactory. The reason for this is that the probe is so close to the antenna that it only detects the signal from each individual slot. The test with the open-ended waveguide probe did show the null in the pattern; that is, it gave a good correlation with the far-field pattern. The combination of the two tests, dipole and open-ended waveguide, made it easier to locate the problem. The short dipole did exclude a faulty harness or antenna, and the waveguide indicated that there would be a null in the pattern. This led to the conclusion that there must be another source causing an interference null. The problem was identified as a small gap between the antenna and the vehicle. This illustrates that the probes may be used together as a diagnostic tool. It should be emphasized that the small dipole located close to the test antenna should not be used as the sole testing device.

7.0 INTERFERENCE DUE TO REFLECTIONS

Since it is not always possible to make the field tests in a reflection-free space, some tests were made at the antenna range after deliberately introducing reflections into the environment. The reflector was a 2x2 ft. aluminum sheet that was moved about while probing the field. All tests were negative; that is, no significant change was registered in the amplitude of the signal received by the probe.

8.0 SAFETY CONSIDERATIONS

The subject of RF hazards is rather complex. No attempt is made in this section to present the subject in any depth. The intent is only to make the operator aware of the problem. For more detailed information references [1] through [4] may be consulted. The few approximate calculations, shown below, are intended to show the order of magnitude of the field that an operator may be exposed to during a typical measurement.

In this example the antenna will be a 20 element slot array mounted on a 20 inch diameter vehicle. The frequency will be 2.25 GHz; the transmitter output will be 10 watts. The most simple calculation would be made by assuming isotropic radiation.

Let the operator be 23 cm from the antenna. The power density at that distance would then be:

$$W = \frac{P}{4\pi r^2} = \frac{10}{4\pi\ (25+23)^2} = 0.3\ mW/cm^2$$

Taking antenna gain into account we get the values below.

$$W = \frac{P \times A_e}{\lambda^2 r^2}$$

where r = 48 cm and A_e is the effective area of the antenna. For G = -5 dB:

$$A_1 = \frac{G\lambda^2}{4\pi} = \frac{56.14}{4\pi} = 4.47 \text{ cm}^2$$

Or for G = 5 dB:

$$A_2 = 44.68 \text{ cm}^2$$

So that

$$W_1 = \frac{4.47 \times 10^4}{\lambda^2 r^2} = 0.1 \text{ mW/cm}^2, \text{ and}$$

$$W_2 = \frac{44.68 \times 10^4}{\lambda^2 r^2} = 1.1 \text{ mW/cm}^2.$$

The calculated values above can be compared to measured values obtained during a recent field test on project ELK-1. The power input to the TM antenna, a slot array, was approximately 40 dBm. The power recorded with the probe was 4 dBm. The probe end was a half wave dipole located 22 cm from the test antenna. The cable loss between the probe and the power meter was 5 dB. Therefore the power received by the dipole was

$$9 \text{ dBm} = 7.9 \text{ mW}.$$

The effective area of the dipole given in reference [5] is

$$A_e = 0.13\lambda^2 = 23.1 \text{ cm}^2,$$

giving a power density of 0.34 mW/cm^2.

The above, admittedly crude, calculations show power densities that are considered to be acceptable exposure levels. However, given the uncertainties in the calculations, it would be preferable to have the operator several feet, rather than 9 inches, from the antenna, or to obtain additional protection through the use of RF absorber shields.

9.0 RECOMMENDATIONS FOR THE TEST SETUP

It appears that two conditions may be encountered under which the measurements have to be performed. The preferable condition occurs when the vehicle can be moved outside the building and set on a rotator. The other condition occurs when the vehicle remains in a horizontal position inside the building and can not be mounted on a standard rotator.

The basic equipment required to cover both conditions is as follows:

1. variable power supply
2. variable attenuator
3. Boonton power meter
4. rectangular recorder
5. synchro-receiver

If the vehicle is set up on the rotator in a vertical position outside the building, the probe will be mounted on a stand next to the antenna. The output from the rotator will drive the synchro-receiver whose shaft rotation will be sensed to drive the recorder. If the vehicle is in a horizontal position inside the building there are two possible approaches: One is to move the probe, mounted on a carriage with wheels, around the vehicle and synchronize the recorder with the wheel rotation. The other is to have the probe mounted the same way as for the vertical vehicle position measurement and construct a drive for rotating the vehicle in a horizontal position. The advantage of having the probe fixed is that the operator does not have to be close to the antenna so that the power radiated by the antenna is not likely

to present a health problem. If the probe is moved around the vehicle by the operator, the power output of the antenna has to be considered, but the setup is quite simple. The radiation hazard could be minimized with shield of RF absorbent material. It would be possible to construct a machine that would drive the probe around the vehicle, but it appears that such a design would be more complex than the one required to drive the vehicle.

10.0 SUMMARY

Radiation pattern measurements were made on a cylindrical slot array. Correlation was established between the far-field measurements and the near-field probing. Both the intact antenna and the simulated damaged antenna were measured. Three different probes and various probe positions were used and the responses of the probes were compared. The possibility of radiation hazard was discussed. Suggestions for a field setup were made, and the basic equipment required for it was listed.

11.0 CONCLUSIONS

The measurements show that sufficient correlation exists between the far-field pattern of a cylindrical slot array and the pattern obtained by a dipole or open-ended waveguide probe to detect pattern changes due to a nonradiating slot or subarray. Either a disk dipole or an open-ended waveguide could be used for a probe. The probe placement is not critical. The probe position could vary from 4 to 8 inches from the antenna with little effect on the measurement. However, a small probe placed very close to the antenna detects only the signal from individual elements and would give erroneous results if there were phasing nulls in the far-field pattern. Reflections from nearby objects did not affect the measurement when the probe was within 6 inches of the test antenna. The surrounding clutter becomes more of a problem if the probe is far from the test antenna.

From the measurements it appears to be quite feasible to assemble a setup for preflight testing of the antenna in the field. It should be emphasized that intermittent problems like bent or pinched cables or loose connectors may not be detected by such a preflight test. Those problems could probably be detected if the probe were used during a vibration test.

REFERENCES

[1] "Some Technical Aspects of Microwave Radiation Hazards," W.W. Munford, Proceedings of the IRE, Feb. '61, pp. 427-447.

[2] "Biological Effects and Health Hazards of Microwave Radiation," Proceedings of an International Symposium, Warsaw, 15-18 Oct. 1973.

[3] "RF Radiation: Biological Effects," IEEE Spectrum, Dec. 1980.

[4] "IEEE Standard Test Procedures for Antennas," published by IEEE, distributed by John Wiley & Sons, Inc., December 19, 1979, pp. 127-129.

[5] Reference Data for Radio Engineers, published by Howard W. Sams & Co., Inc., October 1968, ITT 5th Edition.

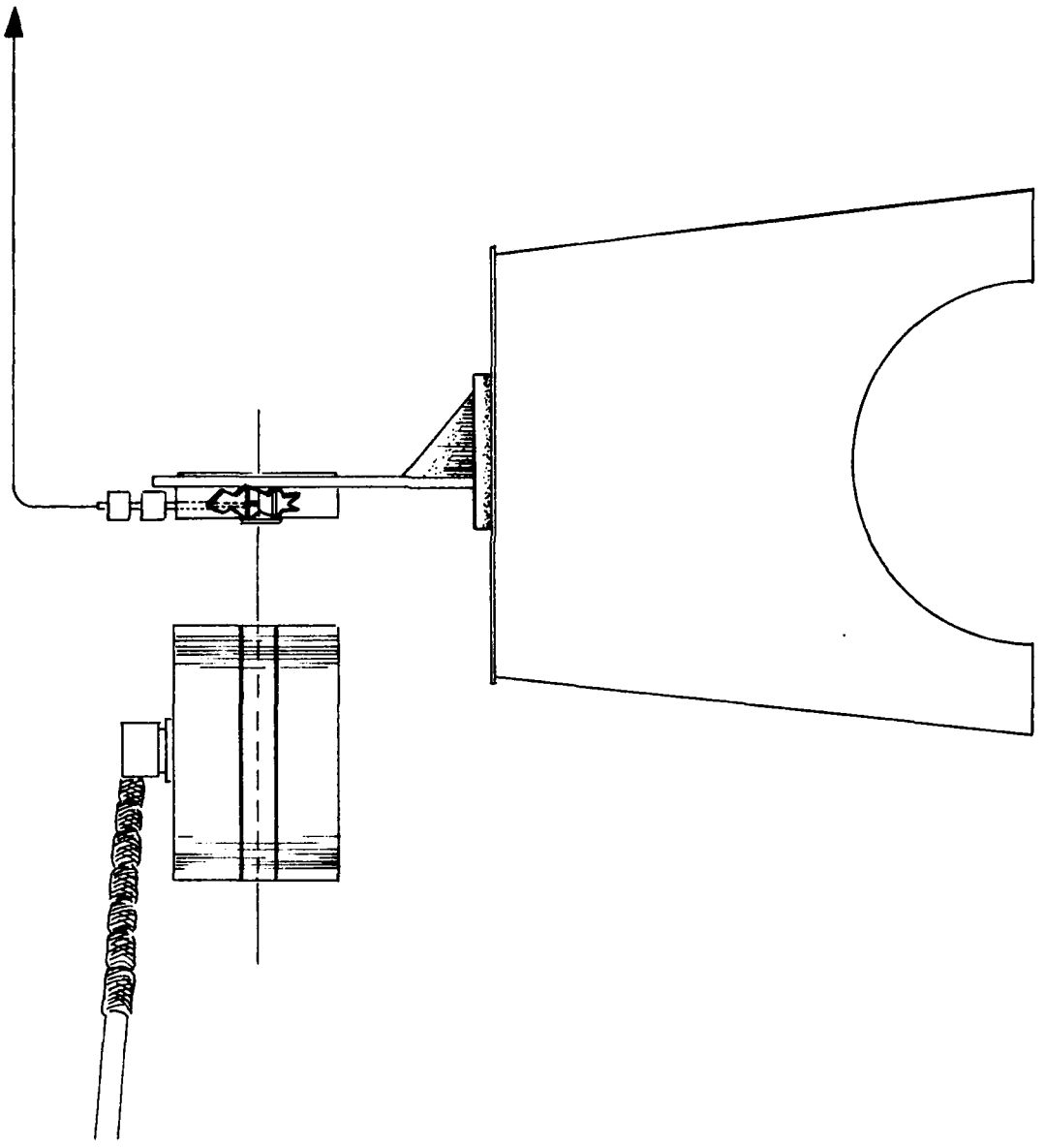

Figure 1. Near-field measurement setup.

TITLE DATE

IMPEDANCE COORDINATES—50-OHM CHARACTERISTIC IMPEDANCE

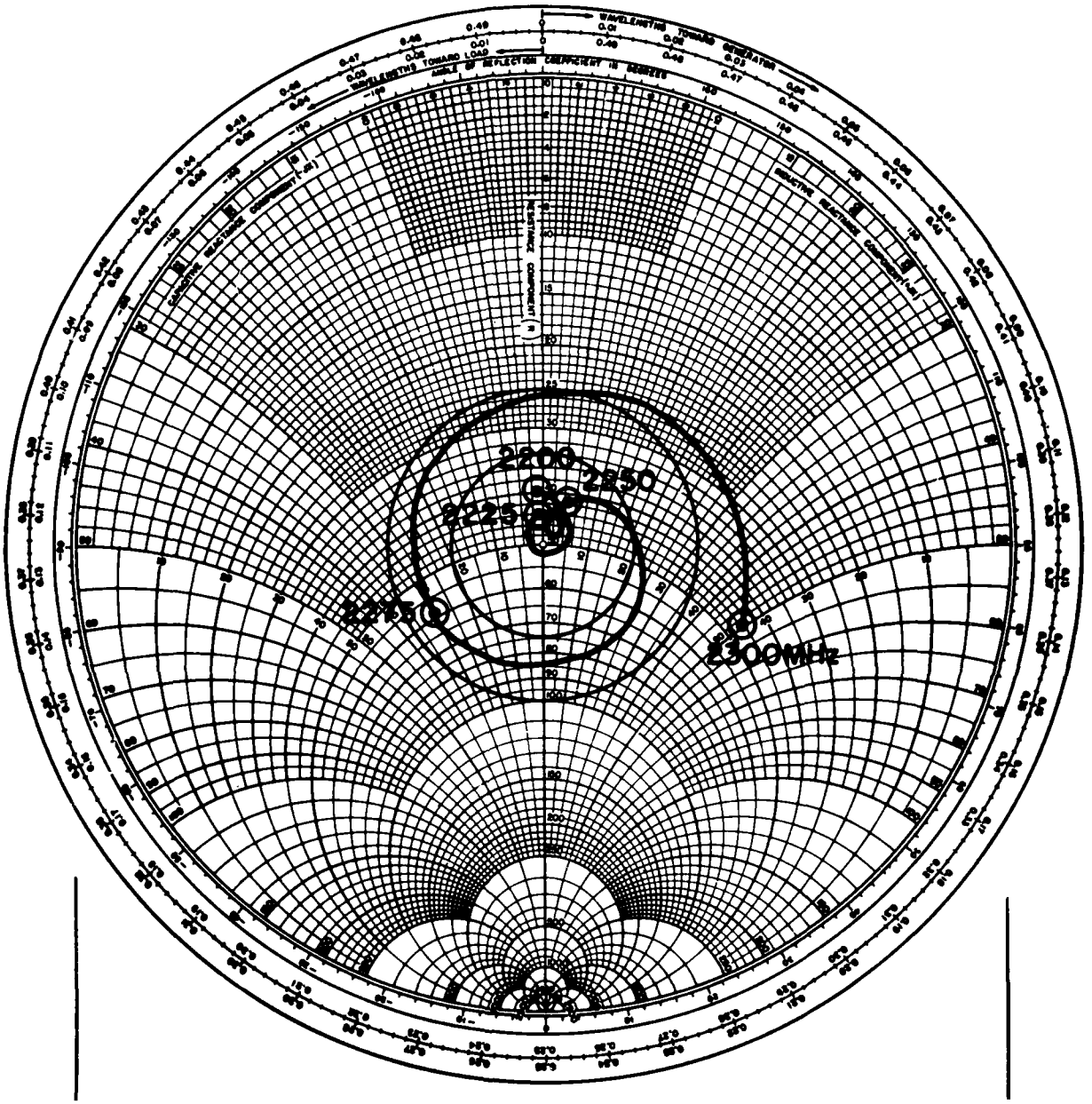

Figure 2. Impedance versus frequency curve of six Model 55.385 subarrays fed in phase and measured at end of feed cable.

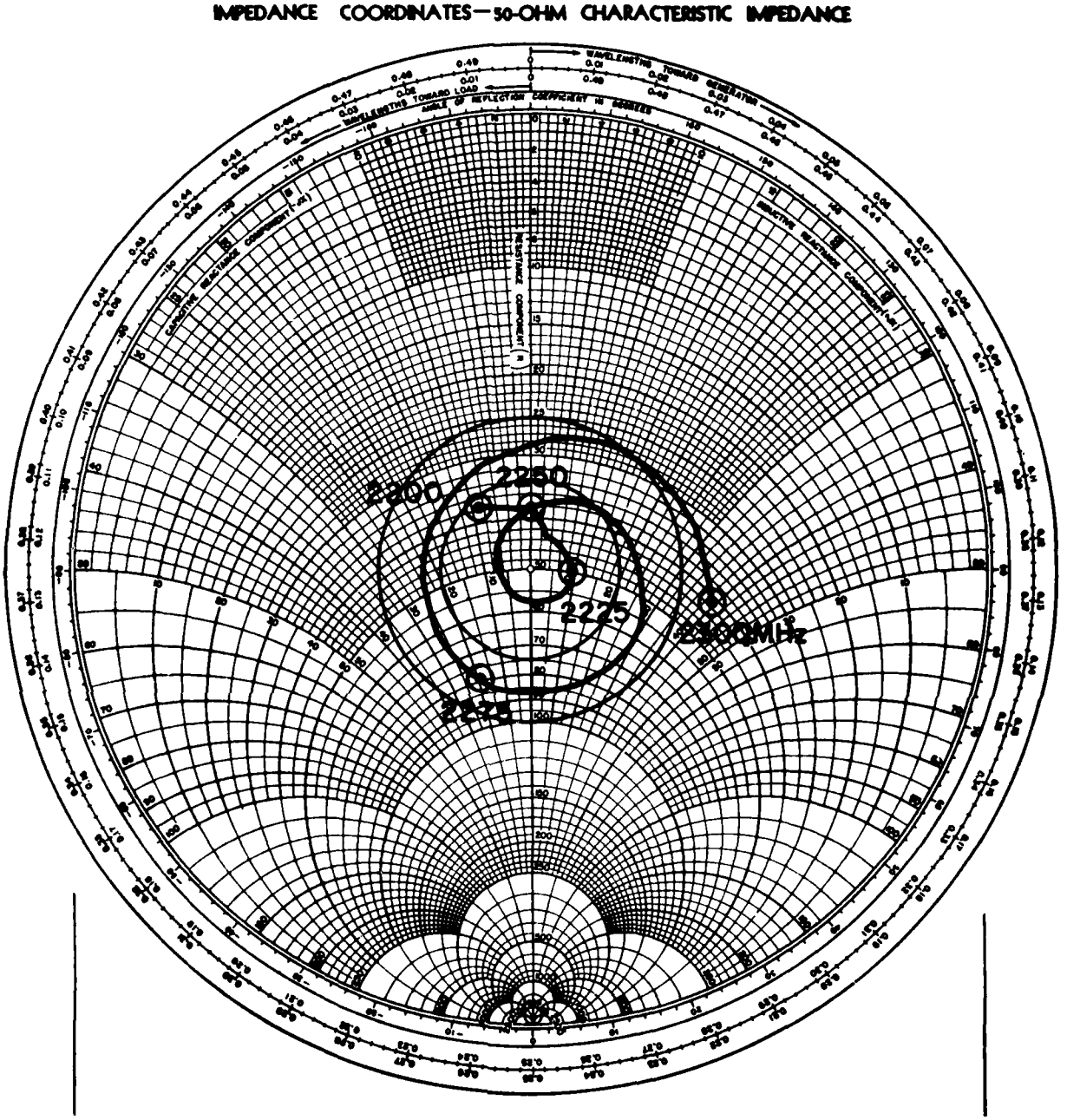

Figure 3. Same setup as data in Figure 2 but with subarray AE265 disconnected at the subarray driving point.

TITLE DATE

IMPEDANCE COORDINATES—50-OHM CHARACTERISTIC IMPEDANCE

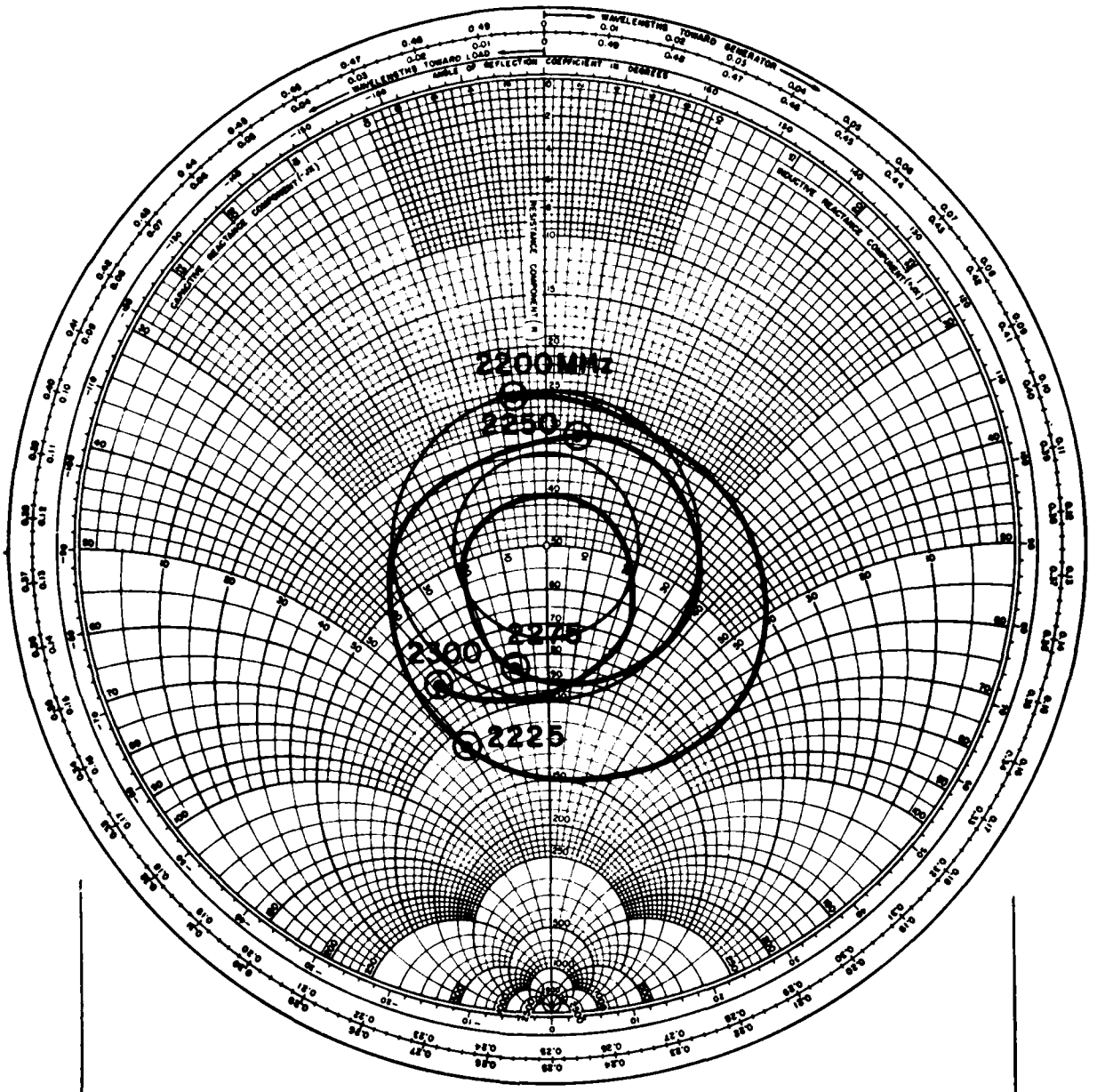

Figure 5. Same setup as for data in Figure 2 but with subarrays AE265 and AE279 disconnected at the Tee-junction.

TITLE DATE

IMPEDANCE COORDINATES—50-OHM CHARACTERISTIC IMPEDANCE

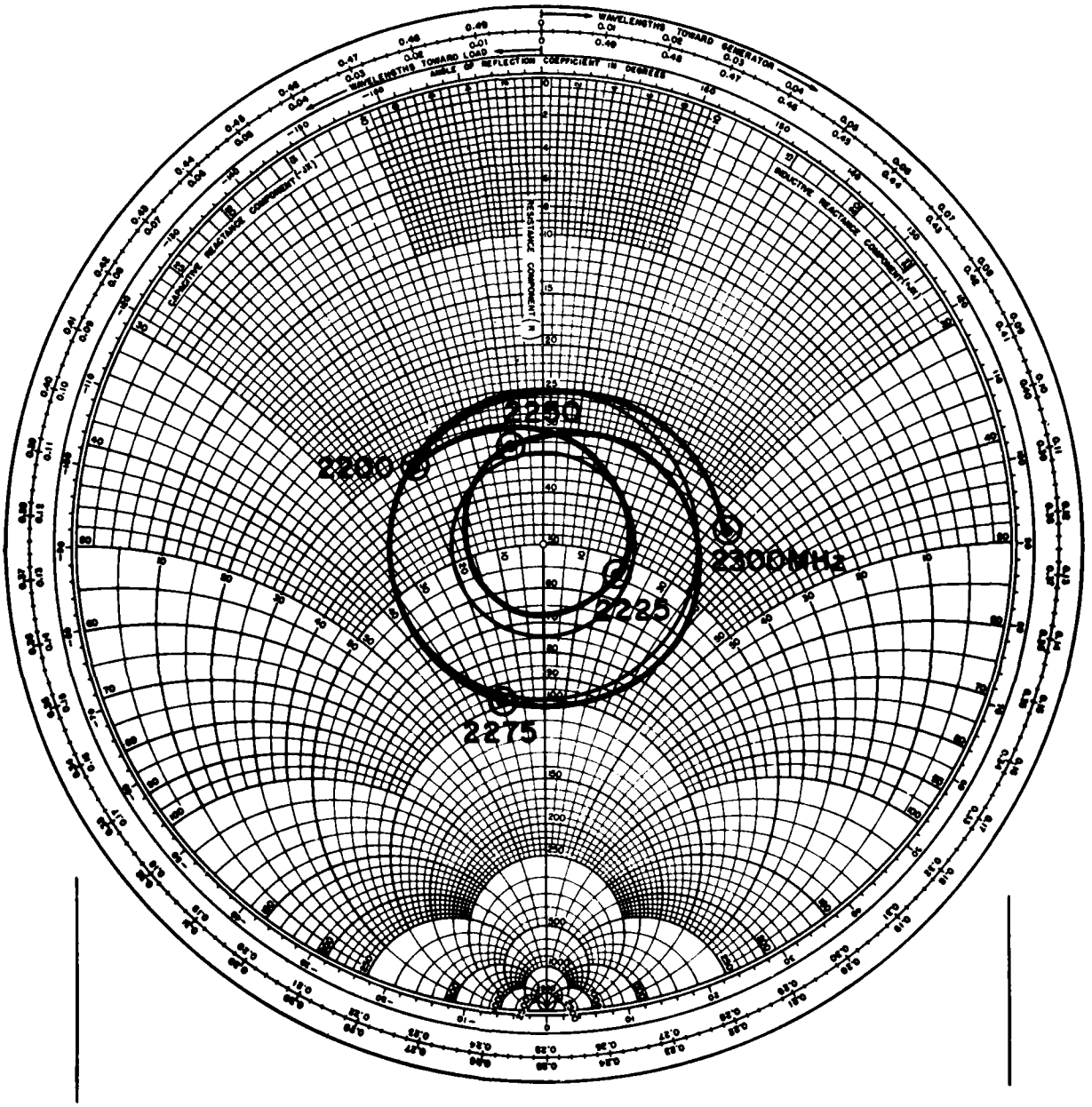

Figure 4. Same setup as for data in Figure 2 but with subarrays AE265 and AE301 disconnected at the driving point.

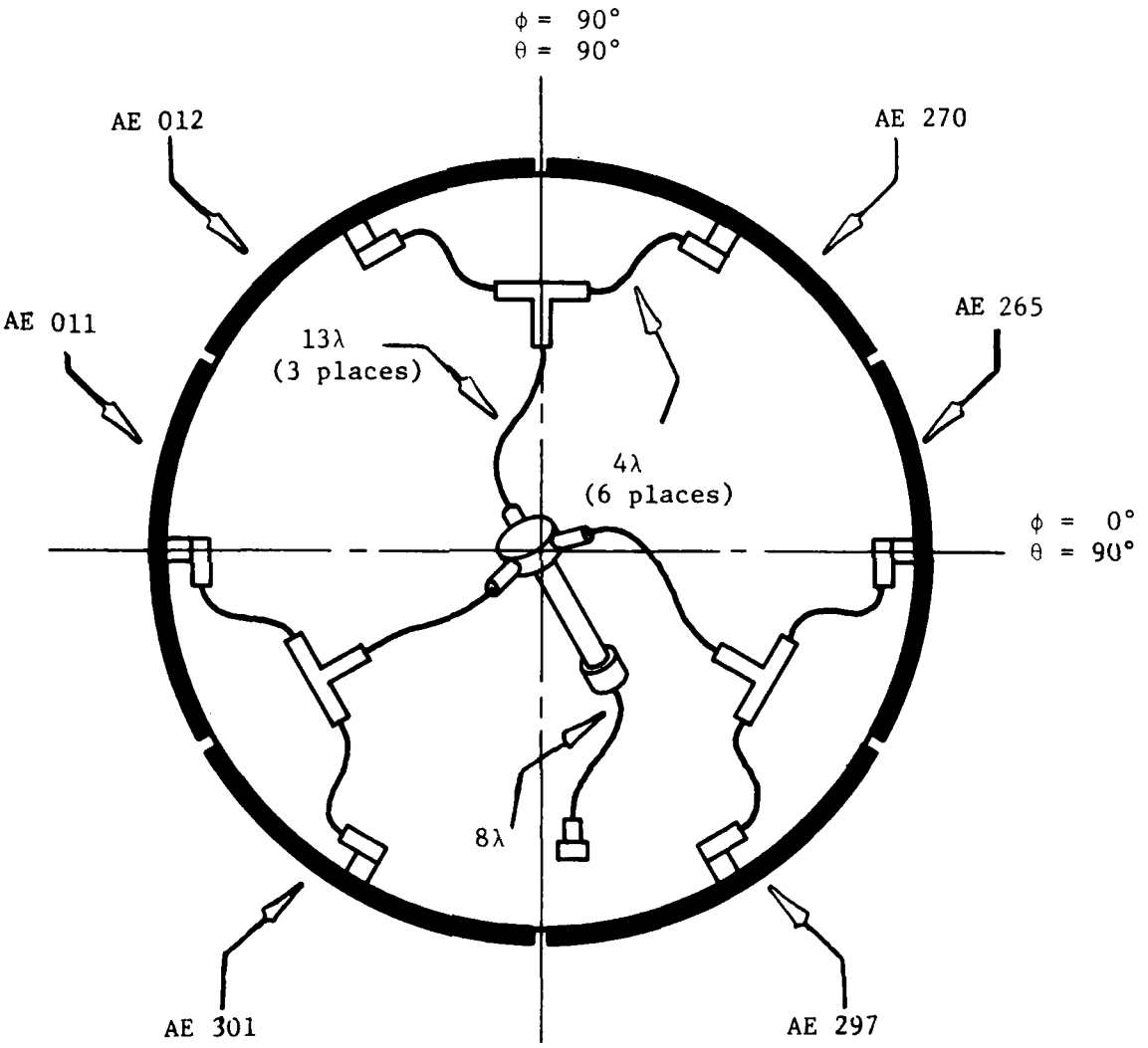

Figure 6. Antenna mounting locations and phasing harness.

POLARIZATION

- ☐ GAIN REF.
- ☒ Eθ
- ☐ Eφ
- ☐ R.C.
- ☐ L.C.
- ☐ OTHER AS NOTED UNDER REMARKS.

φ = ___° θ = 0 °

COORDINATE REFERENCE

φ = 0 °
θ = 90 °

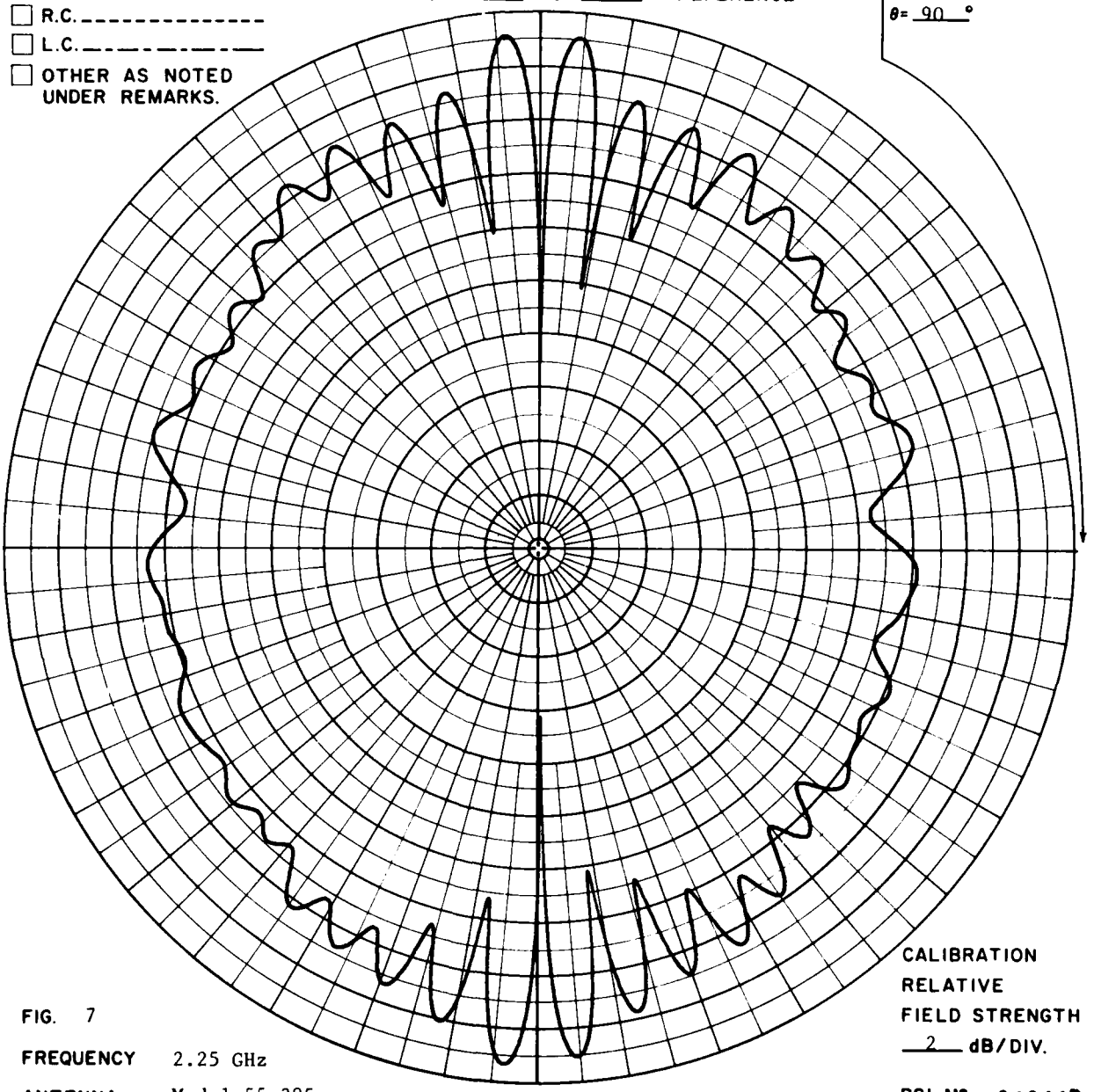

CALIBRATION
RELATIVE
FIELD STRENGTH
2 dB/DIV.

FIG. 7

FREQUENCY 2.25 GHz

ANTENNA Model 55.385

REMARKS Far-field pattern of intact antenna.

PSL № 31841B

RR 2815

POLARIZATION

- ☐ GAIN REF.
- ☒ Eθ
- ☐ Eφ
- ☐ R.C.
- ☐ L.C.
- ☐ OTHER AS NOTED UNDER REMARKS.

φ = 0 ° θ = 90 °

COORDINATE REFERENCE

φ = 90 °
θ = 90 °

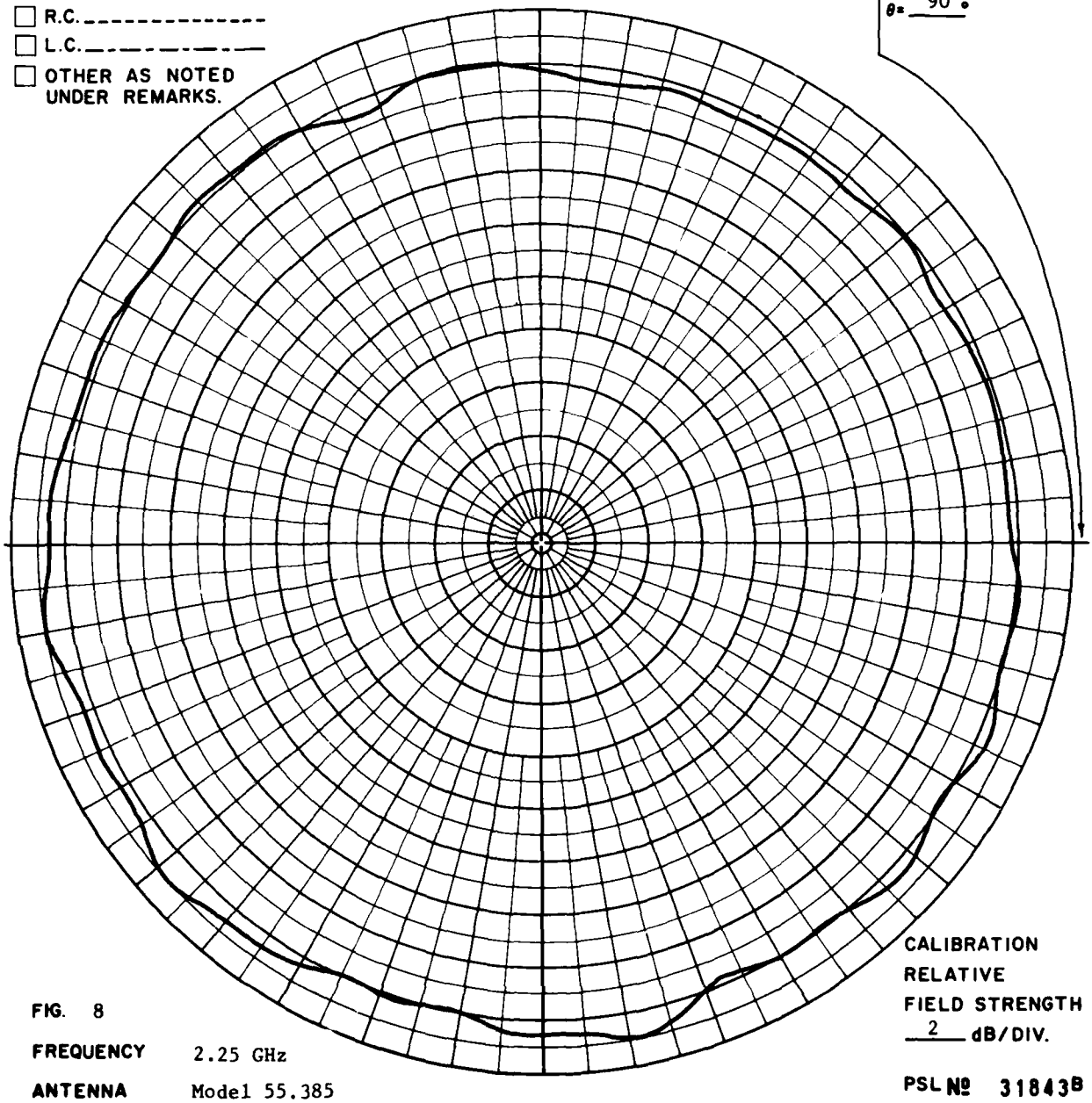

CALIBRATION
RELATIVE
FIELD STRENGTH
2 dB/DIV.

FIG. 8

FREQUENCY 2.25 GHz

ANTENNA Model 55.385

REMARKS Far-field pattern of intact antenna.

PSL № 31843B

RR 2815

POLARIZATION

- ☐ GAIN REF.
- ☒ Eθ
- ☐ Eφ
- ☐ R.C.
- ☐ L.C.
- ☐ OTHER AS NOTED UNDER REMARKS.

φ= ___ ° θ= 0 °

COORDINATE REFERENCE

φ= 0 °
θ= 90 °

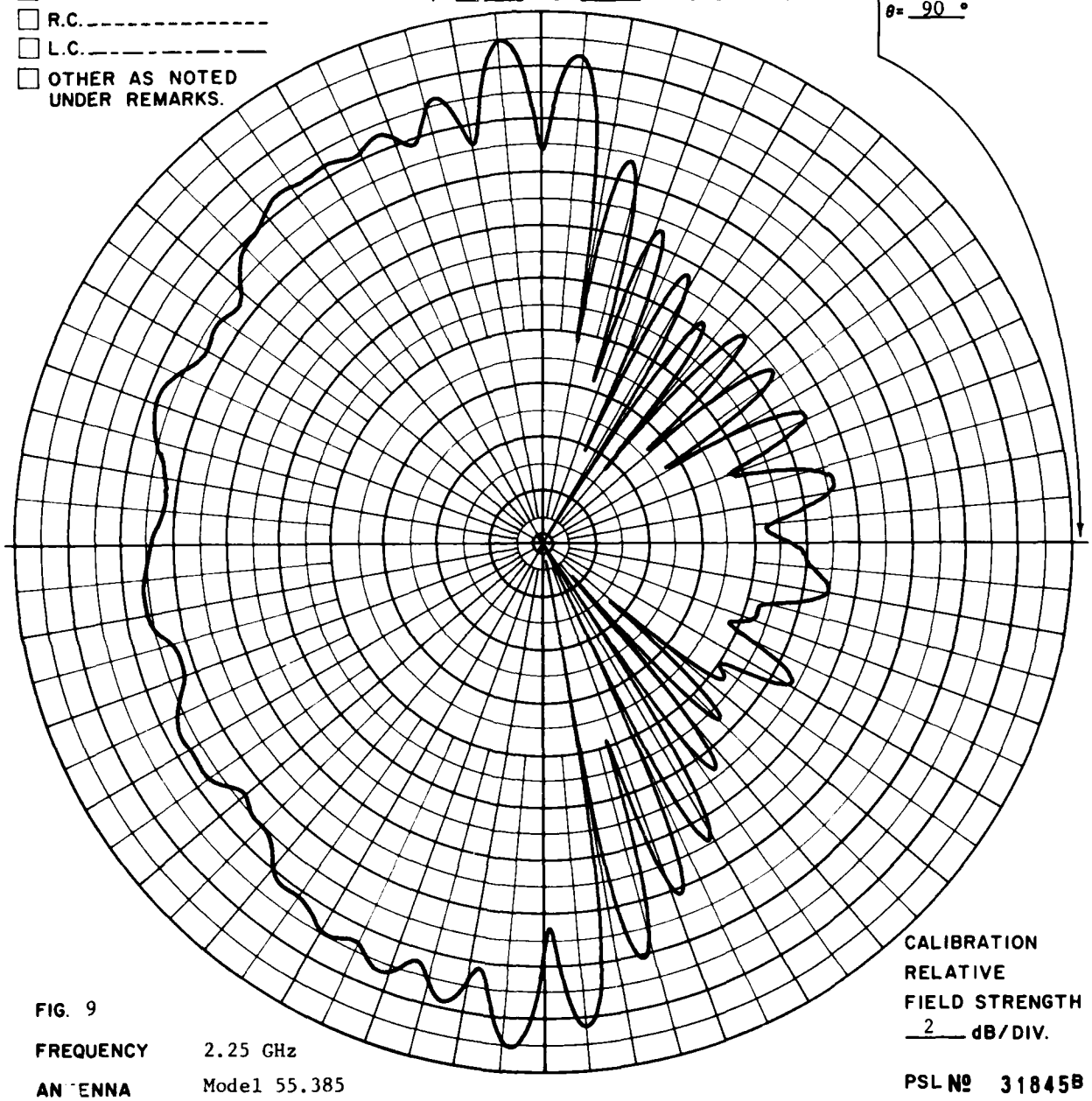

CALIBRATION
RELATIVE
FIELD STRENGTH
2 dB/DIV.

FIG. 9

FREQUENCY 2.25 GHz

ANTENNA Model 55.385

PSL Nº 31845B

REMARKS Far-field pattern. One subarray disconnected.

RR 2815

POLARIZATION

- ☐ GAIN REF.
- ☒ Eθ
- ☐ Eϕ
- ☐ R.C.
- ☐ L.C.
- ☐ OTHER AS NOTED UNDER REMARKS.

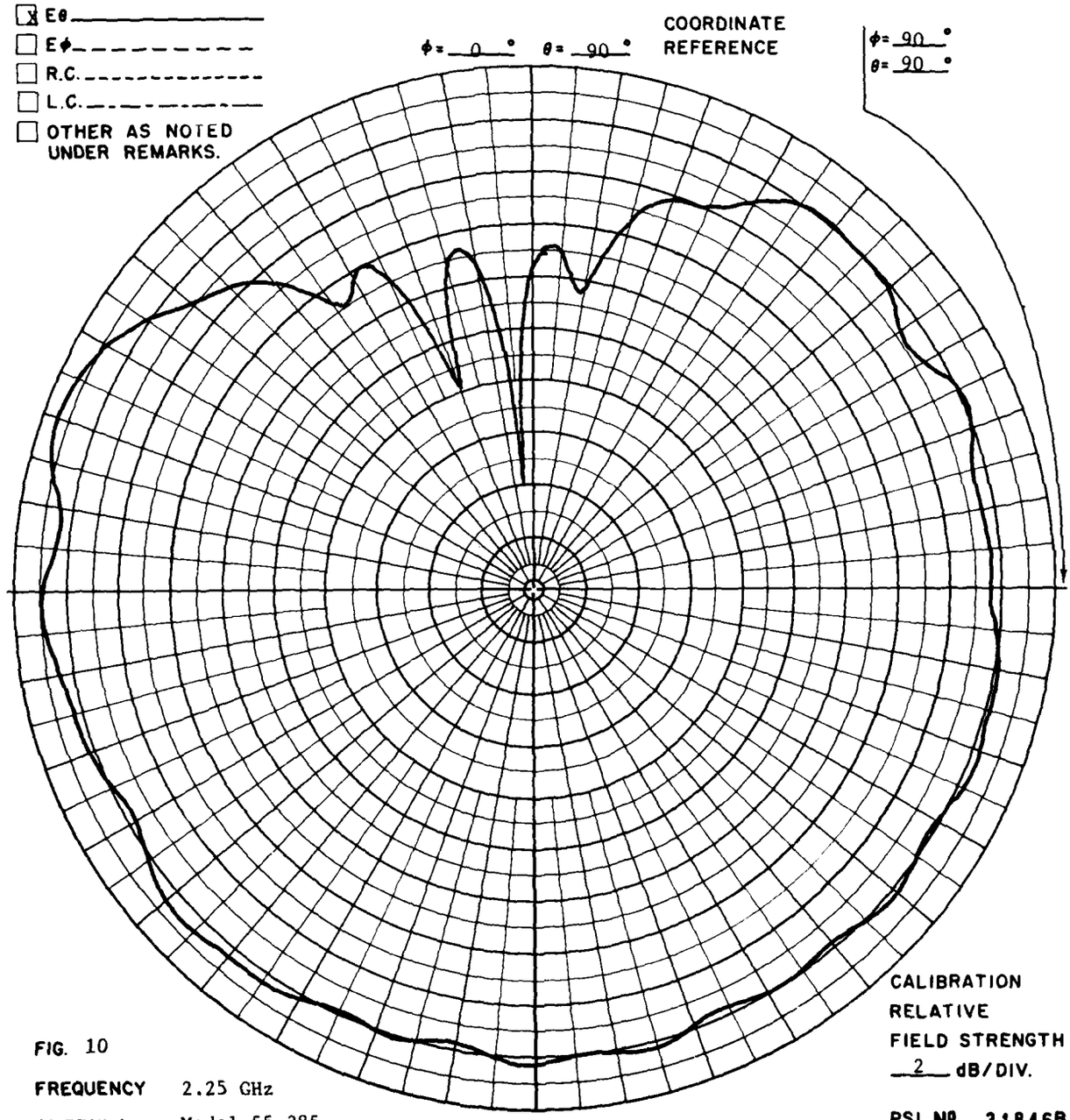

CALIBRATION
RELATIVE
FIELD STRENGTH
2 dB/DIV.

FIG. 10

FREQUENCY 2.25 GHz

ANTENNA Model 55.385

REMARKS Far-field pattern. One subarray disconnected.

PSL № 31846B

RR 2815

POLARIZATION

- ☐ GAIN REF.
- ☒ Eθ
- ☐ Eφ
- ☐ R.C.
- ☐ L.C.
- ☐ OTHER AS NOTED UNDER REMARKS.

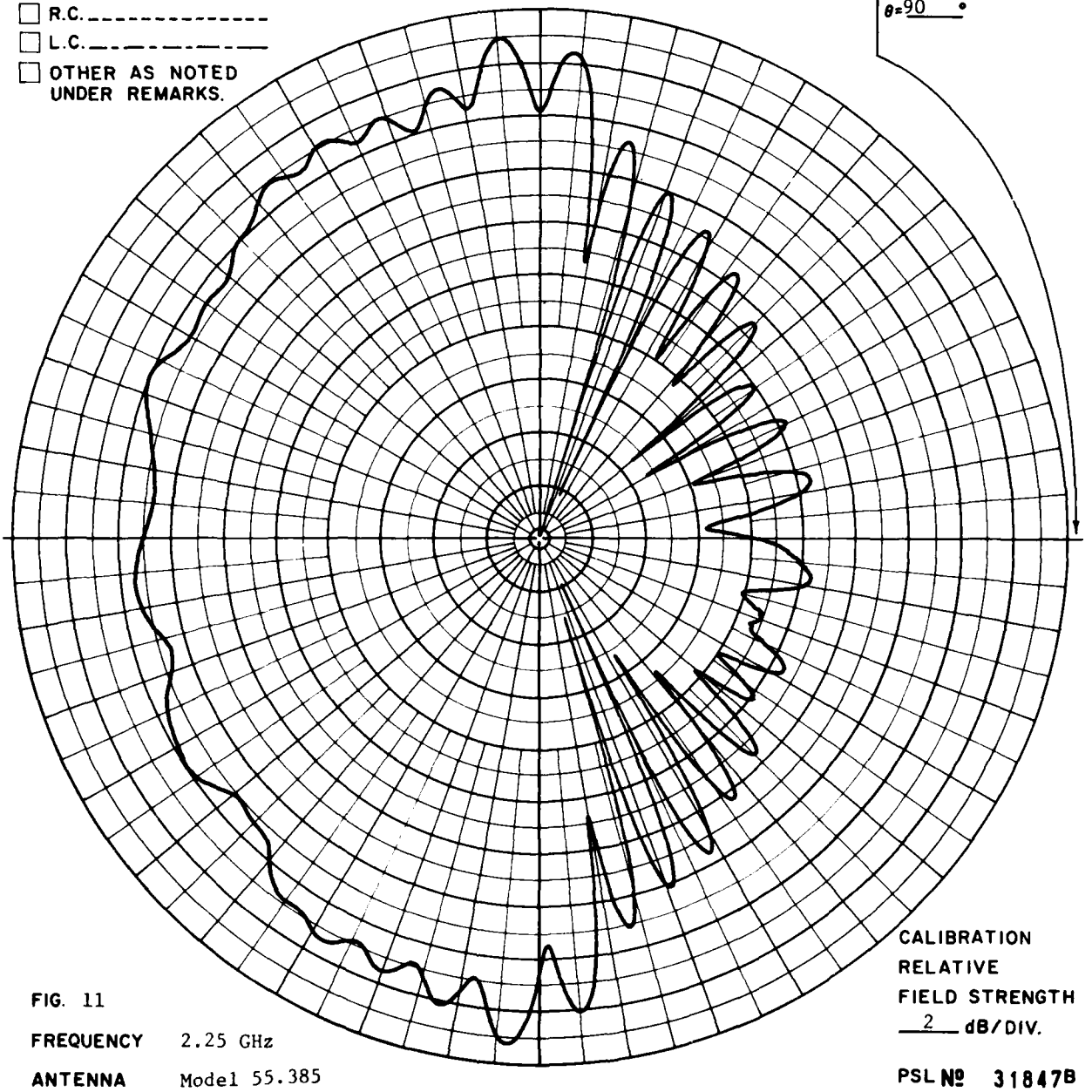

CALIBRATION
RELATIVE
FIELD STRENGTH
2 dB/DIV.

FIG. 11

FREQUENCY 2.25 GHz

ANTENNA Model 55.385

REMARKS Far-field pattern. Two subarrays disconnected.

PSL Nº 31847B

RR 2815

POLARIZATION

- ☐ GAIN REF.
- ☒ Eθ
- ☐ Eφ
- ☐ R.C.
- ☐ L.C.
- ☐ OTHER AS NOTED UNDER REMARKS.

COORDINATE REFERENCE

φ= 0 ° θ= 90 °

φ= 90 °
θ= 90 °

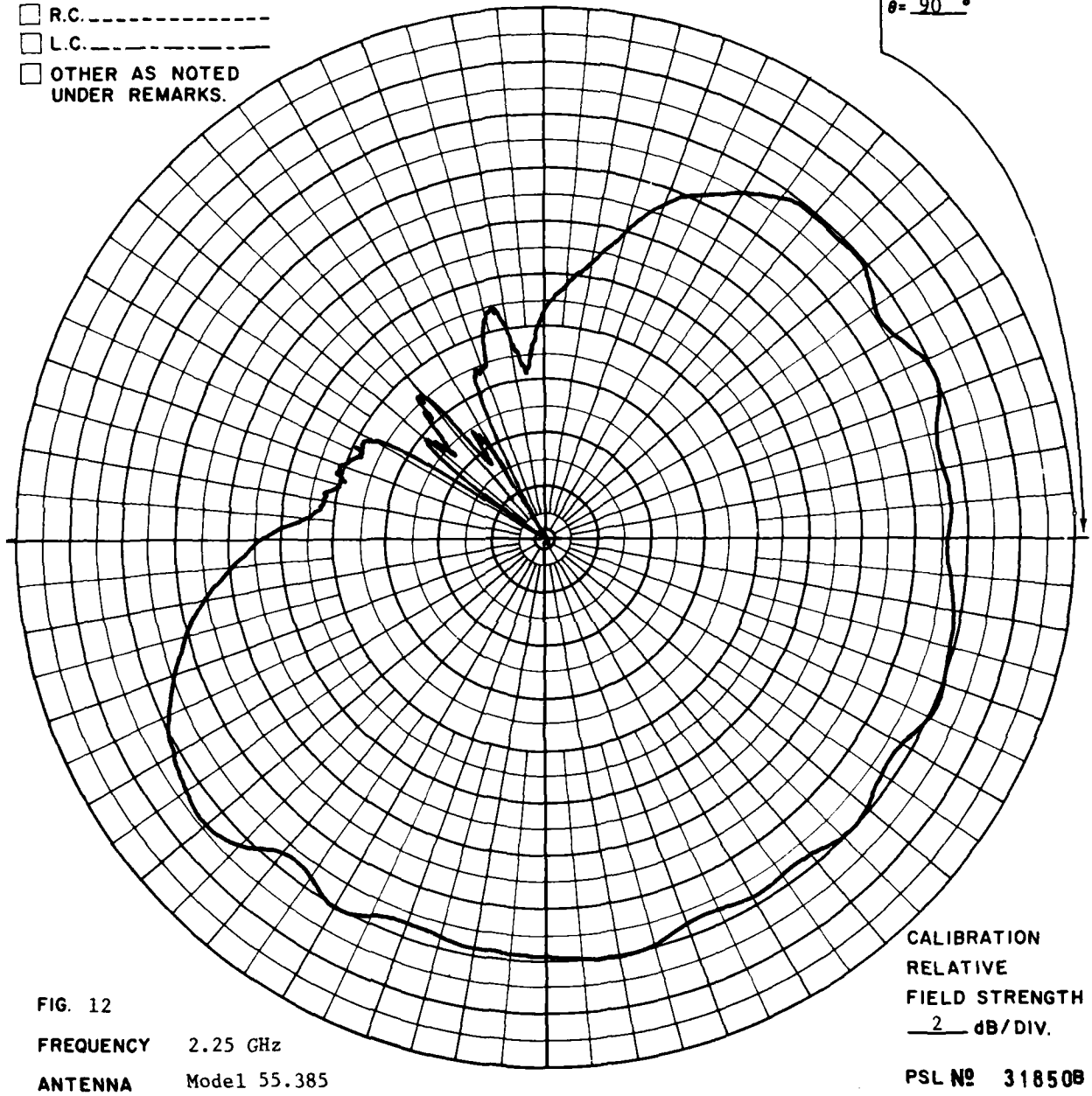

CALIBRATION
RELATIVE
FIELD STRENGTH
2 dB/DIV.

FIG. 12

FREQUENCY 2.25 GHz

ANTENNA Model 55.385

PSL № 318508

REMARKS Far-field pattern. Two subarrays disconnected.

RR 2815

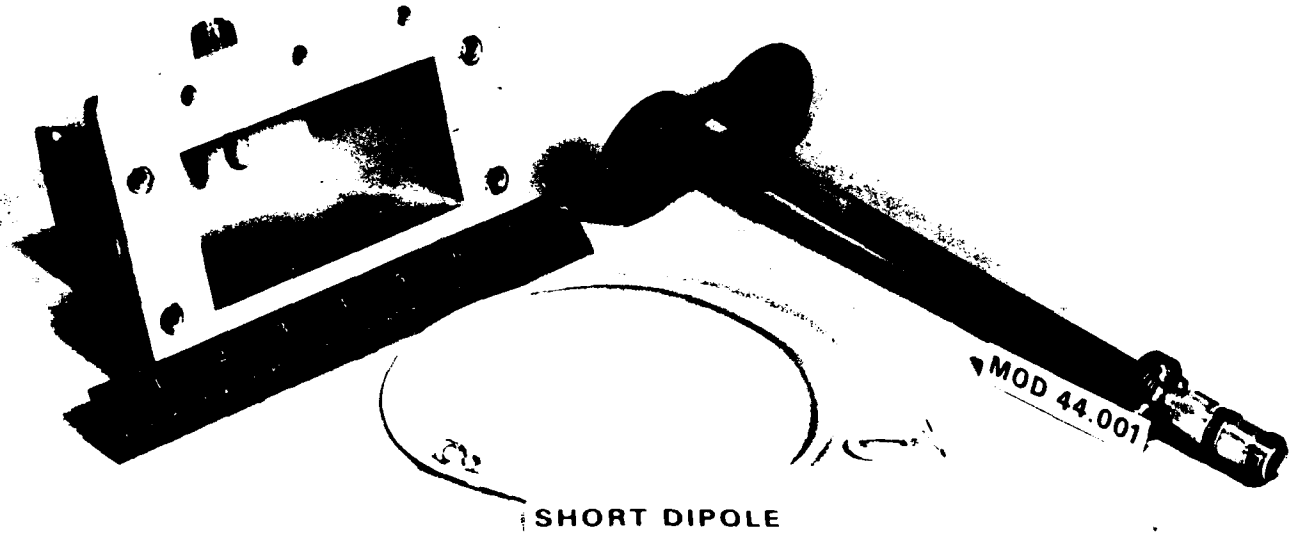

Figure 13. Near-field probes.

POLARIZATION

- ☐ GAIN REF.
- ☒ Eθ
- ☒ Eϕ
- ☐ R.C.
- ☐ L.C.
- ☐ OTHER AS NOTED UNDER REMARKS.

ϕ= ___ ° θ= 0 °

COORDINATE REFERENCE

ϕ= 0 °
θ= 90 °

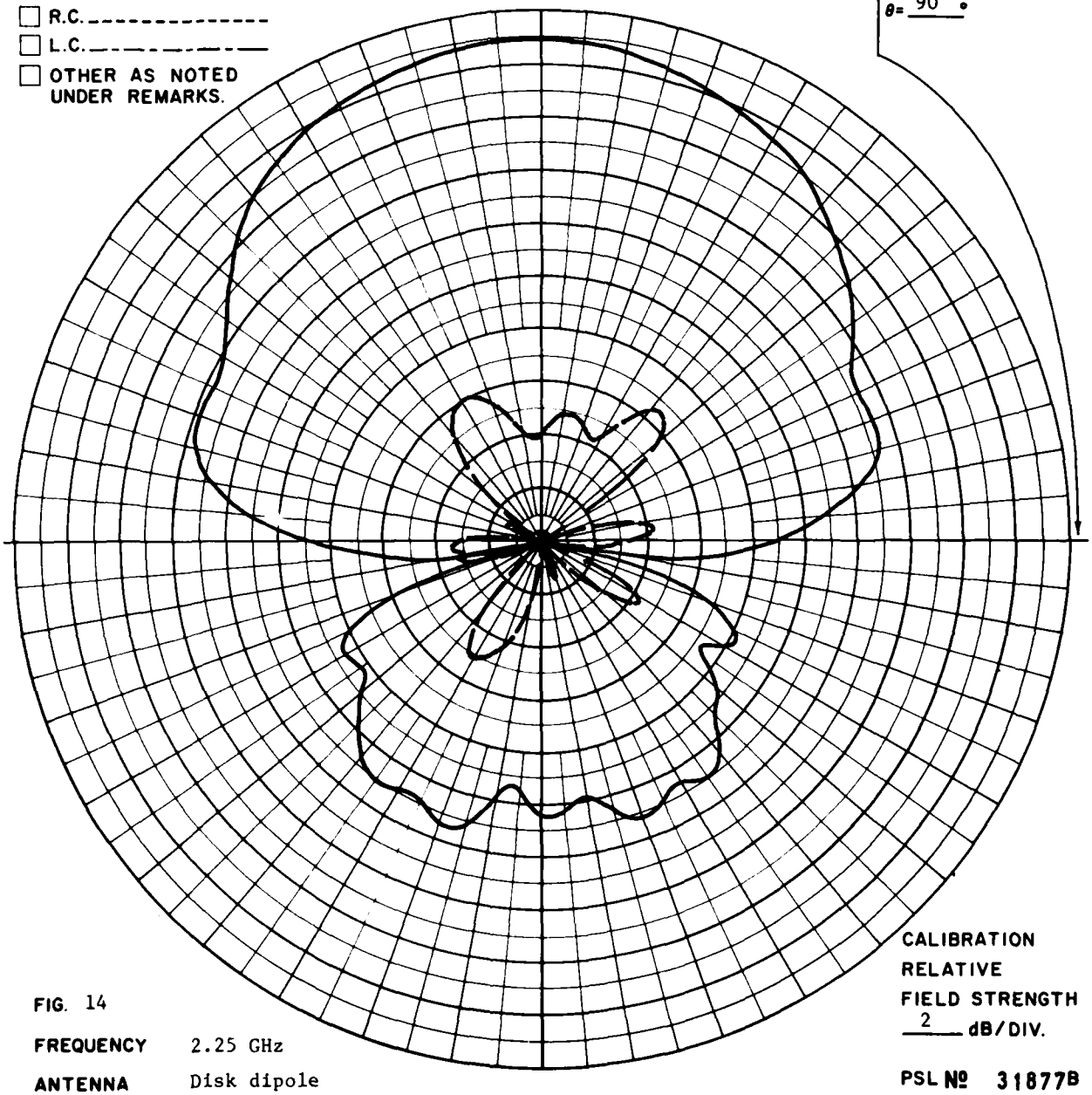

CALIBRATION
RELATIVE
FIELD STRENGTH
2 dB/DIV.

FIG. 14

FREQUENCY 2.25 GHz

ANTENNA Disk dipole

REMARKS Probe documentation.

PSL № 31877B

RR 2817

POLARIZATION

☐ GAIN REF.-- -- -- -- --
☒ Eθ_____
☒ Eφ- - - - - - - - - -
☐ R.C.- - - - - - - - - - - - -
☐ L.C._-_-_-_-_-_-_
☐ OTHER AS NOTED UNDER REMARKS.

φ= _ _ ° θ= 0 °

COORDINATE REFERENCE

φ= 90 °
θ= 90 °

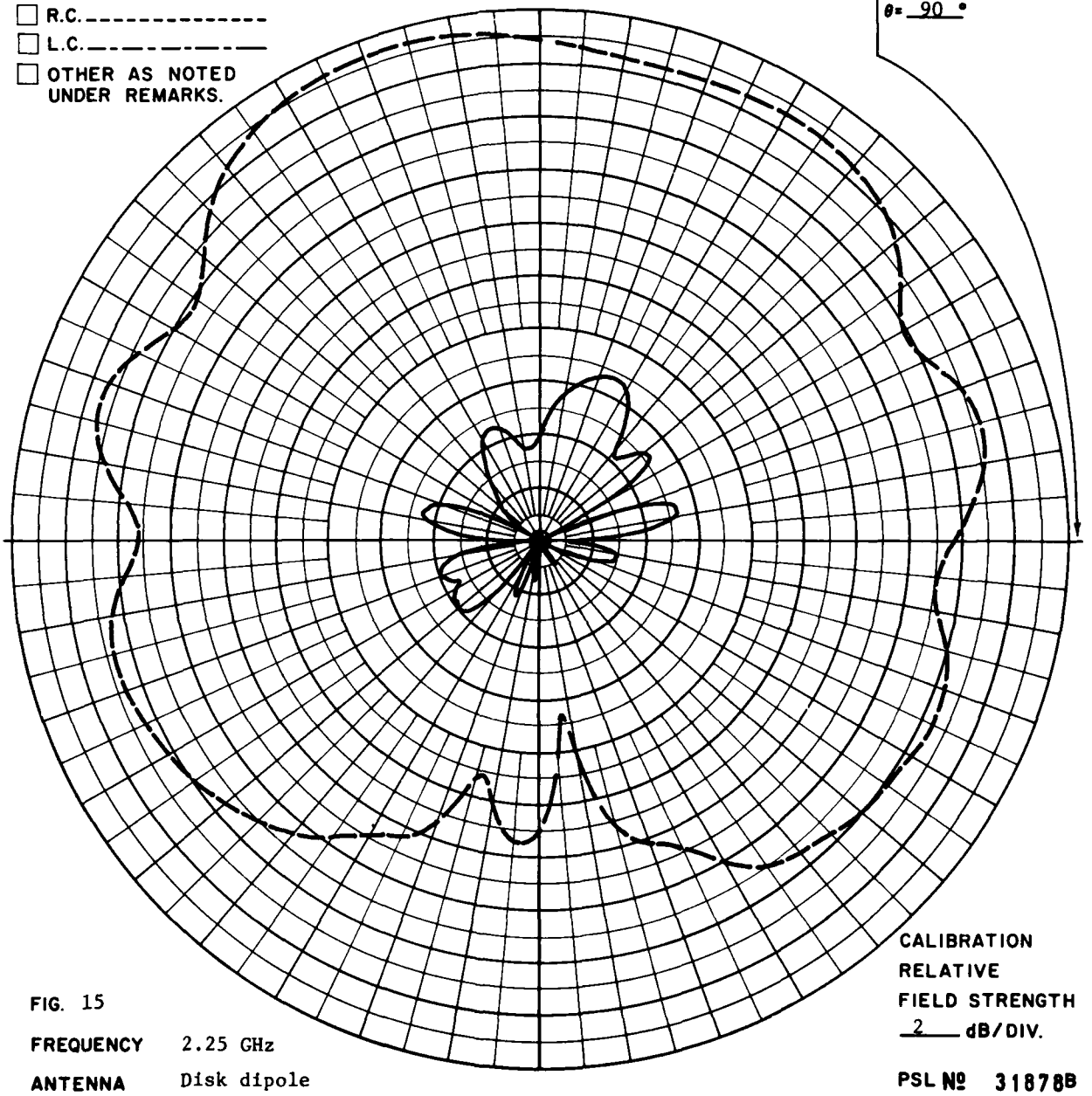

CALIBRATION
RELATIVE
FIELD STRENGTH
2 dB/DIV.

FIG. 15

FREQUENCY 2.25 GHz

ANTENNA Disk dipole

REMARKS Probe documentation.

PSL № 31878B

RR 2817

POLARIZATION

- ☐ GAIN REF.
- ☒ Eθ
- ☒ Eφ
- ☐ R.C.
- ☐ L.C.
- ☐ OTHER AS NOTED UNDER REMARKS.

φ= ___° θ= 0 ° COORDINATE REFERENCE

φ= 0 °
θ= 90 °

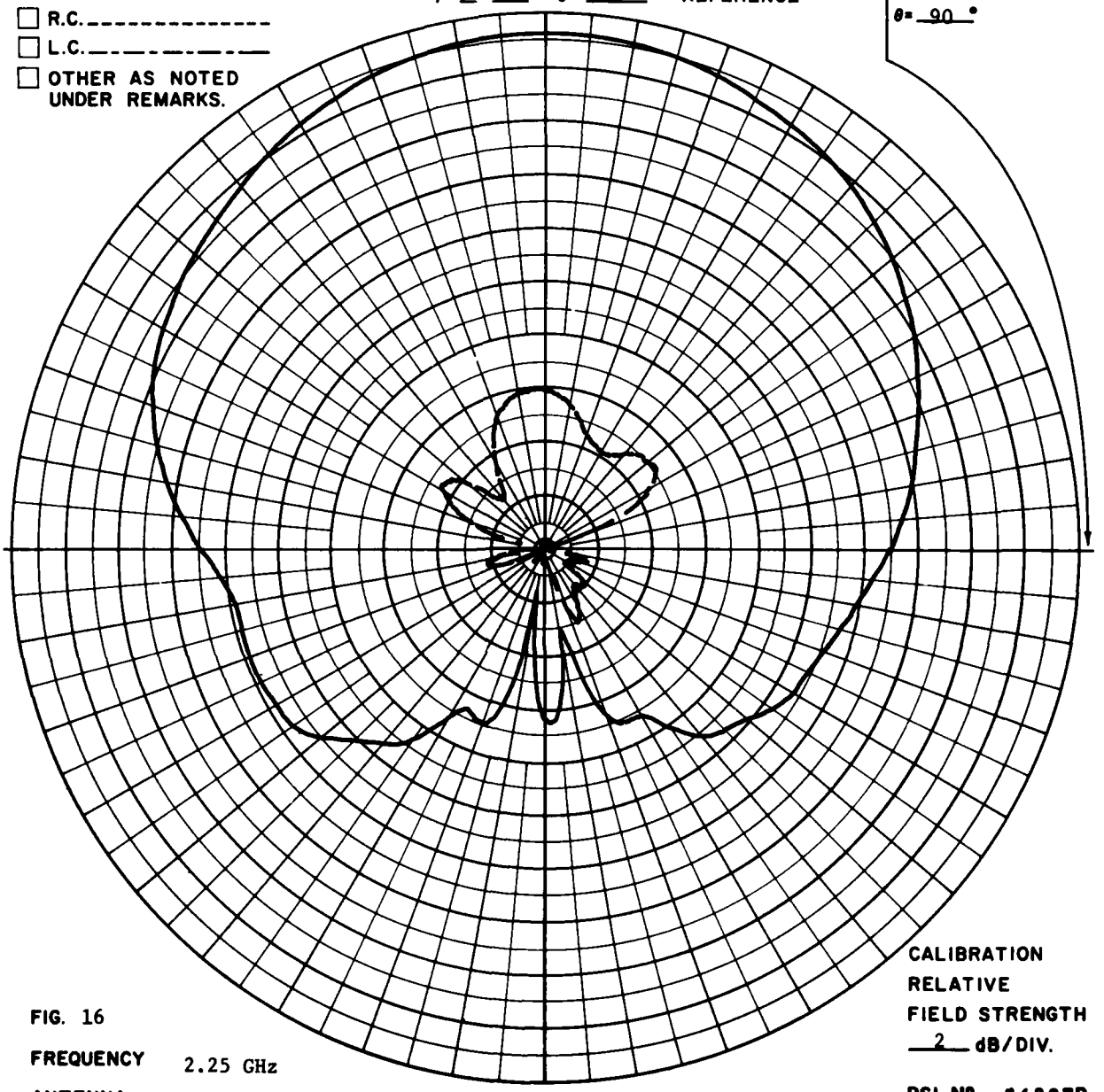

CALIBRATION
RELATIVE
FIELD STRENGTH
2 dB/DIV.

FIG. 16

FREQUENCY 2.25 GHz

ANTENNA Coaxial to waveguide adapter

REMARKS Probe documentation.

PSL № 31887B

RR 2817

POLARIZATION

- ☐ GAIN REF.
- ☒ Eθ
- ☒ Eϕ
- ☐ R.C.
- ☐ L.C.
- ☐ OTHER AS NOTED UNDER REMARKS.

ϕ= ___ ° θ= 0 °

COORDINATE REFERENCE

ϕ= 90 °
θ= 90 °

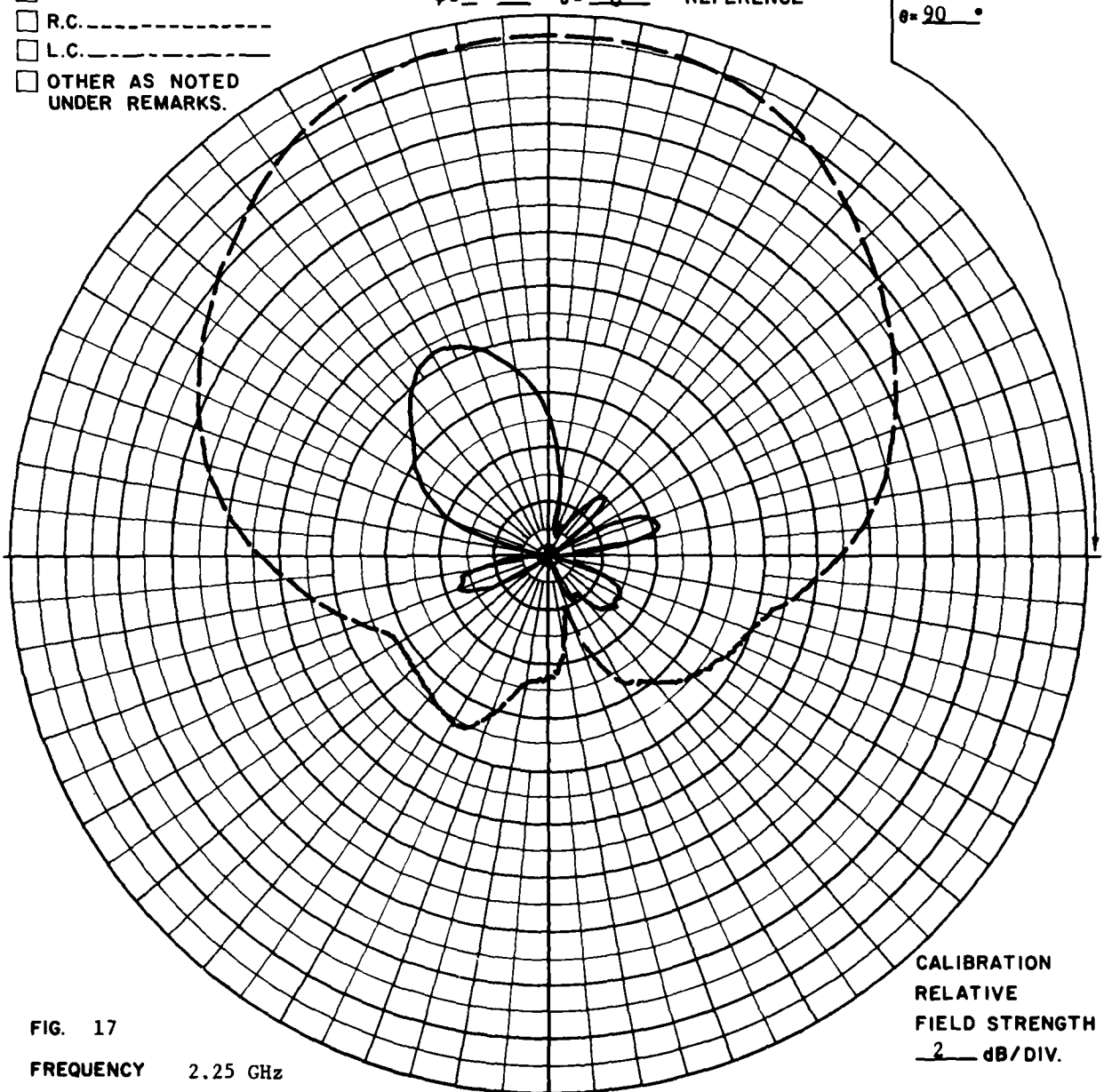

CALIBRATION
RELATIVE
FIELD STRENGTH
2 dB/DIV.

FIG. 17

FREQUENCY 2.25 GHz

ANTENNA Coaxial to waveguide adapter

REMARKS Probe documentation.

PSL Nº 31889B

RR 2817

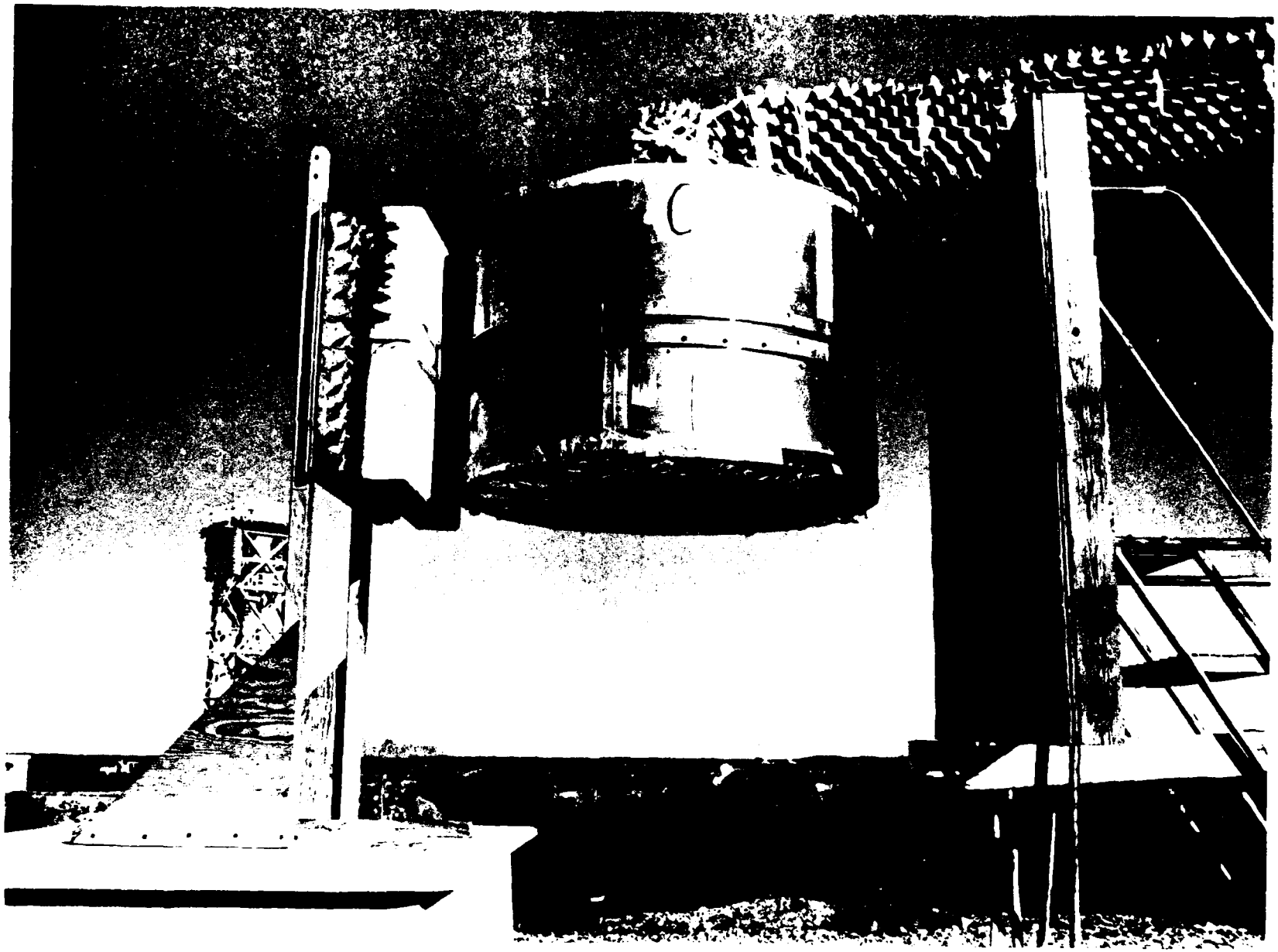

Figure 18. View of the test setup.

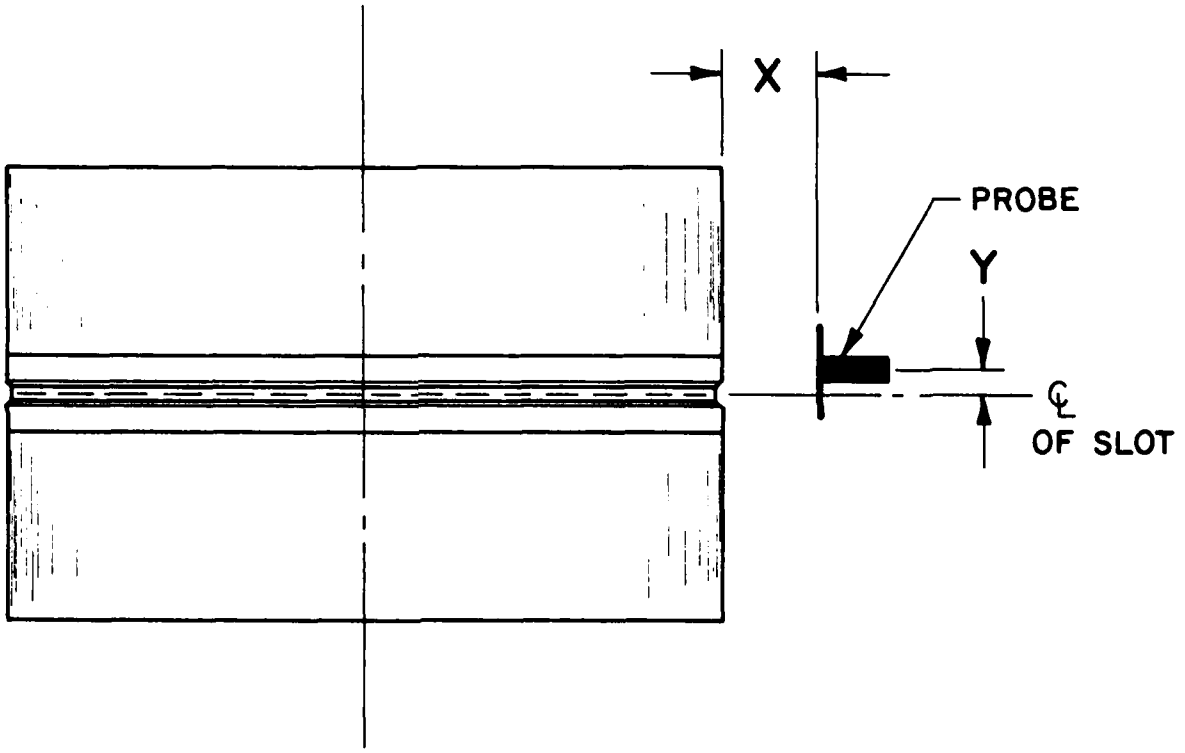

DISPLACEMENT		PATTERN NO.
X	Y	PSL No.
4	0	31896B
6	0	31897B
8	0	31898B
6	2	31899B
6	4	31900B

Figure 19. Sketch showing the various probe positions.

POLARIZATION

- ☐ GAIN REF.
- ☒ Eθ
- ☐ Eφ
- ☐ R.C.
- ☐ L.C.
- ☐ OTHER AS NOTED UNDER REMARKS.

COORDINATE REFERENCE

φ= 0 ° θ= 90 °

φ= 90 °
θ= 90 °

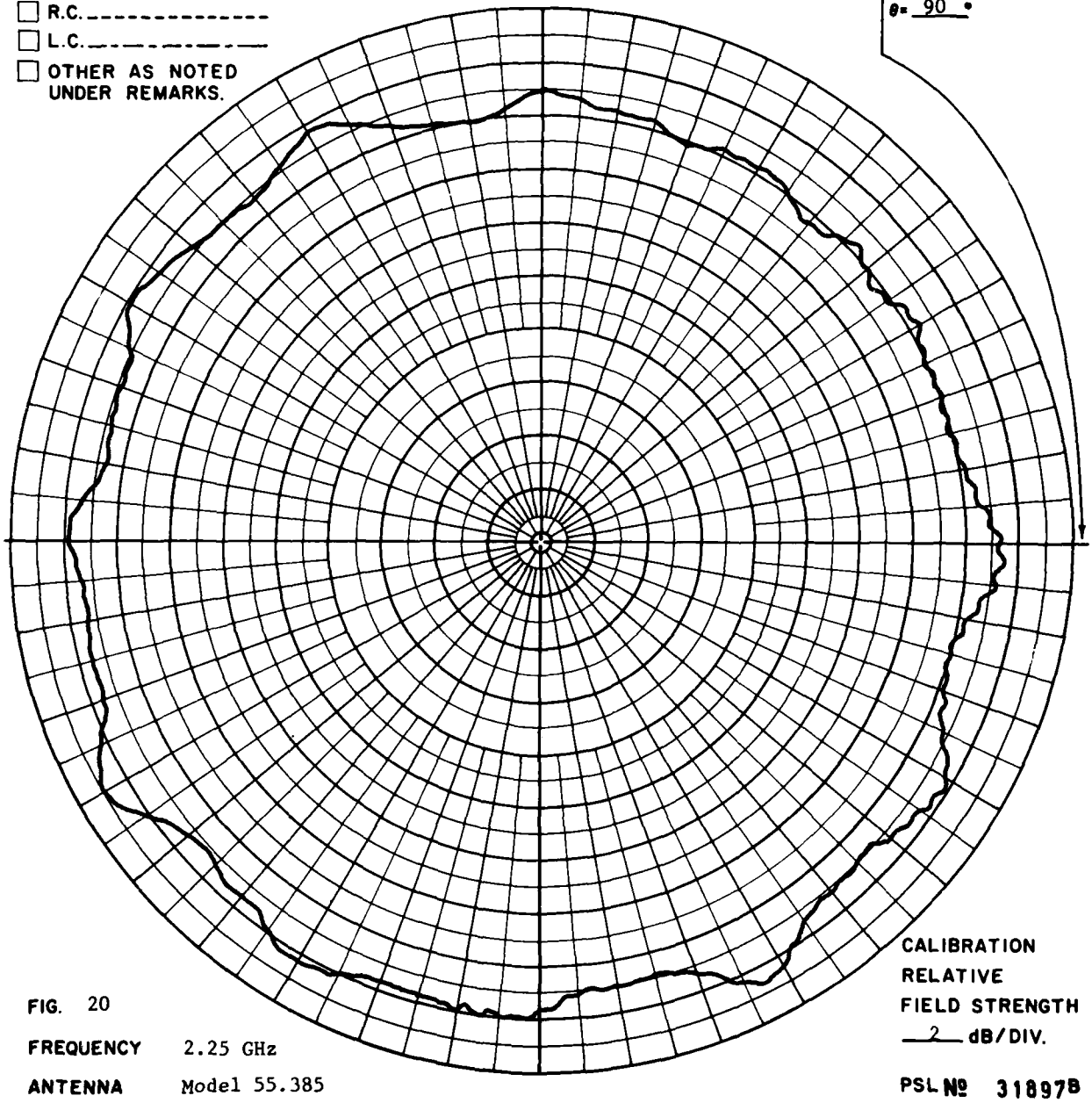

CALIBRATION
RELATIVE
FIELD STRENGTH
2 dB/DIV.

FIG. 20

FREQUENCY 2.25 GHz

ANTENNA Model 55.385

REMARKS Testing effect of probe position
X=4" Y=0"

PSL № 31897B

RR 2818

POLARIZATION

- ☐ GAIN REF.
- ☒ Eθ
- ☐ Eφ
- ☐ R.C.
- ☐ L.C.
- ☐ OTHER AS NOTED UNDER REMARKS.

COORDINATE REFERENCE

φ= 0 ° θ= 90 °

φ= 90 °
θ= 90 °

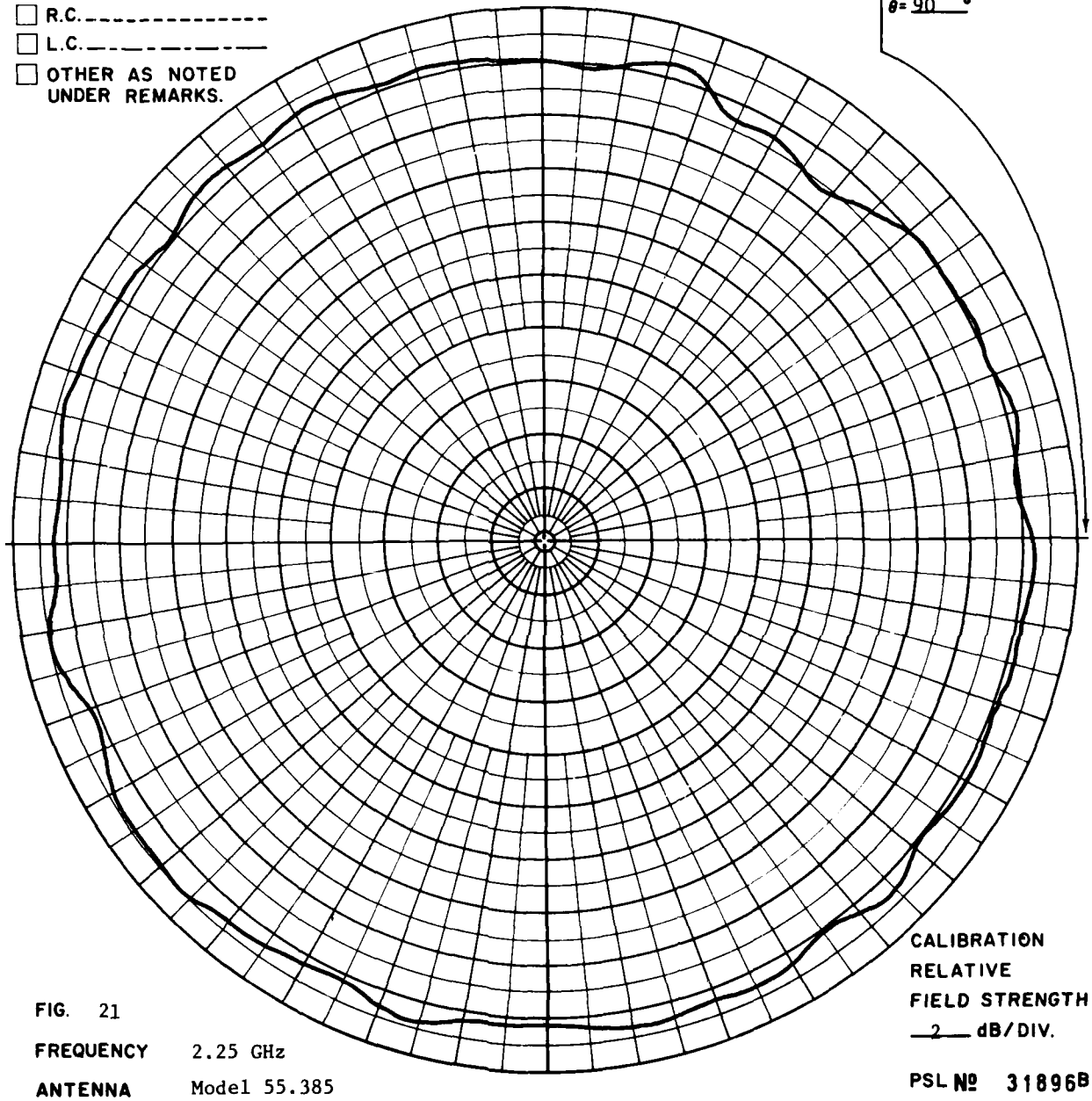

CALIBRATION
RELATIVE
FIELD STRENGTH
2 dB/DIV.

PSL № 31896B

RR 2818

FIG. 21

FREQUENCY 2.25 GHz

ANTENNA Model 55.385

REMARKS Testing effect of probe position
X=6" Y=0"

POLARIZATION

- ☐ GAIN REF.
- ☒ Eθ
- ☐ Eφ
- ☐ R.C.
- ☐ L.C.
- ☐ OTHER AS NOTED UNDER REMARKS.

COORDINATE REFERENCE

φ= 0 ° θ= 90 °

φ= 90 °
θ= 90 °

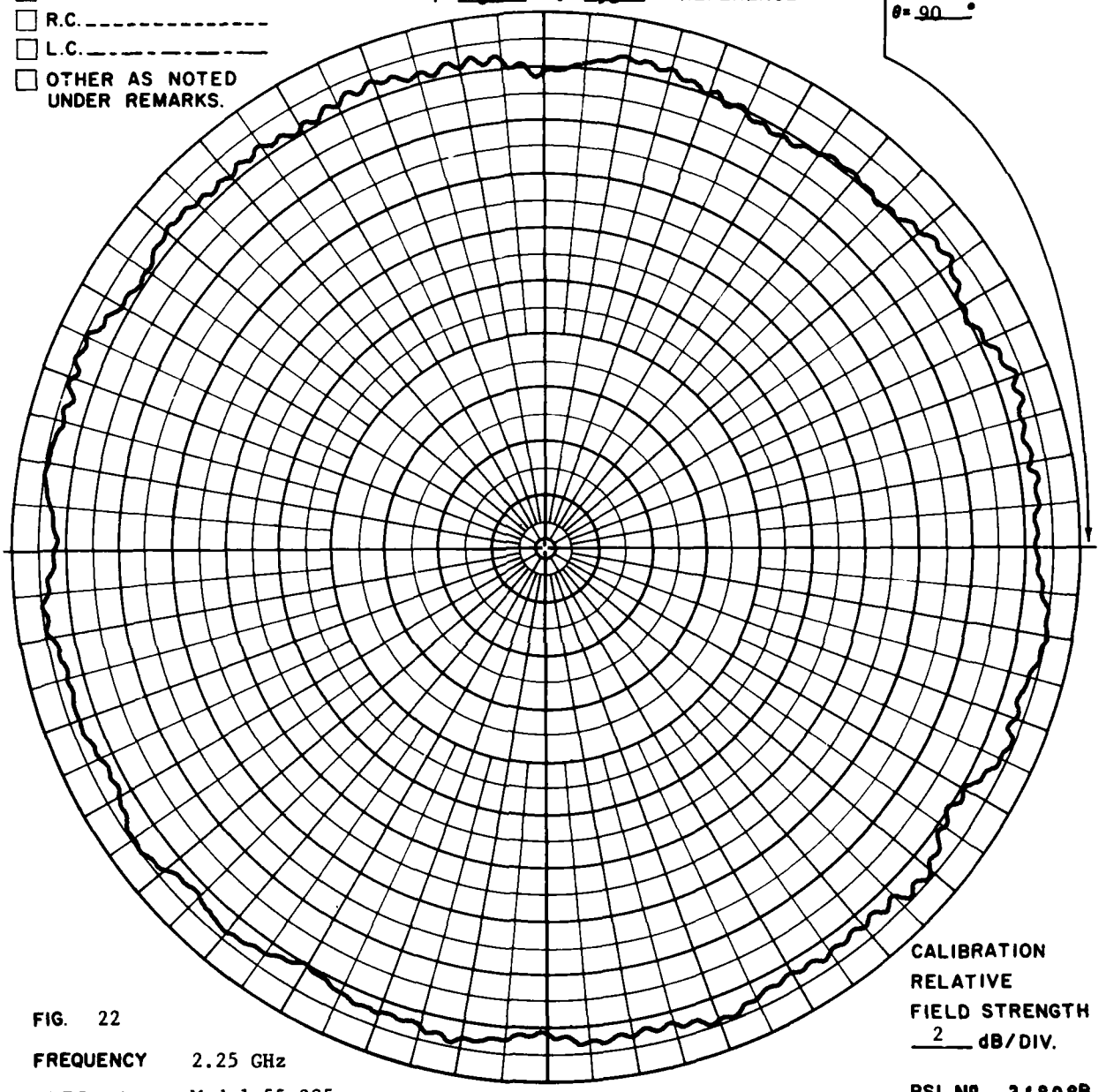

CALIBRATION
RELATIVE
FIELD STRENGTH
2 dB/DIV.

FIG. 22

FREQUENCY 2.25 GHz

ANTENNA Model 55.385

REMARKS Testing effect of probe position
X=8" Y=0"

PSL Nº 31898B

RR 2818

POLARIZATION

- ☐ GAIN REF.
- ☒ Eθ
- ☐ Eϕ
- ☐ R.C.
- ☐ L.C.
- ☐ OTHER AS NOTED UNDER REMARKS.

ϕ= 0 • θ= 90 • COORDINATE REFERENCE

ϕ= 90 •
θ= 90 •

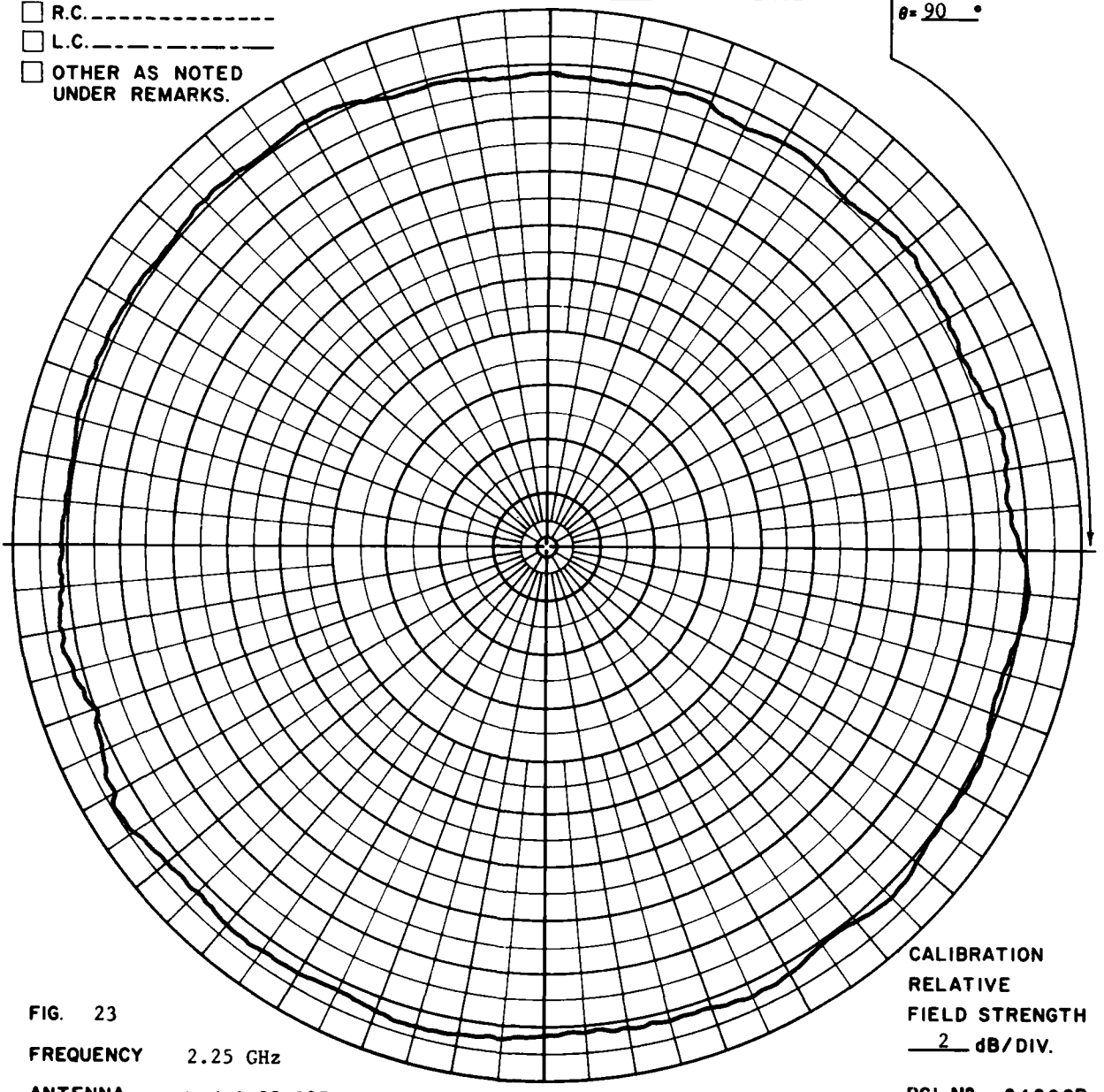

CALIBRATION
RELATIVE
FIELD STRENGTH
2 dB/DIV.

FIG. 23

FREQUENCY 2.25 GHz

ANTENNA Model 55.385

REMARKS Testing effect of probe position
X=6" Y=2"

PSL № 31899B

RR 2818

POLARIZATION

- ☐ GAIN REF.
- ☒ Eθ
- ☐ Eφ
- ☐ R.C.
- ☐ L.C.
- ☐ OTHER AS NOTED UNDER REMARKS.

COORDINATE REFERENCE

φ= 0 ° θ= 90 °

φ= 90 °
θ= 90 °

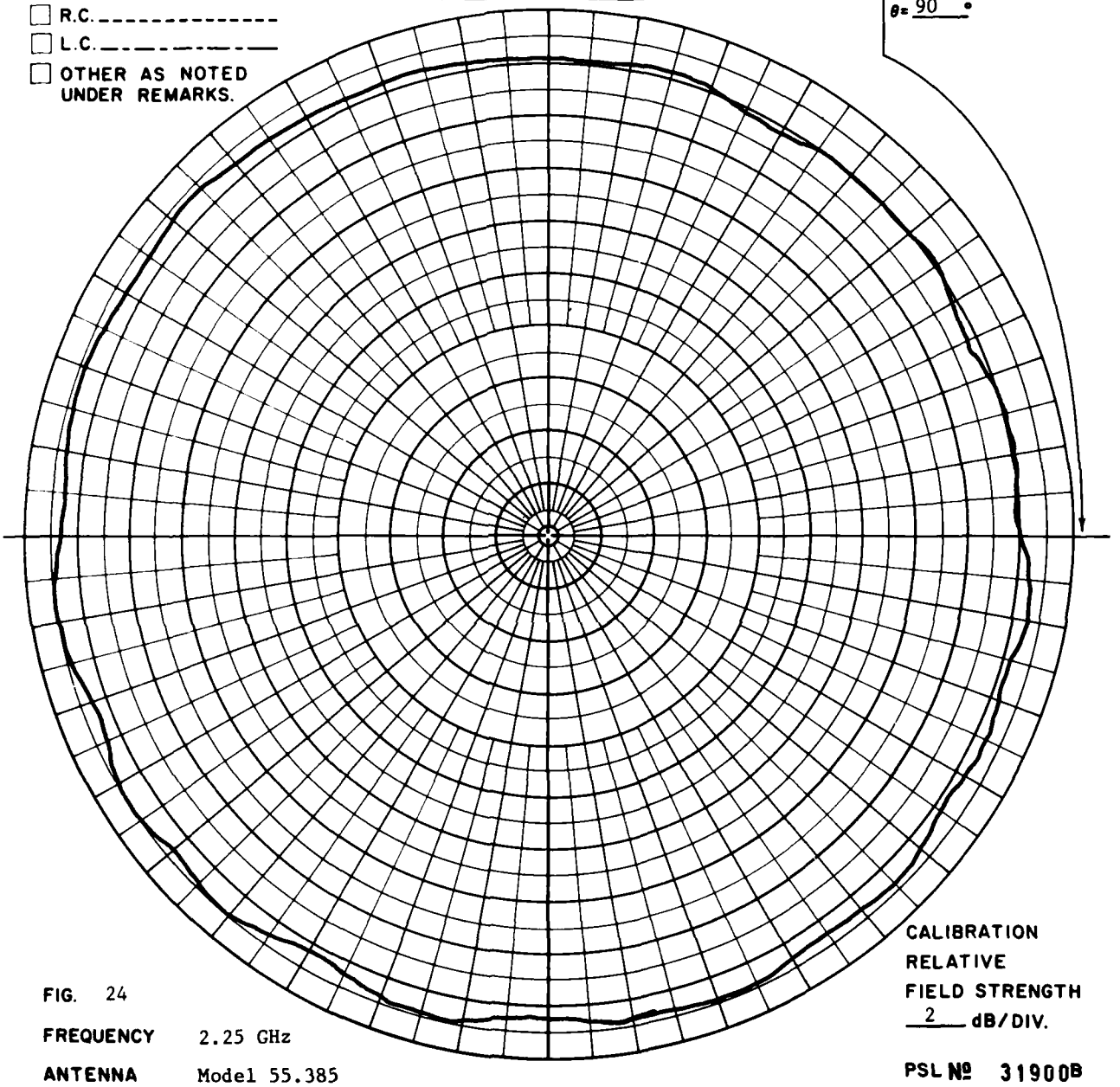

CALIBRATION
RELATIVE
FIELD STRENGTH
2 dB/DIV.

FIG. 24

FREQUENCY 2.25 GHz

ANTENNA Model 55.385

REMARKS Testing effect of probe position
X=6" Y=4"

PSL № 31900B

RR 2818

POLARIZATION

- ☐ GAIN REF.
- ☒ Eθ
- ☐ Eφ
- ☐ R.C.
- ☐ L.C.
- ☐ OTHER AS NOTED UNDER REMARKS.

COORDINATE REFERENCE

φ= 0 ° θ= 90 °

φ= 90 °
θ= 90 °

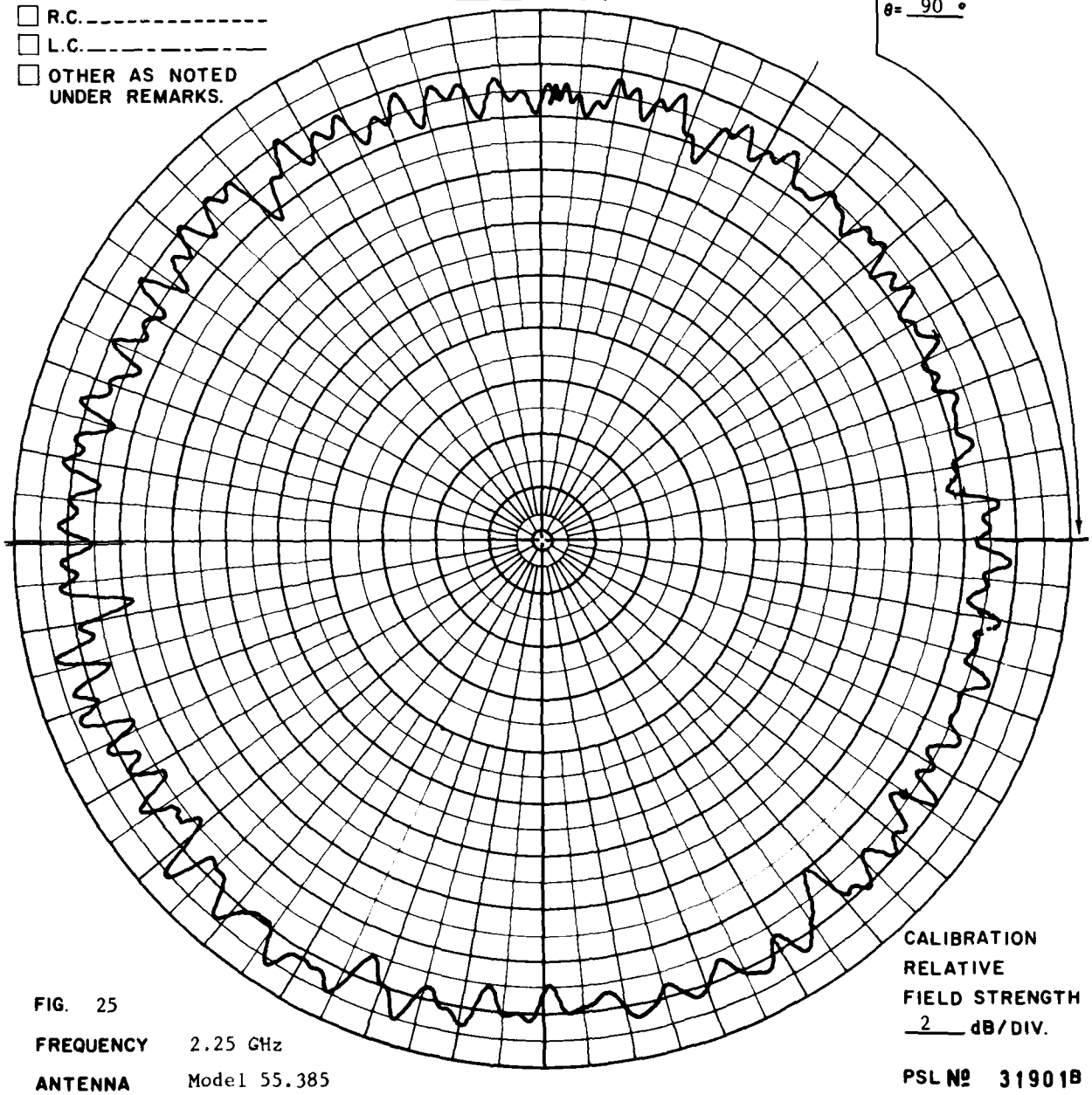

CALIBRATION
RELATIVE
FIELD STRENGTH
2 dB/DIV.

FIG. 25

FREQUENCY 2.25 GHz

ANTENNA Model 55.385

REMARKS Short dipole probe. Antenna and harness intact.

PSL № 31901B

RR 2818

POLARIZATION

- ☐ GAIN REF.
- ☒ Eθ
- ☐ Eϕ
- ☐ R.C.
- ☐ L.C.
- ☐ OTHER AS NOTED UNDER REMARKS.

ϕ = 0 ° θ = 90 ° COORDINATE REFERENCE

ϕ = 1 °
θ = 5 °

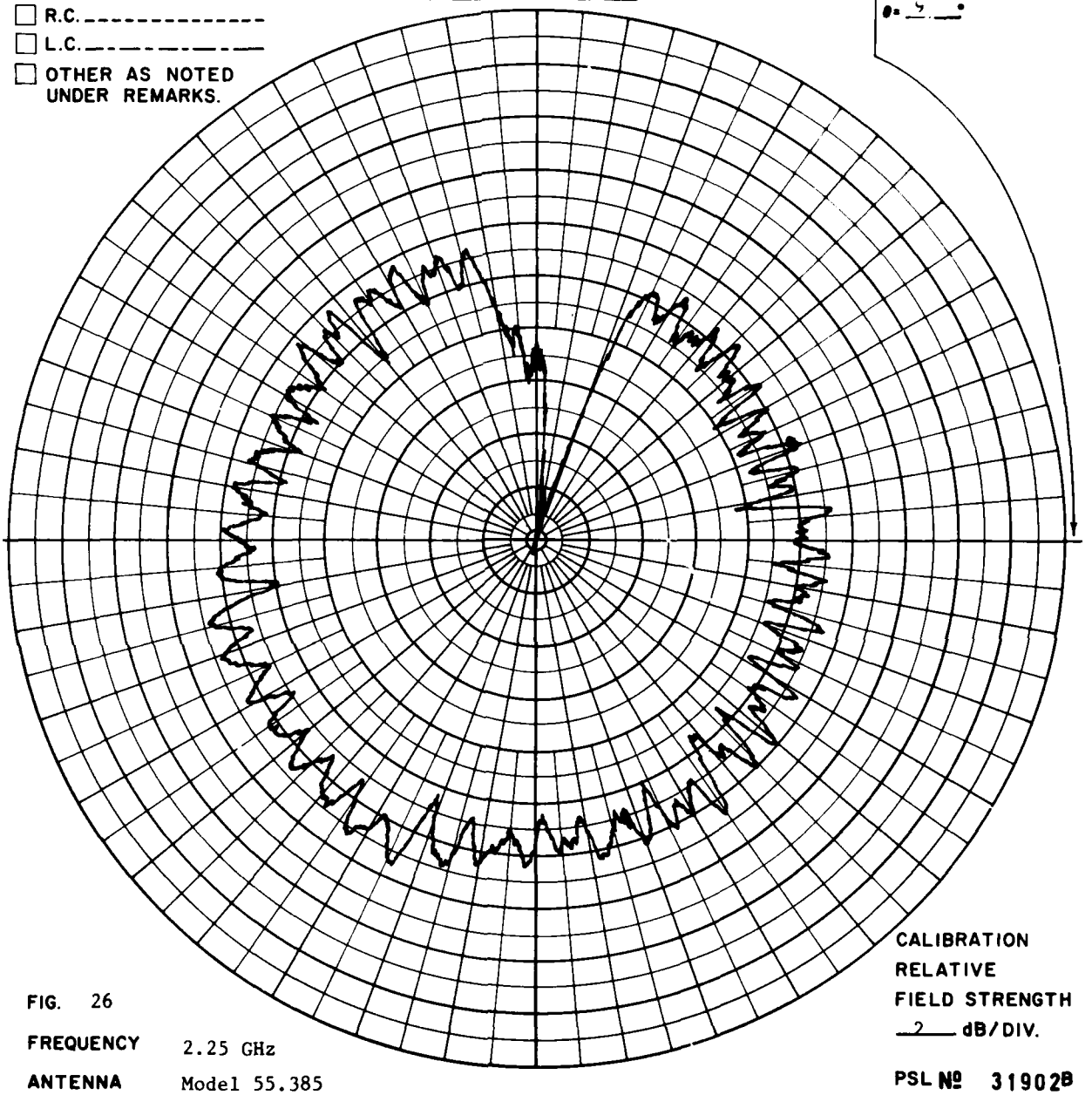

CALIBRATION
RELATIVE
FIELD STRENGTH
2 dB/DIV.

FIG. 26

FREQUENCY 2.25 GHz

ANTENNA Model 55.385

REMARKS Short dipole probe. One element covered with metal foil.

PSL № 31902B

RR 2818

POLARIZATION

- ☐ GAIN REF.
- ☒ Eθ
- ☐ Eφ
- ☐ R.C.
- ☐ L.C.
- ☐ OTHER AS NOTED UNDER REMARKS.

φ= 0 ° θ= 90 ° COORDINATE REFERENCE

φ= 90 °
θ= 90 °

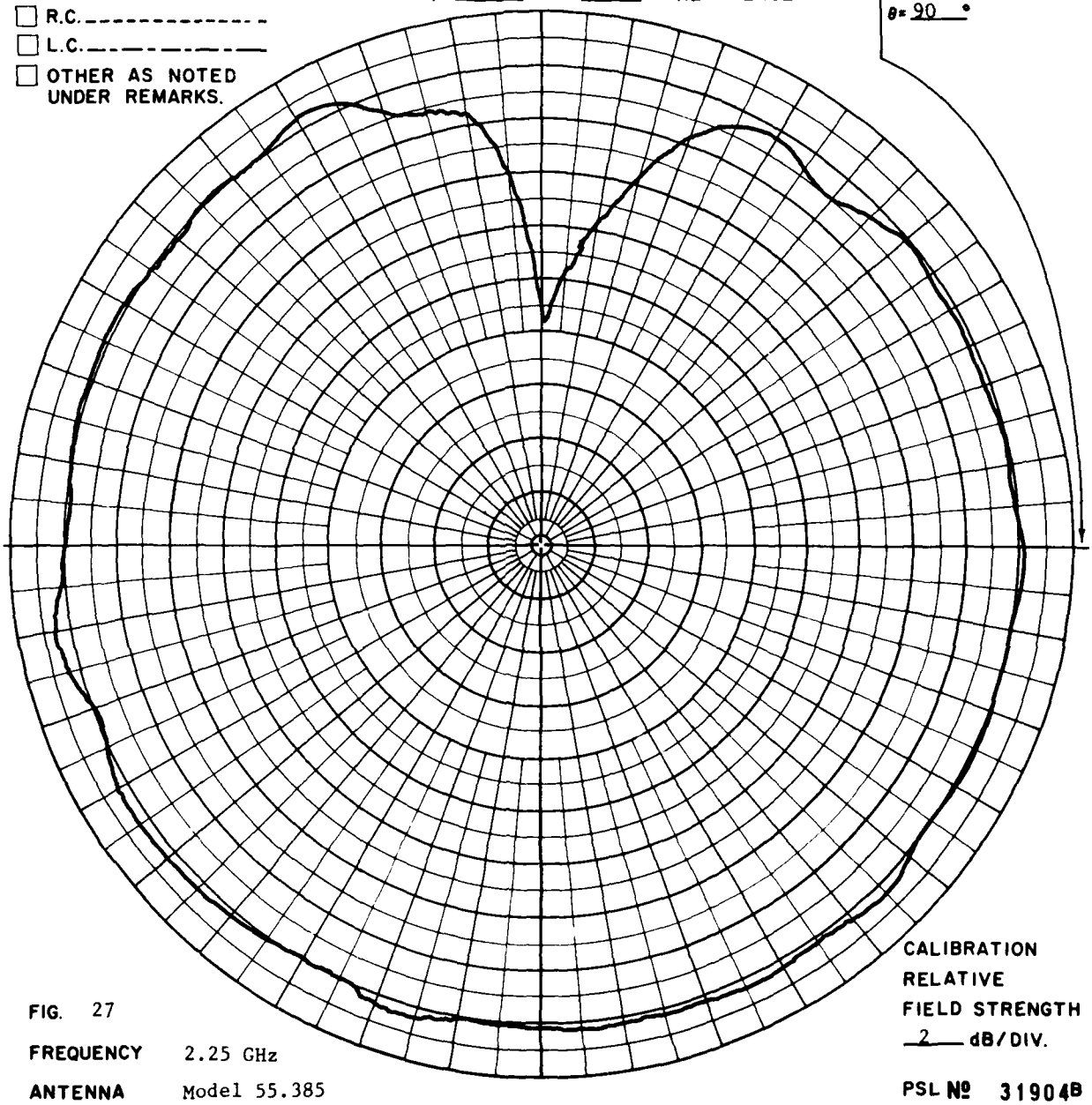

CALIBRATION
RELATIVE
FIELD STRENGTH
2 dB/DIV.

FIG. 27

FREQUENCY 2.25 GHz

ANTENNA Model 55.385

REMARKS Coaxial to waveguide adaptor probe. One element covered with metal foil.

PSL Nº 31904B

RR 2818

POLARIZATION

- ☐ GAIN REF.
- ☒ Eθ
- ☐ Eφ
- ☐ R.C.
- ☐ L.C.
- ☐ OTHER AS NOTED UNDER REMARKS.

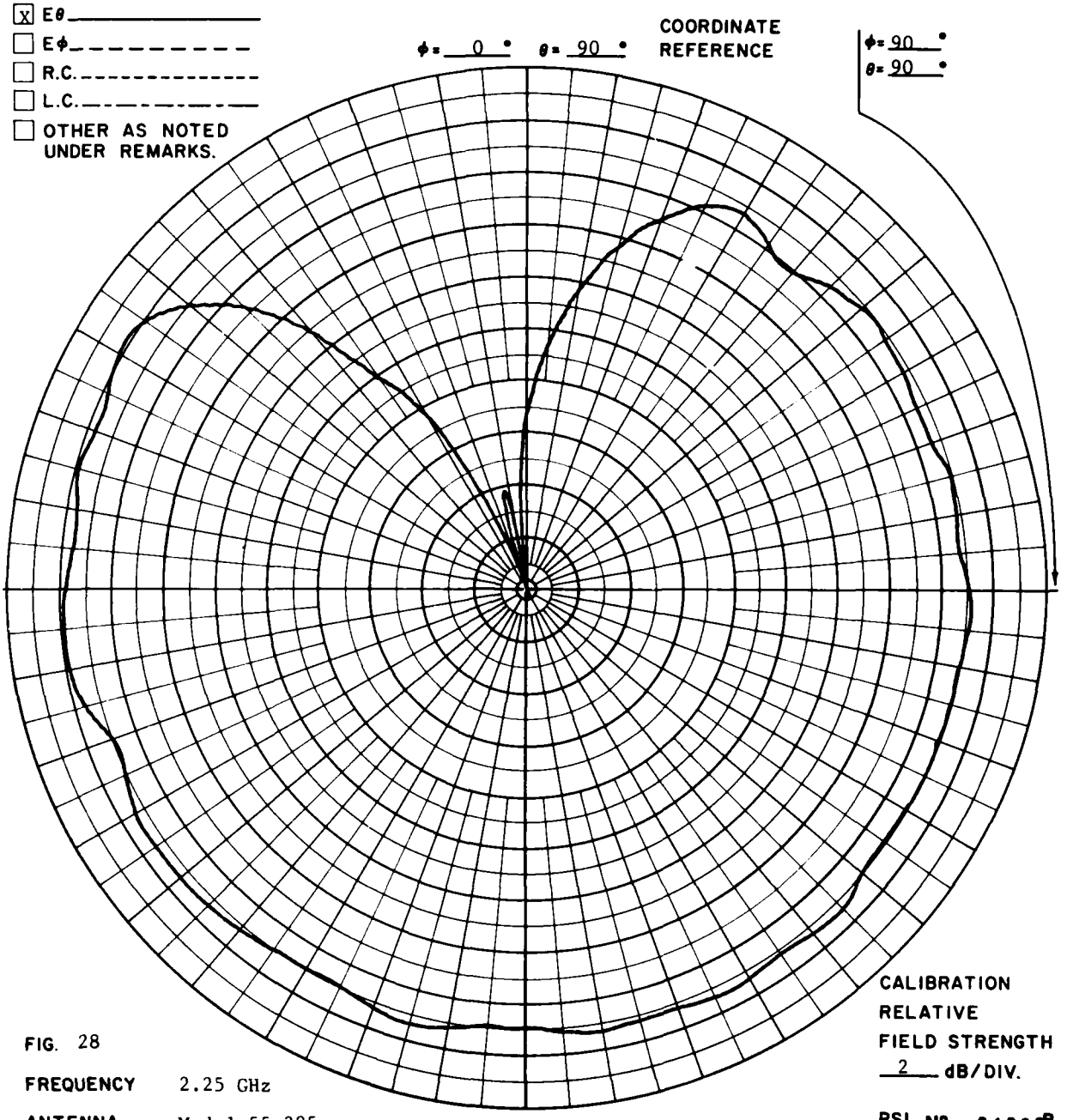

CALIBRATION
RELATIVE
FIELD STRENGTH
2 dB/DIV.

FIG. 28

FREQUENCY 2.25 GHz

ANTENNA Model 55.385

REMARKS Coaxial to waveguide adaptor probe. One subarray disconnected.

PSL № 31909B

RR 2818

POLARIZATION

- ☐ GAIN REF.
- ☒ Eθ
- ☐ Eϕ
- ☐ R.C.
- ☐ L.C.
- ☐ OTHER AS NOTED UNDER REMARKS.

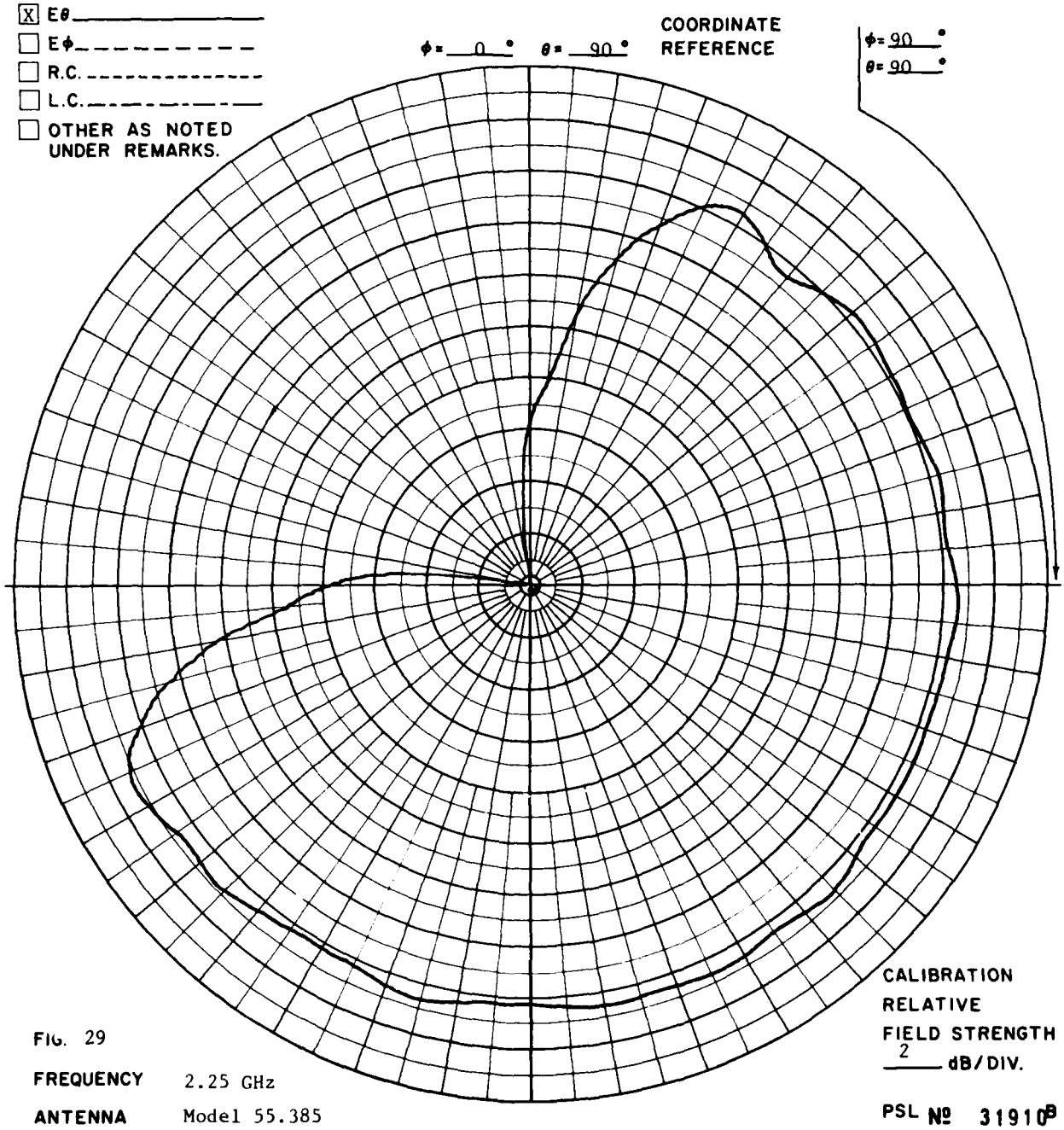

CALIBRATION
RELATIVE
FIELD STRENGTH
2 dB/DIV.

FIG. 29

FREQUENCY 2.25 GHz

ANTENNA Model 55.385

REMARKS Coaxial to waveguide adaptor probe. Two subarrays disconnected.

PSL № 31910[B]

RR 2818

POLARIZATION

- ☐ GAIN REF.
- ☒ Eθ
- ☐ Eϕ
- ☐ R.C.
- ☐ L.C.
- ☐ OTHER AS NOTED UNDER REMARKS.

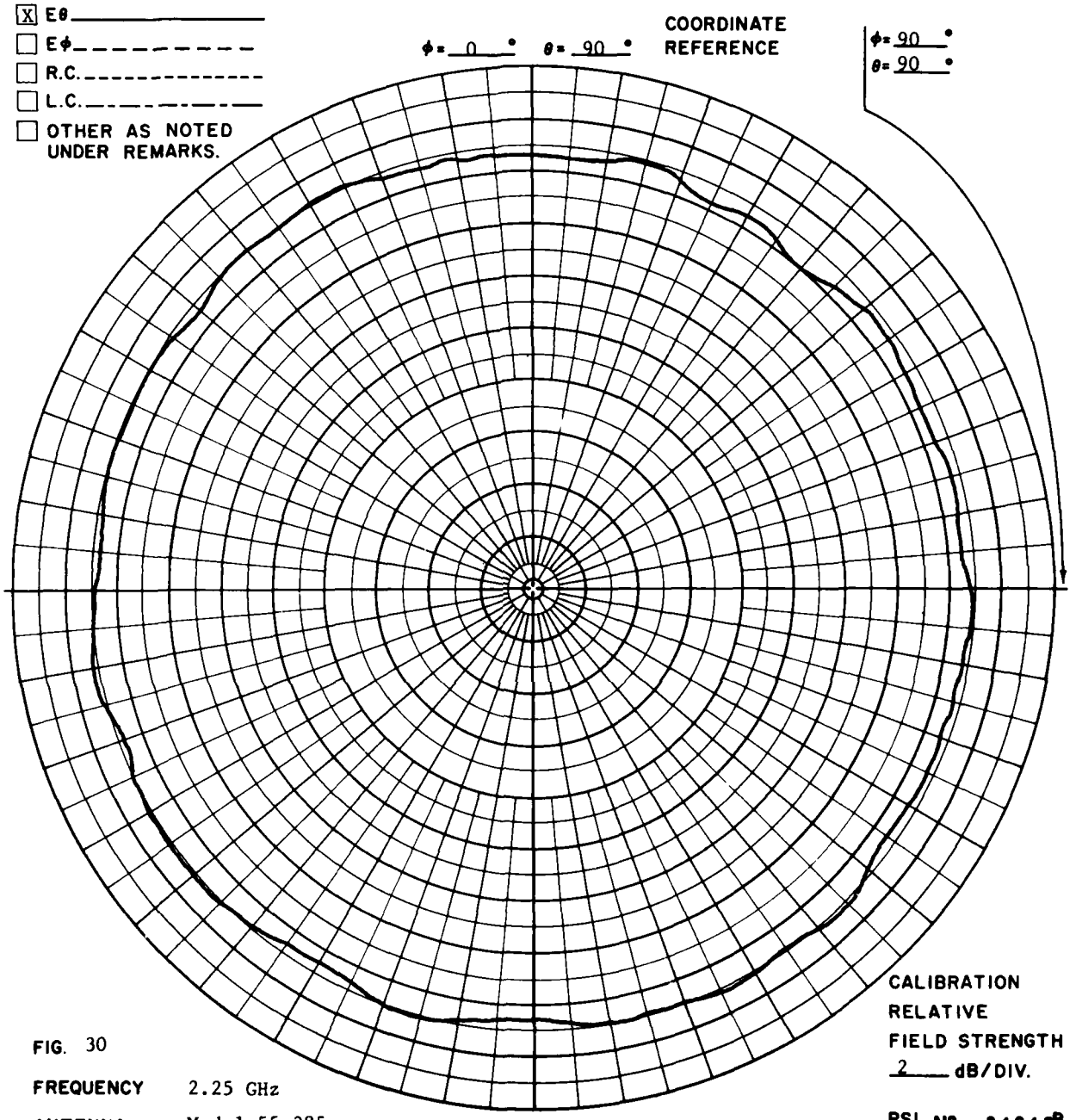

CALIBRATION
RELATIVE
FIELD STRENGTH
2 dB/DIV.

FIG. 30

FREQUENCY 2.25 GHz

ANTENNA Model 1 55.385

REMARKS Coaxial to waveguide adaptor probe. Connector loosened at antenna feed.

PSL № 31912[B]

RR 2818

POLARIZATION

- ☐ GAIN REF.
- ☒ Eθ
- ☐ Eφ
- ☐ R.C.
- ☐ L.C.
- ☐ OTHER AS NOTED UNDER REMARKS.

φ = 0° θ = 90° COORDINATE REFERENCE

φ = 90°
θ = 90°

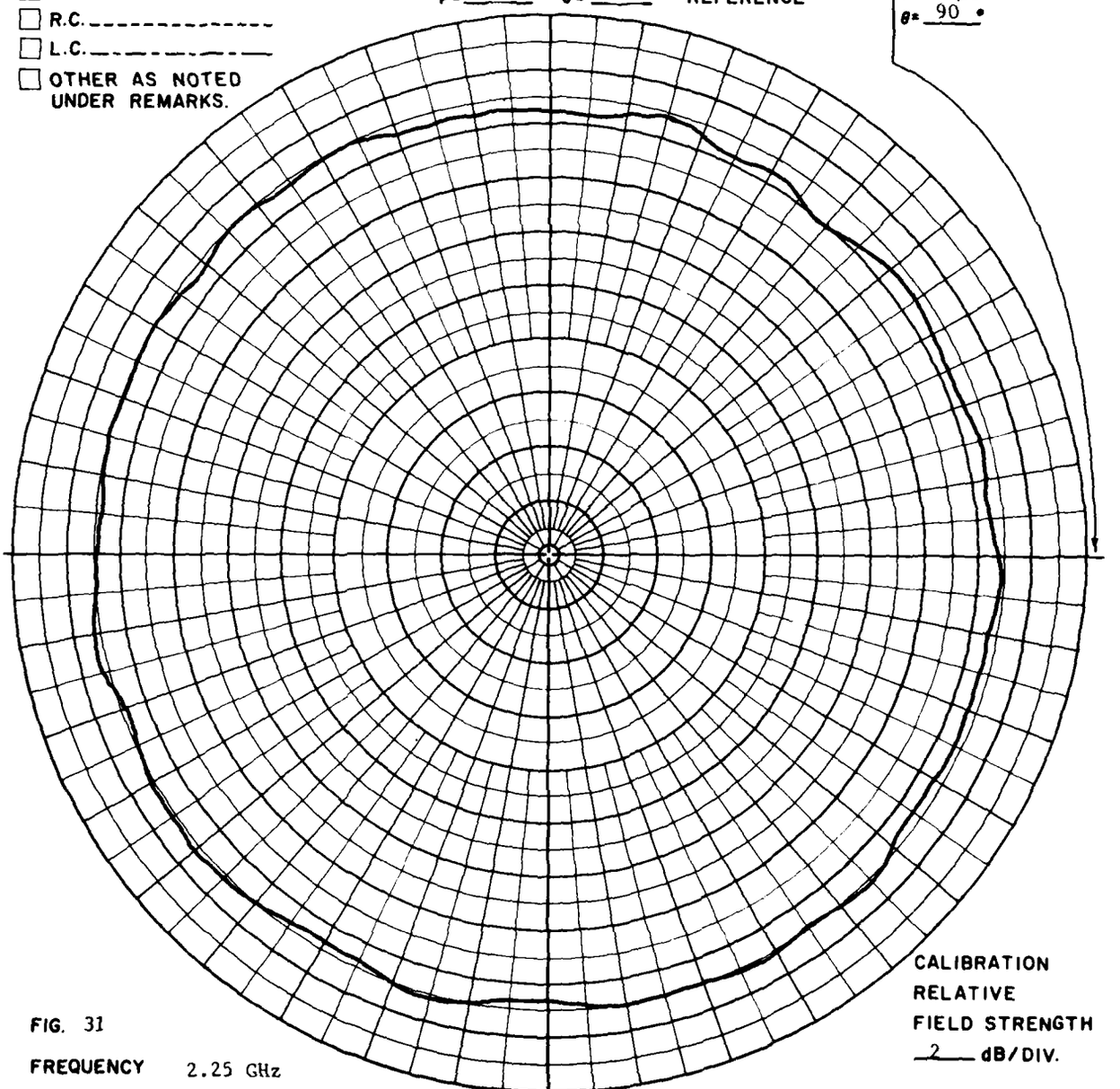

CALIBRATION
RELATIVE
FIELD STRENGTH
2 dB/DIV.

PSL № 31911B

RR 2818

FIG. 31

FREQUENCY 2.25 GHz

ANTENNA Model 55.385

REMARKS Coaxial to waveguide adaptor probe. Connector loosened at three-way power divider.

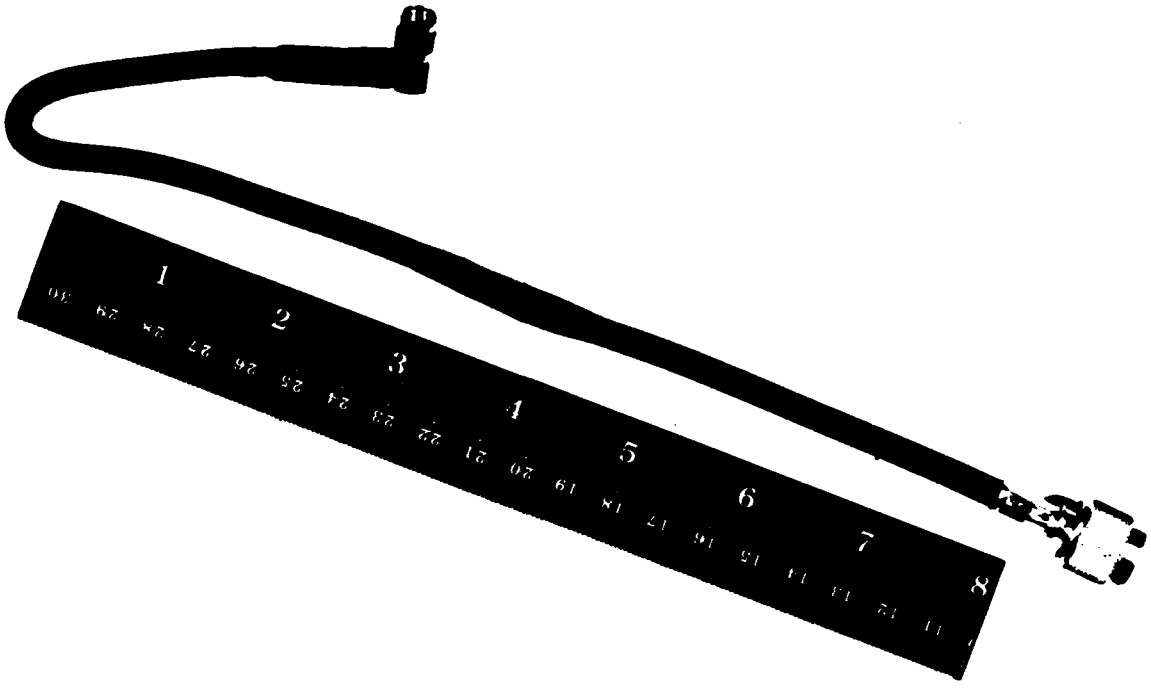

Figure 32. Damaged coaxial cable.

POLARIZATION

- ☐ GAIN REF.
- ☒ Eθ
- ☐ Eφ
- ☐ R.C.
- ☐ L.C.
- ☐ OTHER AS NOTED UNDER REMARKS.

φ= 0 ° θ= 90 ° COORDINATE REFERENCE

φ= 90 °
θ= 90 °

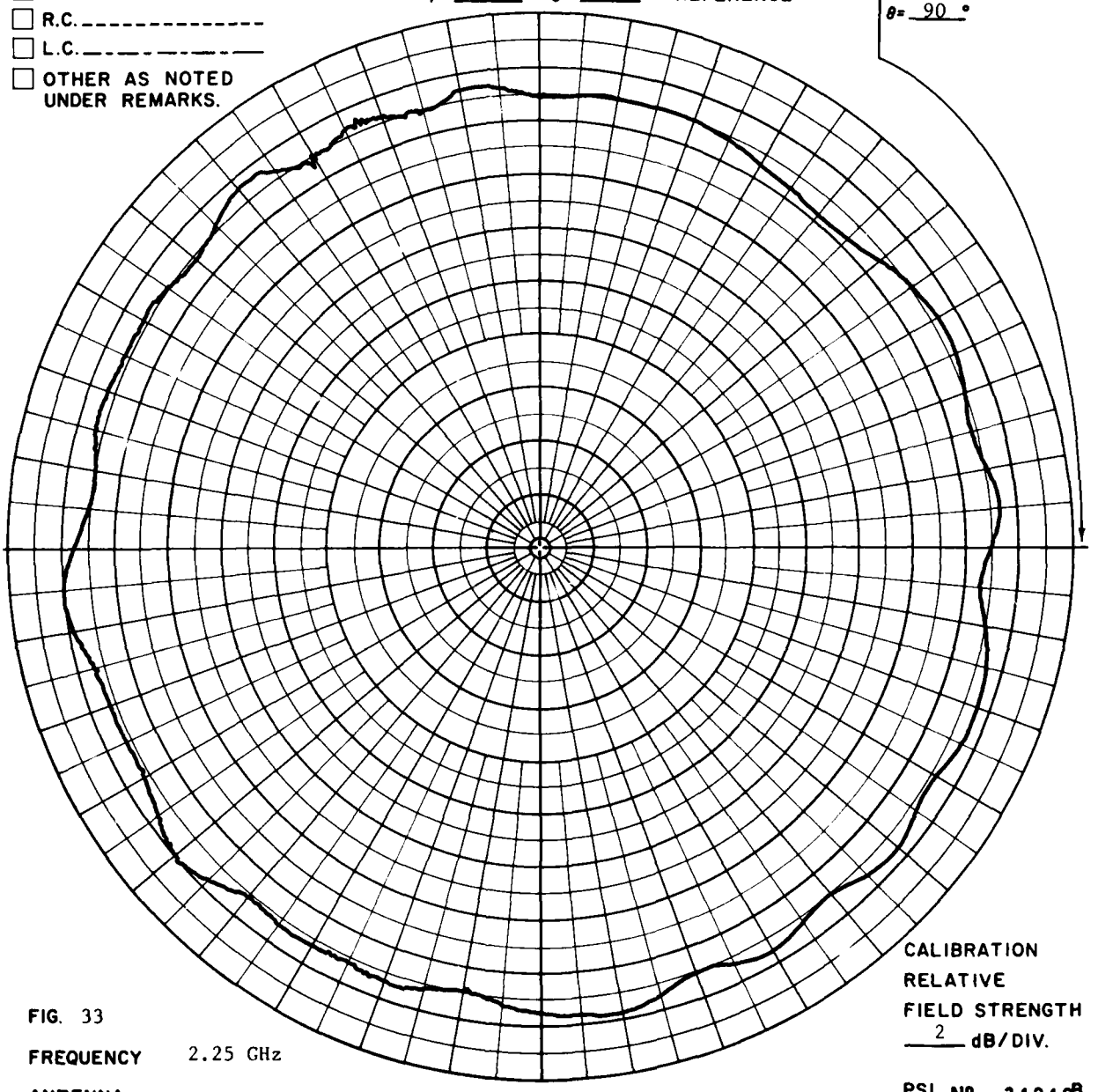

CALIBRATION
RELATIVE
FIELD STRENGTH
2 dB/DIV.

FIG. 33

FREQUENCY 2.25 GHz

ANTENNA Model 55.385

REMARKS Far-field pattern of intact antenna and harness.

PSL № 31916B

RR 2819

POLARIZATION

- ☐ GAIN REF.
- ☒ Eθ
- ☐ Eφ
- ☐ R.C.
- ☐ L.C.
- ☐ OTHER AS NOTED UNDER REMARKS.

φ= 0 • θ= 90 •

COORDINATE REFERENCE

φ= 90 •
θ= 90 •

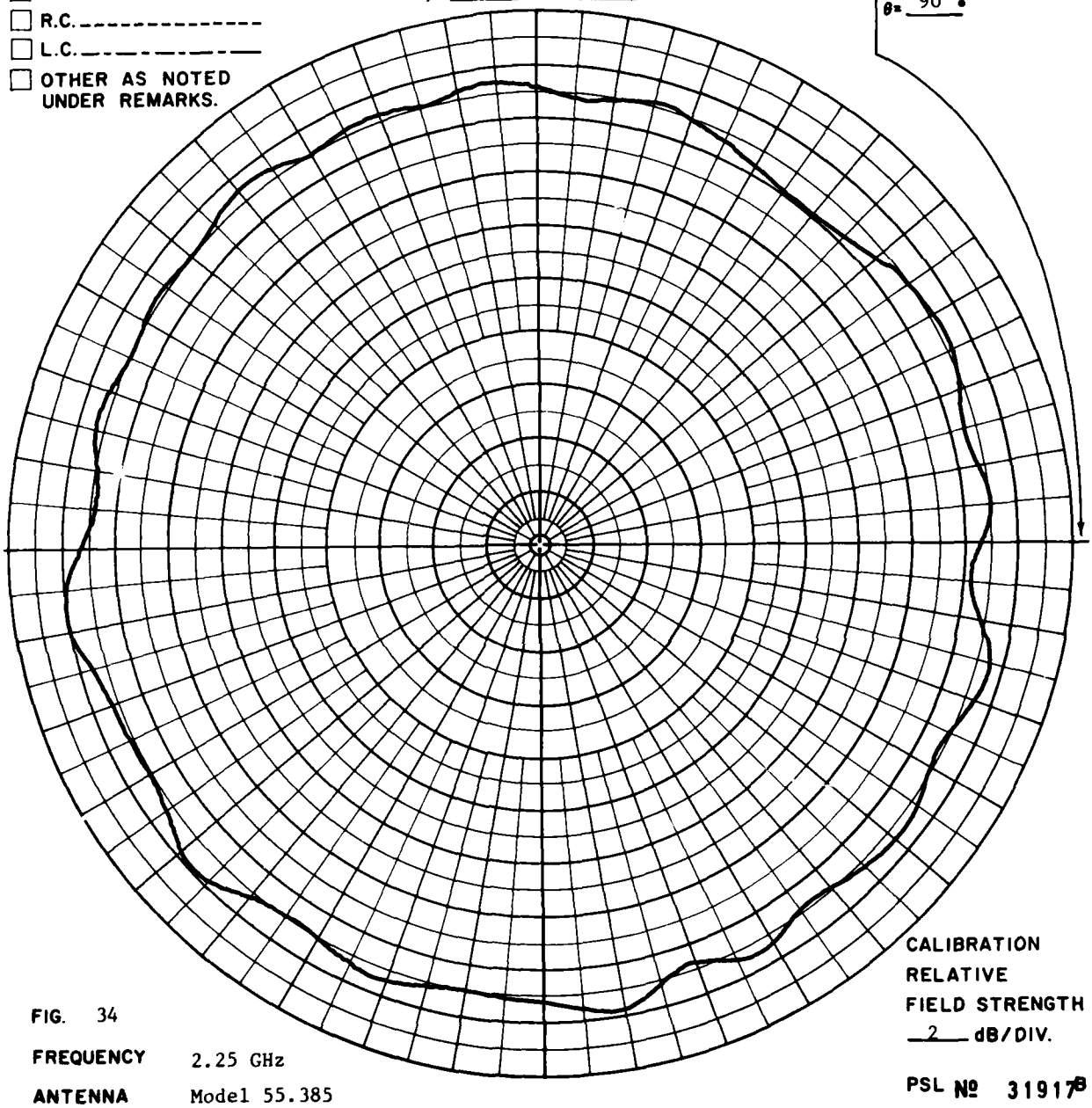

CALIBRATION
RELATIVE
FIELD STRENGTH
2 dB/DIV.

PSL № 31917B

FIG. 34

FREQUENCY 2.25 GHz

ANTENNA Model 55.385

REMARKS Far-field pattern. Sharp bend in the cable attached to the AE265 subarray.

RR 2819

POLARIZATION

- ☐ GAIN REF.
- ☒ Eθ
- ☐ Eφ
- ☐ R.C.
- ☐ L.C.
- ☐ OTHER AS NOTED UNDER REMARKS.

φ= 0° θ= 90°

COORDINATE REFERENCE

φ= 90°
θ= 90°

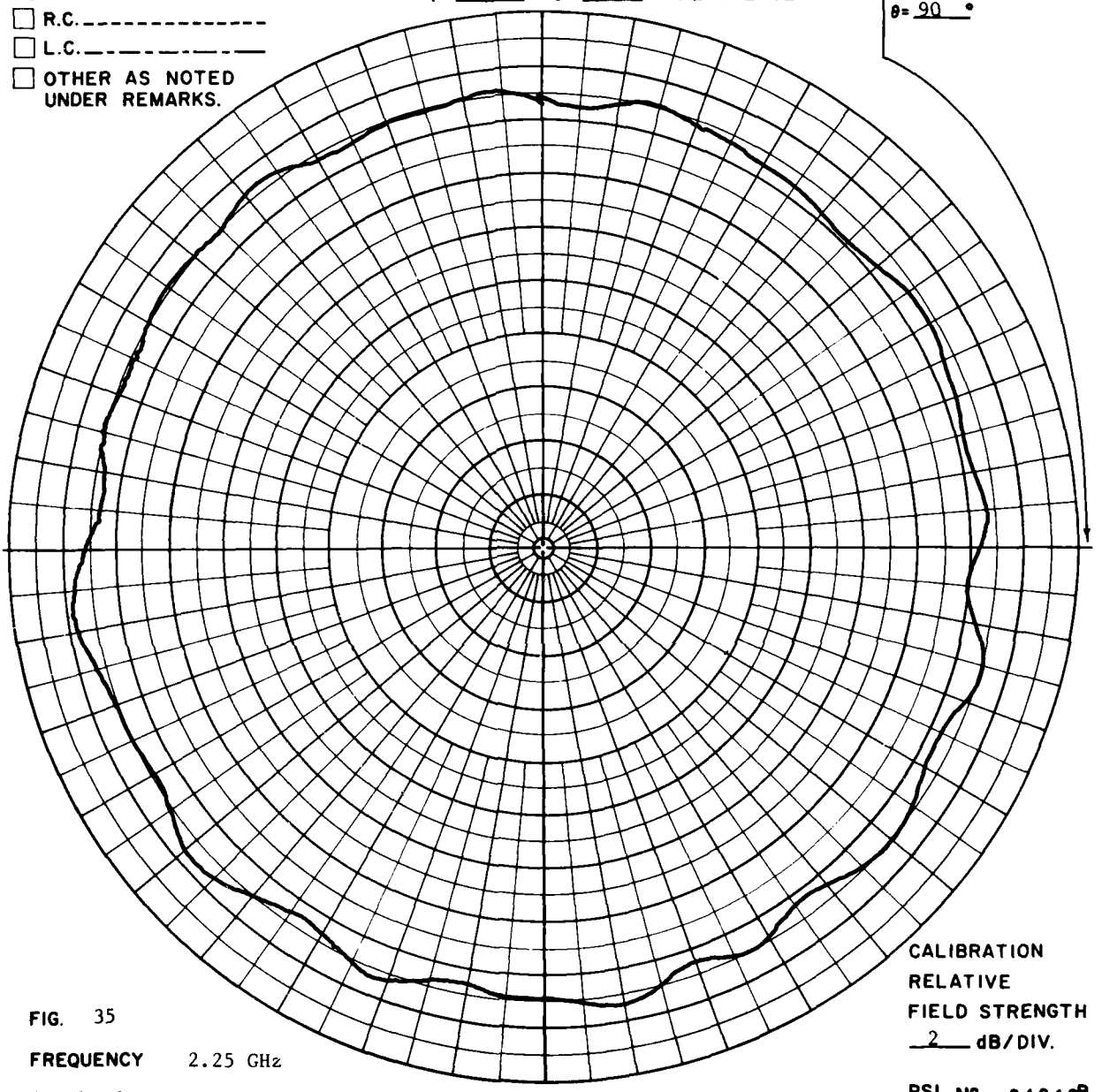

CALIBRATION
RELATIVE
FIELD STRENGTH
2 dB/DIV.

PSL № 31918B

FIG. 35

FREQUENCY 2.25 GHz

ANTENNA Model 55.385

REMARKS Far-field pattern. Sharp bend and flattening of the cable attached to AE265 subarray.

RR 2819

POLARIZATION

- ☐ GAIN REF.
- ☒ Eθ
- ☐ Eϕ
- ☐ R.C.
- ☐ L.C.
- ☐ OTHER AS NOTED UNDER REMARKS.

ϕ = 0 • θ = 90 • COORDINATE REFERENCE

ϕ = 90 •
θ = 90 •

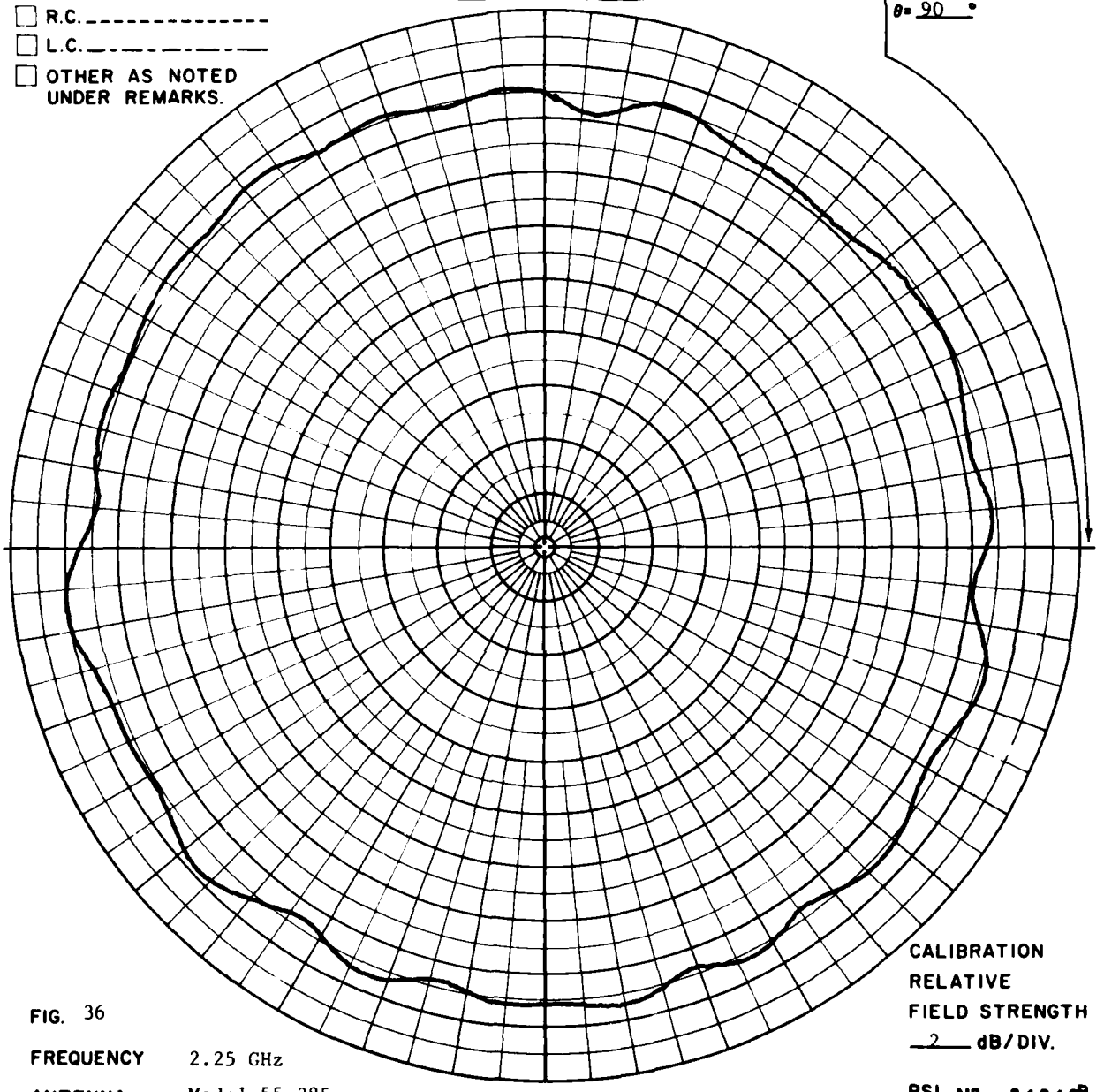

CALIBRATION
RELATIVE
FIELD STRENGTH
2 dB/DIV.

FIG. 36

FREQUENCY 2.25 GHz

ANTENNA Model 55.385

PSL № 31919B

REMARKS Far-field pattern. Sharp bend in cable attached to Tee-junction feeding AE265 and AE297 subarrays.

RR 2819

POLARIZATION

- [ ] GAIN REF.
- [x] Eθ
- [ ] Eφ
- [ ] R.C.
- [ ] L.C.
- [ ] OTHER AS NOTED UNDER REMARKS.

COORDINATE REFERENCE

φ= 0 ° θ= 90 °

φ= 90 °
θ= 90 °

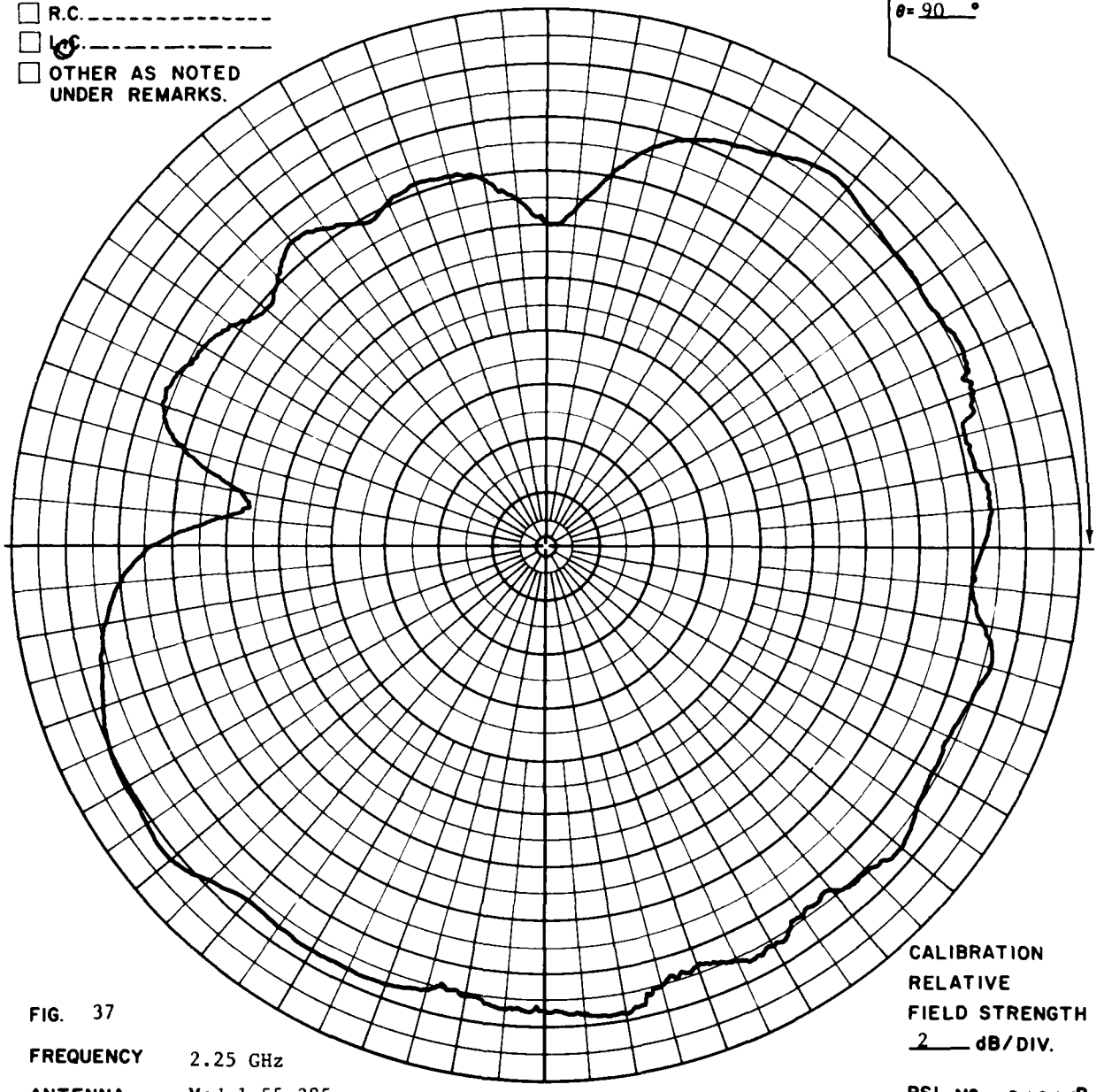

CALIBRATION
RELATIVE
FIELD STRENGTH
2 dB/DIV.

FIG. 37

FREQUENCY 2.25 GHz

ANTENNA Model 55.385

PSL № 31921B

REMARKS Far-field pattern. Sharp bend and flattening of cable attached to Tee-junction feeding the AE265 and AE297 subarrays.

RR 2819

POLARIZATION

- ☐ GAIN REF.
- ☒ Eθ
- ☐ Eφ
- ☐ R.C.
- ☐ L.C.
- ☐ OTHER AS NOTED UNDER REMARKS.

φ= 0 ° θ= 90 ° COORDINATE REFERENCE

φ= 90 °
θ= 90 °

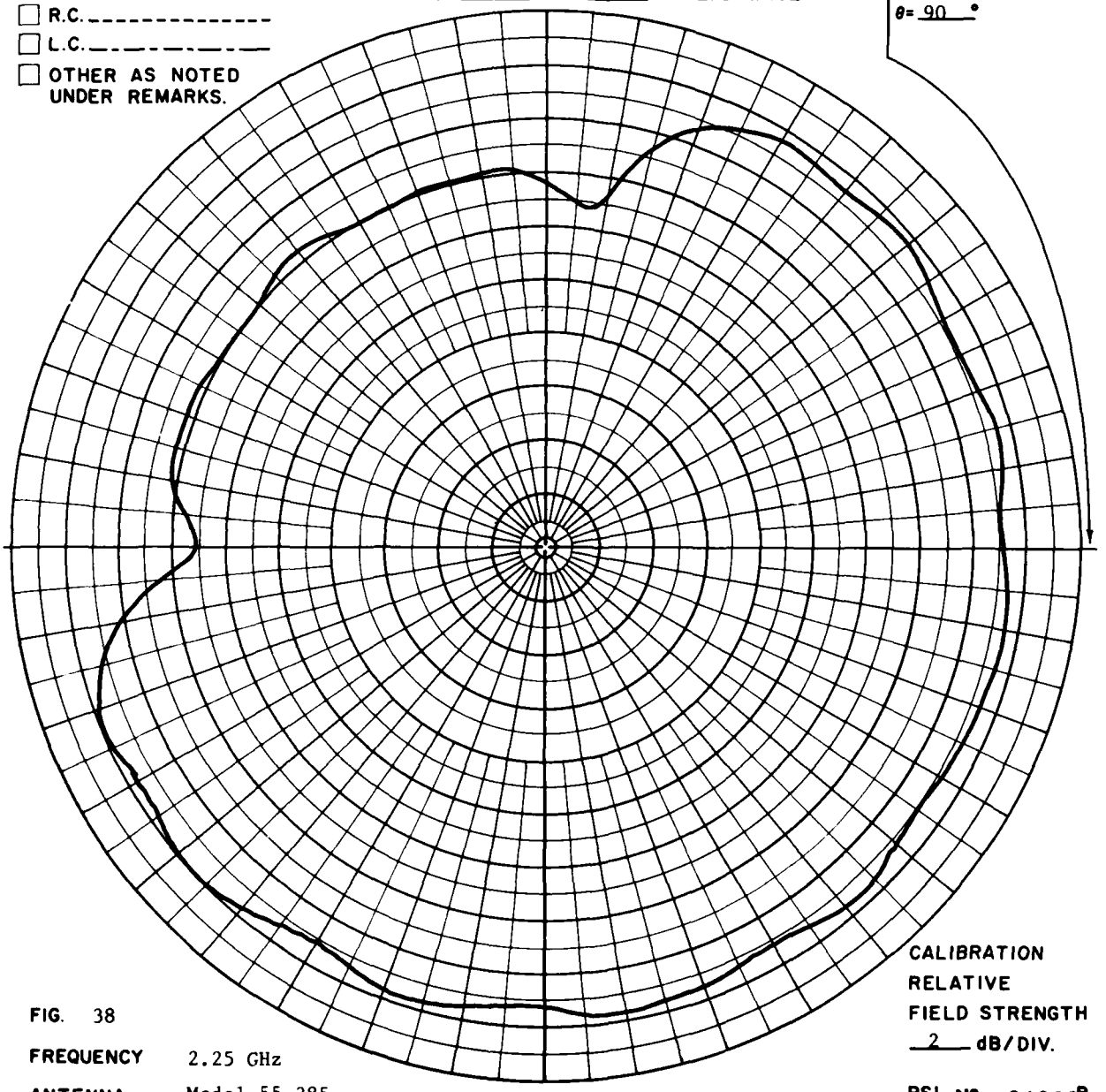

CALIBRATION
RELATIVE
FIELD STRENGTH
2 dB/DIV.

FIG. 38

FREQUENCY 2.25 GHz

ANTENNA Model 55.385

PSL № 31923B

REMARKS Near-field probe with coaxial to waveguide adaptor. Same cable conditions as with PSL 31921B (Fig. 37).

RR 2819

POLARIZATION

- ☐ GAIN REF.
- ☒ Eθ
- ☐ Eφ
- ☐ R.C.
- ☐ L.C.
- ☐ OTHER AS NOTED UNDER REMARKS.

φ= 0 ° θ= 90 ° COORDINATE REFERENCE

φ= 90 °
θ= 90 °

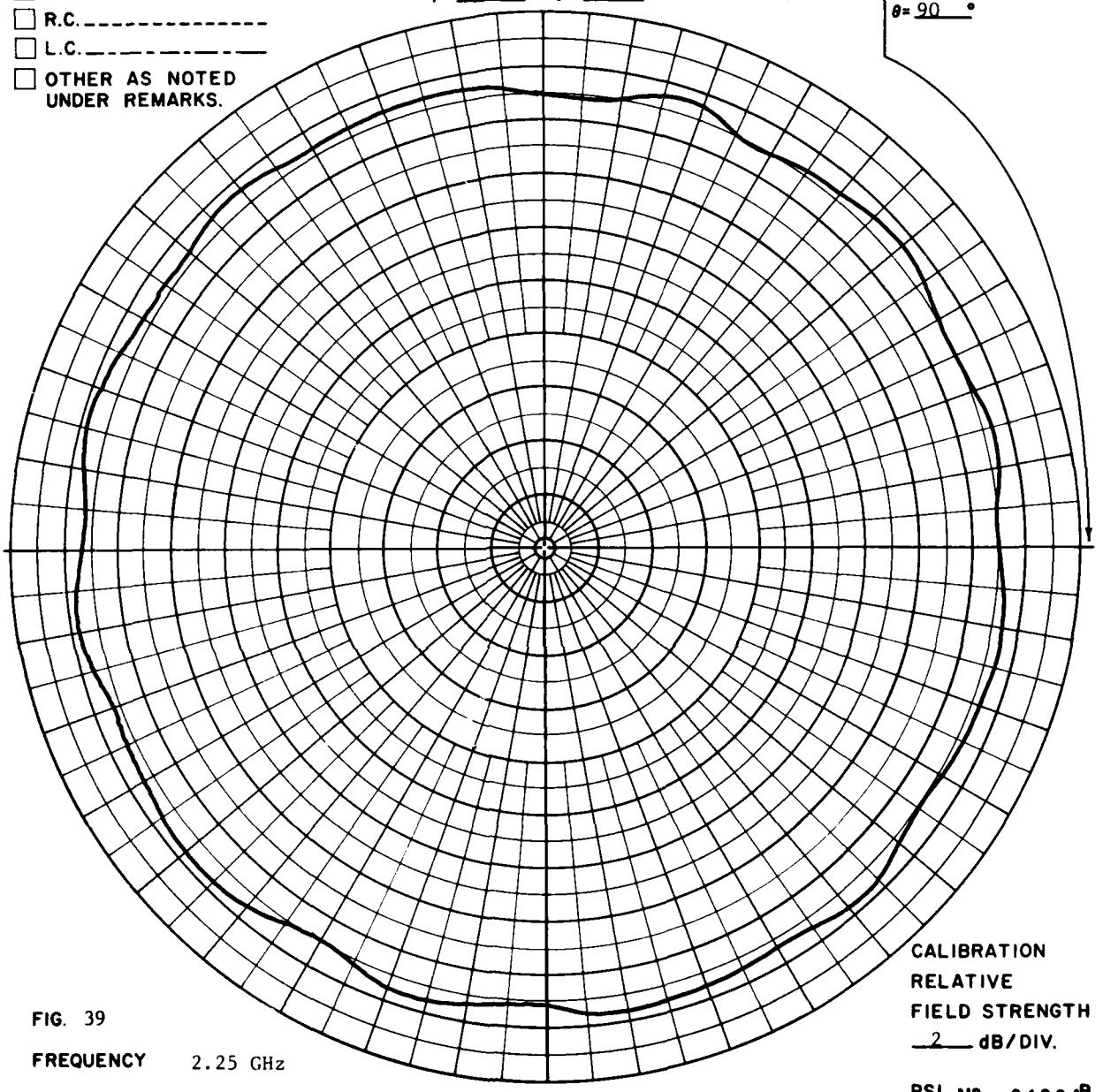

CALIBRATION
RELATIVE
FIELD STRENGTH
2 dB/DIV.

FIG. 39

FREQUENCY 2.25 GHz

ANTENNA Model 55.385

REMARKS Far-field pattern. Intact antenna and harness.
End of sequence. Repeatability check.

PSL № 31924B

RR 2819

POLARIZATION

- ☐ GAIN REF.
- ☒ Eθ
- ☐ Eφ
- ☐ R.C.
- ☐ L.C.
- ☐ OTHER AS NOTED UNDER REMARKS.

φ= 0 ° θ= 90 °

COORDINATE REFERENCE

φ= 90 °
θ= 90 °

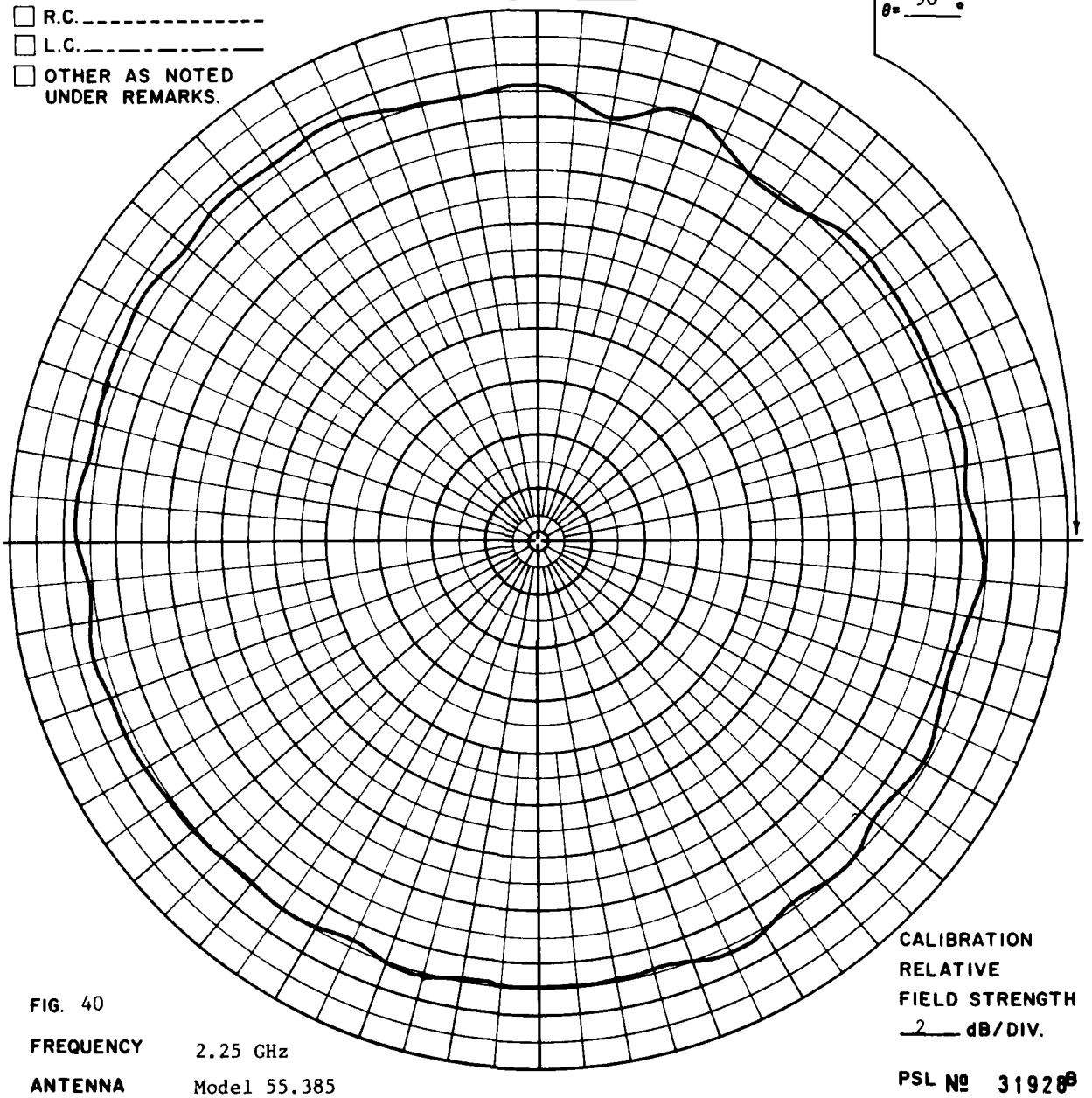

CALIBRATION
RELATIVE
FIELD STRENGTH
2 dB/DIV.

FIG. 40

PSL № 31928B

FREQUENCY	2.25 GHz
ANTENNA	Model 55.385
REMARKS	Near-field pattern. Coaxial to waveguide adaptor probe. Antenna and harness condition is the same as for pattern shown as PSL 31923B (Fig. 38).

RR 2819

POLARIZATION

- ☐ GAIN REF.
- ☒ Eθ
- ☐ Eφ
- ☐ R.C.
- ☐ L.C.
- ☐ OTHER AS NOTED UNDER REMARKS.

φ= 0 ° θ= 90 °

COORDINATE REFERENCE

φ= 90 °
θ= 90 °

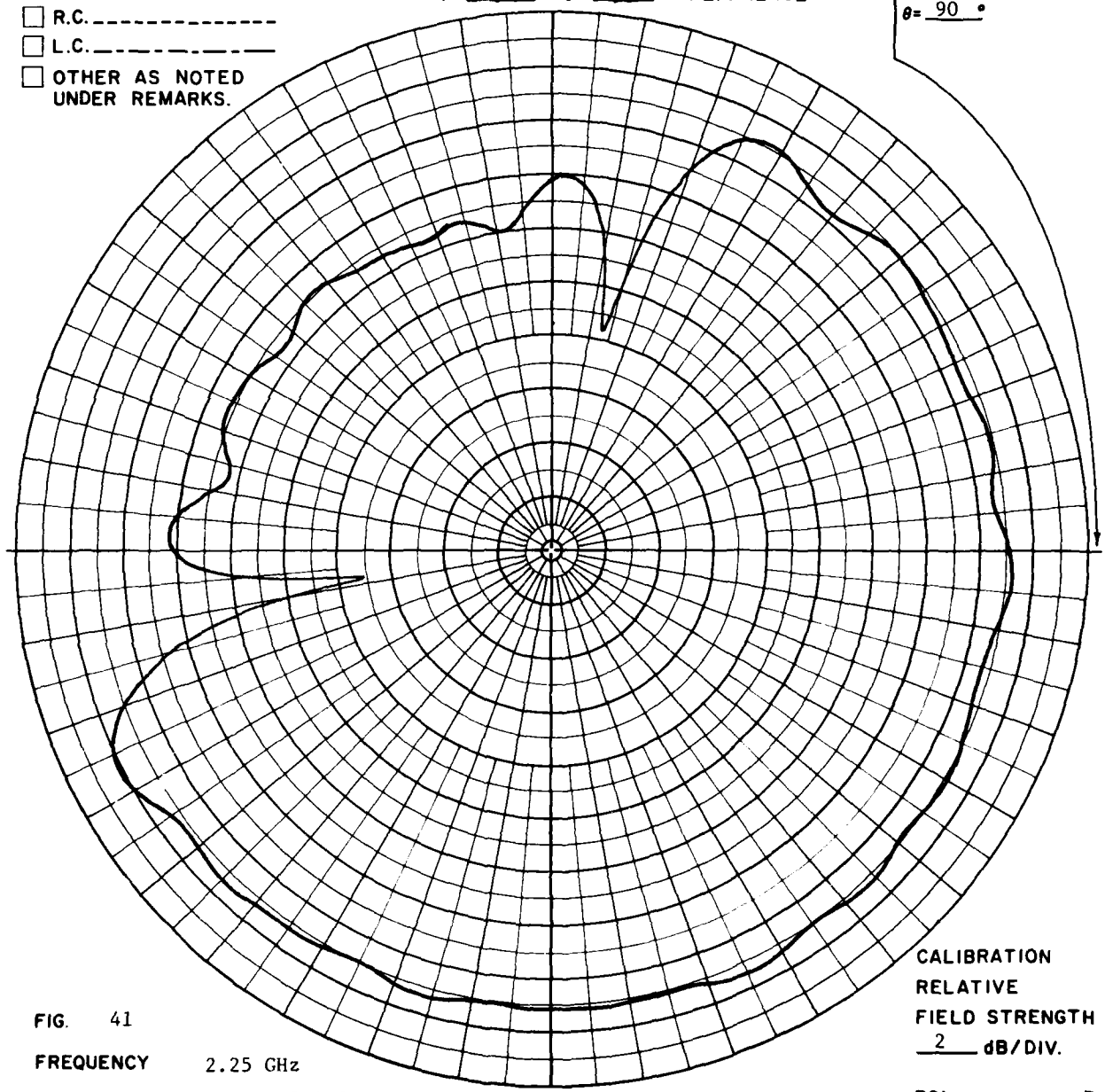

CALIBRATION
RELATIVE
FIELD STRENGTH
2 dB/DIV.

PSL № 31929B

RR 2819

FIG. 41

FREQUENCY 2.25 GHz

ANTENNA Model 55.385

REMARKS Near-field. Coaxial to waveguide adaptor probe. After additional handling of the damaged cable.

POLARIZATION

- ☐ GAIN REF.
- ☒ Eθ
- ☐ Eφ
- ☐ R.C.
- ☐ L.C.
- ☐ OTHER AS NOTED UNDER REMARKS.

φ = 0 • θ = 90 • COORDINATE REFERENCE

φ = 90 •
θ = 90 •

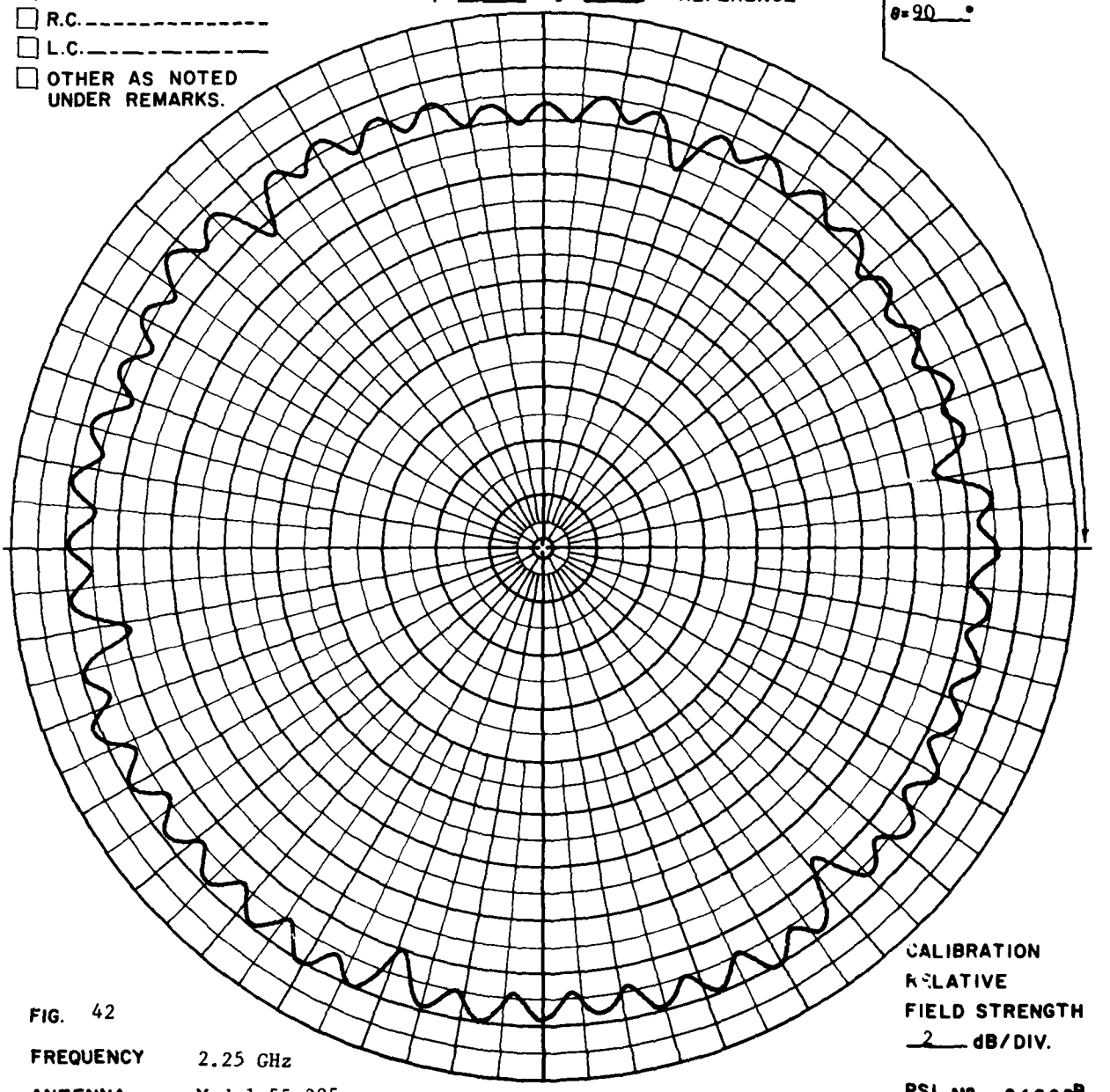

CALIBRATION
RELATIVE
FIELD STRENGTH
2 dB/DIV.

FIG. 42

FREQUENCY 2.25 GHz

ANTENNA Model 55.385

REMARKS Near-field probe with small dipole. Intact antenna and harness.

PSL № 31926[B]

RR 2819

POLARIZATION

- ☐ GAIN REF.
- ☒ Eθ
- ☐ Eϕ
- ☐ R.C.
- ☐ L.C.
- ☐ OTHER AS NOTED UNDER REMARKS.

ϕ = 0° θ = 90°

COORDINATE REFERENCE

ϕ = 90°
θ = 90°

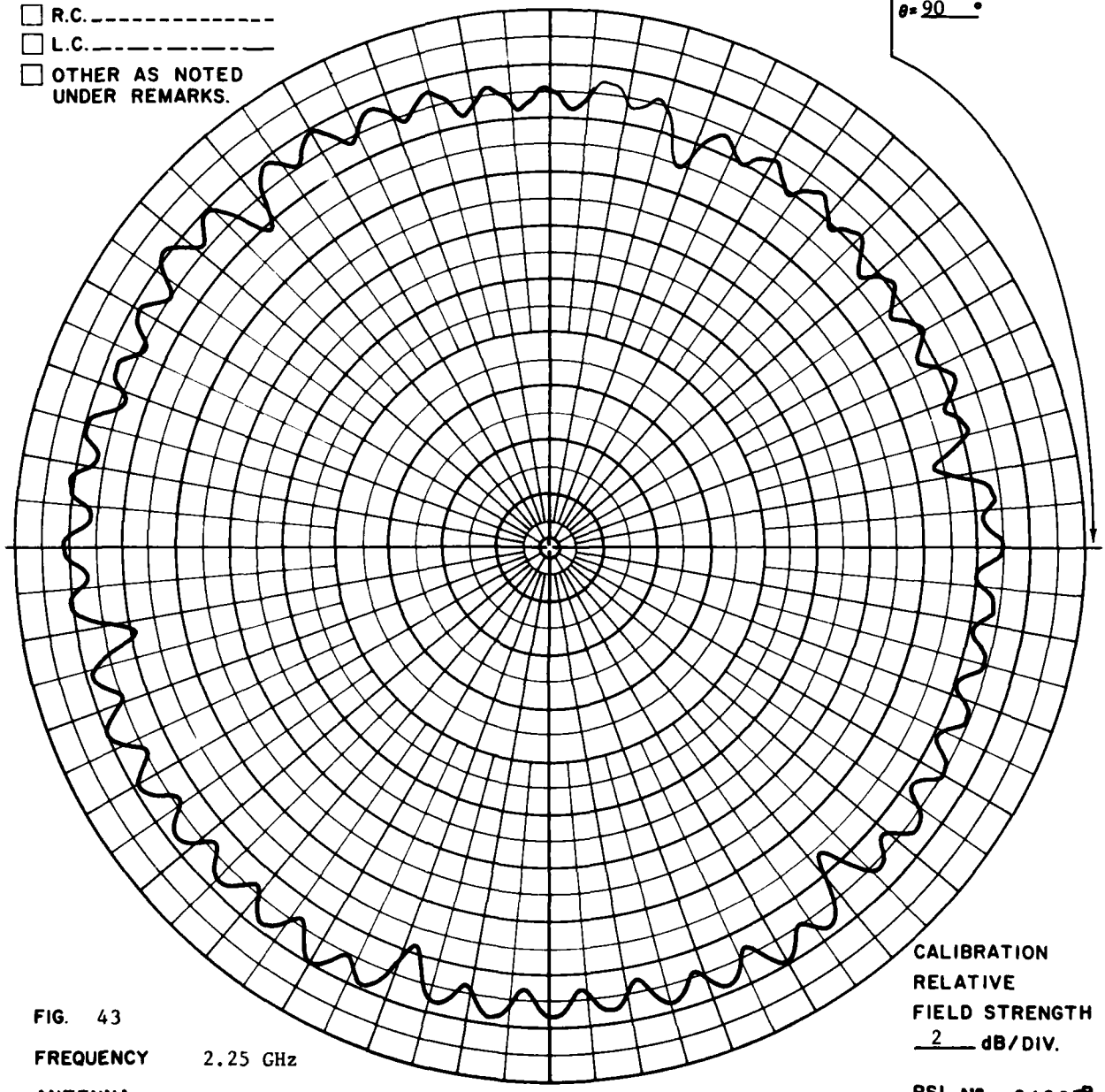

CALIBRATION
RELATIVE
FIELD STRENGTH
2 dB/DIV.

FIG. 43

FREQUENCY 2.25 GHz

ANTENNA Model 55.385

REMARKS Near-field pattern. Short dipole probe. Intact cables were replaced by the damaged cables. Note that the pattern shown in PSL 31928B (Fig. 40) did not repeat.

PSL № 31927B

RR 2819

POLARIZATION

- ☐ GAIN REF.
- ☒ Eθ
- ☐ Eϕ
- ☐ R.C.
- ☐ L.C.
- ☐ OTHER AS NOTED UNDER REMARKS.

ϕ = 0° θ = 90°

COORDINATE REFERENCE

ϕ = 90°
θ = 90°

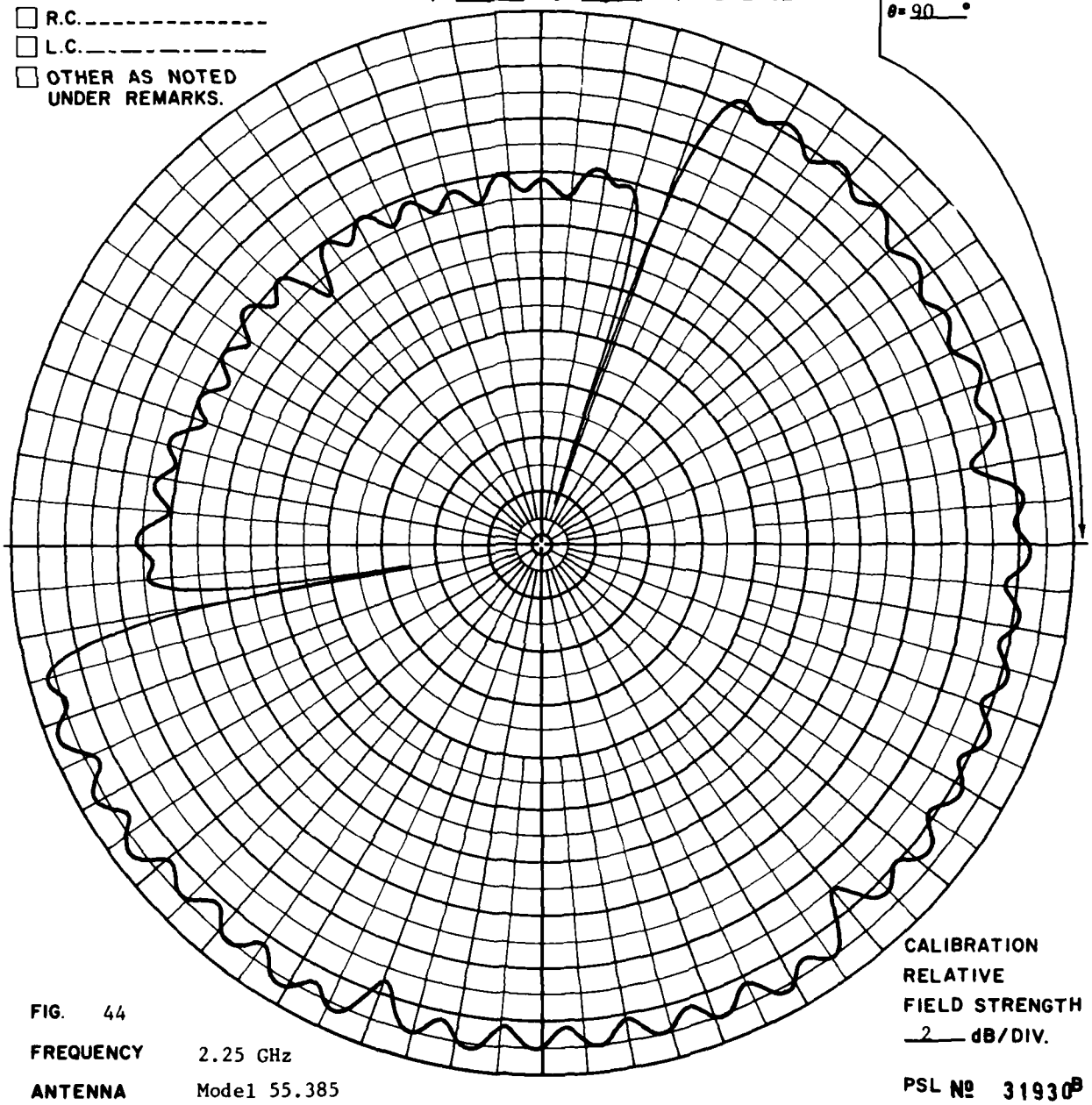

CALIBRATION
RELATIVE
FIELD STRENGTH
2 dB/DIV.

FIG. 44

FREQUENCY 2.25 GHz

ANTENNA Model 55.385

PSL № 31930B

REMARKS Near-field. Short dipole probe. Same cable condition as for pattern PSL 31929B (Fig. 41).

RR 2819

POLARIZATION

- ☐ GAIN REF.
- ☒ Eθ
- ☒ Eφ
- ☐ R.C.
- ☐ L.C.
- ☐ OTHER AS NOTED UNDER REMARKS.

φ= 0 ° θ= 90 ° COORDINATE REFERENCE

φ= 90 °
θ= 90 °

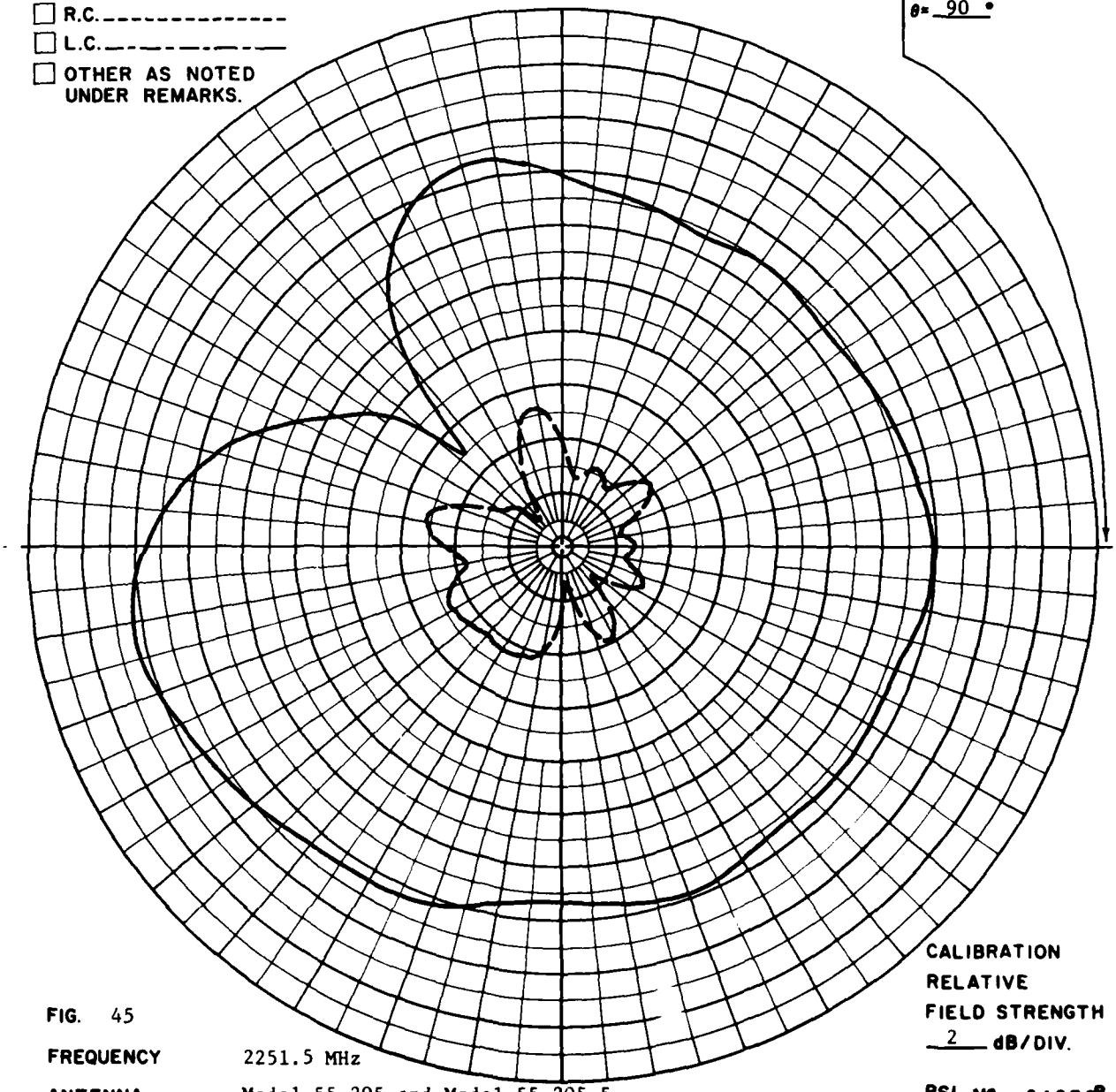

CALIBRATION
RELATIVE
FIELD STRENGTH
2 dB/DIV.

FIG. 45

FREQUENCY 2251.5 MHz

ANTENNA Model 55.205 and Model 55.205.5

PSL № 31970[B]

REMARKS The antenna is mounted on a 17 inch diameter cylinder. Far-field pattern.

RR 2824

APPENDIX A

Documentation of the Antenna Used for the Tests

1.0 The Model 55.385 Stripline Antenna

The Model 55.385 was used for the test antenna. One of the subarrays is shown in Figure 1A. The stripline antenna is an array of eight slots which are fed in phase and with equal power by a corporate harness. The schematic of the harness is shown in Figure 2A. The harness sections are numbered to correspond to the numbers of the NO column of the computer printout.

The parameters of the antenna are documented by the output of APL program H55385 (see page A-5). This program (shown on page A-6), was written strictly for documentation and has no input. The effective dielectric constant used in the program was derived by assuming that the line length between the 2 element junction and the 4 element junction is one wavelength in the dielectric. This assumption is somewhat arbitrary, but is quite acceptable to document the antenna for reproduction.

The antenna is fabricated from printed circuit board by 3M Co. The material designation is Cu Clad 250 (GX-0600-45-11). The trim dimensions of the antenna are shown in Figure 2A.

A representative impedance curve of a single subarray is shown in Figure 3A. The high VSWR at the upper end of the frequency band does not necessarily imply that the antenna cannot be used at that frequency since the pattern bandwidth is probably larger than the impedance bandwidth.

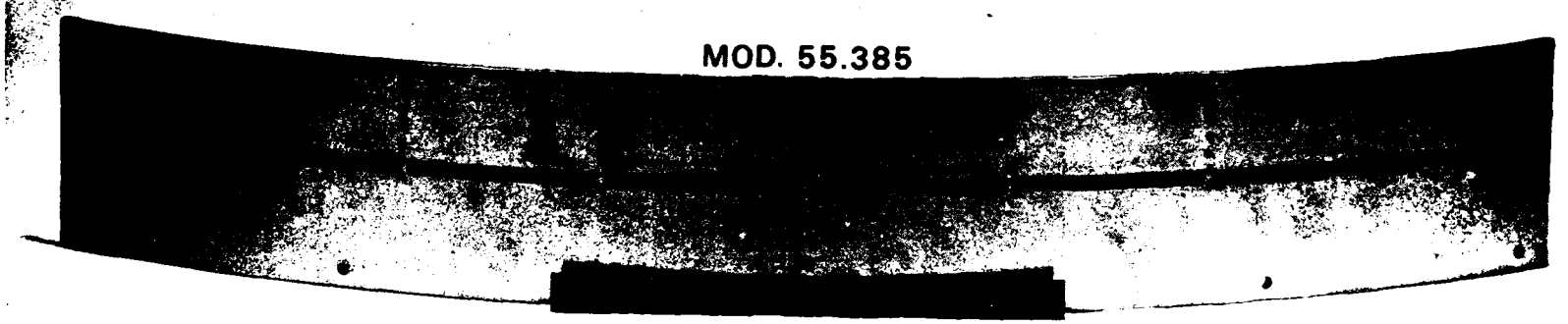

Figure 1A. Model 55.385 subarray.

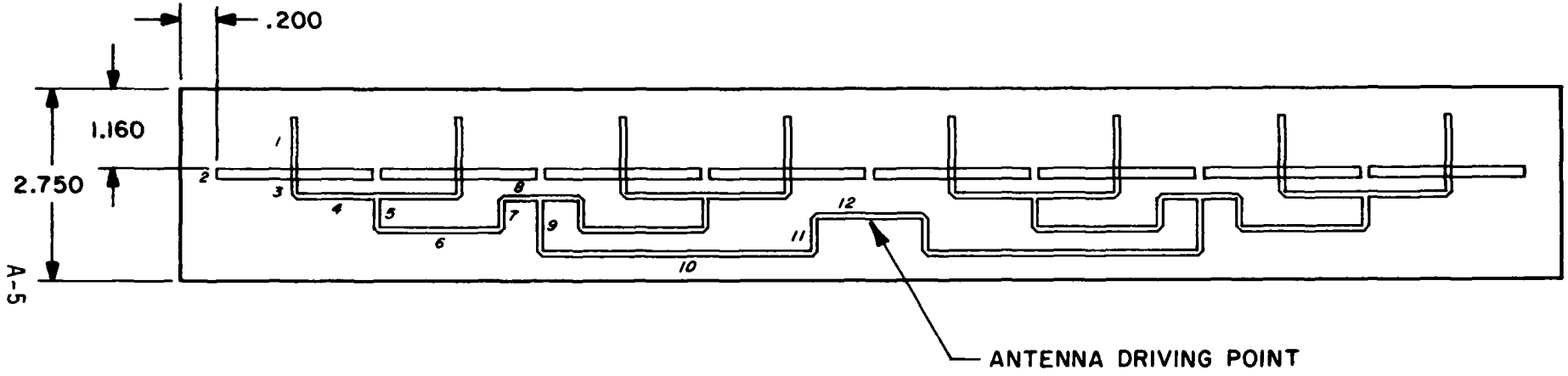

Figure 2A. Model 55.385 harness schematic.

TITLE DATE

IMPEDANCE COORDINATES—50-OHM CHARACTERISTIC IMPEDANCE

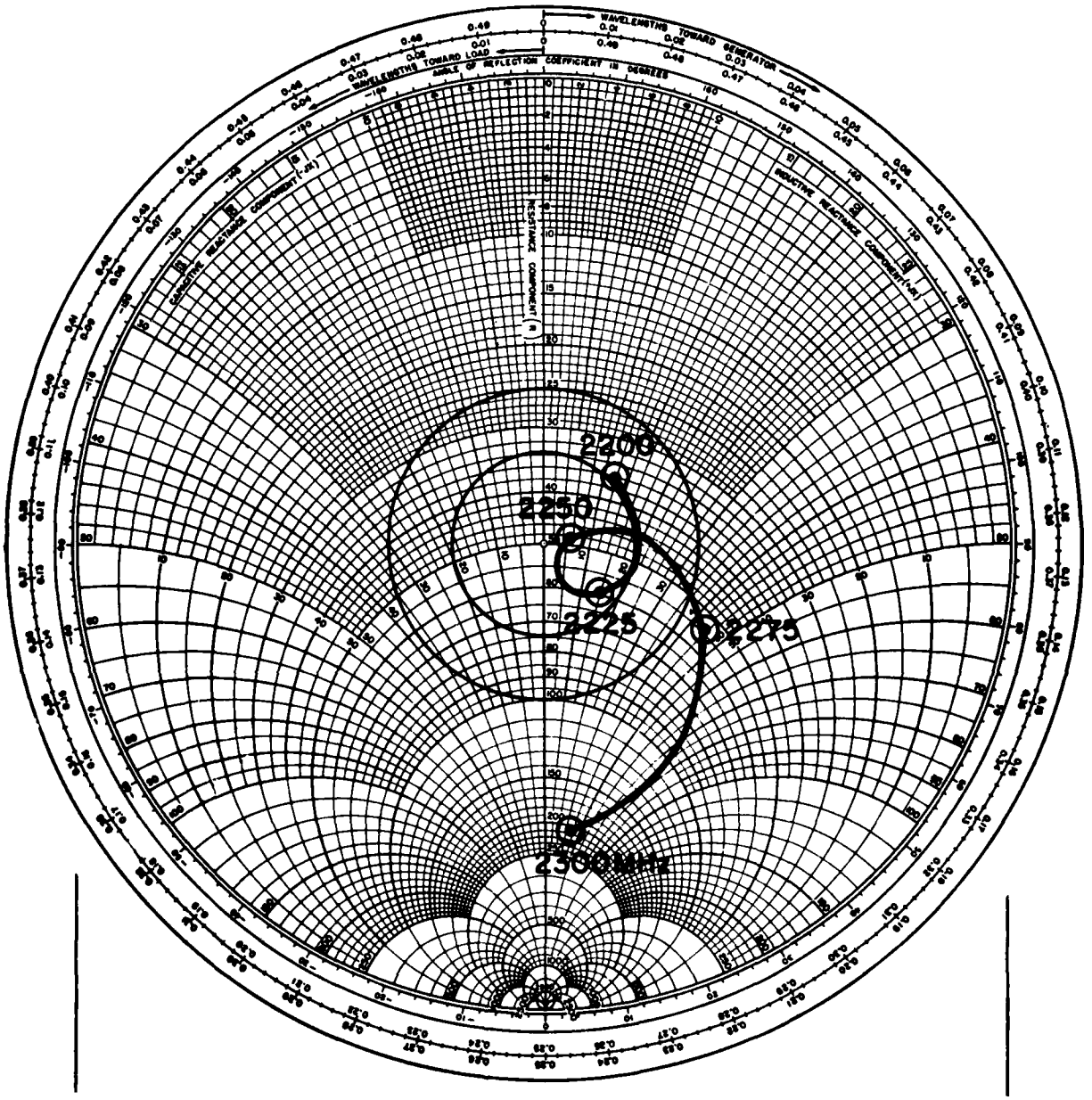

Figure 3A. Representative impedance versus frequency curve for the Model 55.385 eight element slot array.

```
OUTPUT
MOD 55.385; FIELD TEST; AFGL 81101/01369
************************************************
SLOT LENGTH          2.283
SLOT WIDTH           0.157
SUBARRAY LENGTH     19.331
LINE WIDTH           0.079


ELEM. SPA.(INCH)                  2.416
ELEM. SPA.(WAVEL.AIR)             0.461
ELEM. SPA. (WAVEL.DIELEC)         0.715


FROM SLOT TO 2 ELEM. JCT.                  0.456
FROM2 ELEM. JCT. TO 4 ELEM. JCT.           1.000
FROM 4 ELEM. JCT TO 8 ELEM. JCT            1.837


NO    LENGTH(I)    LENGTH(WE)
 1      0.827        0.245
 2      0.157        0.047
 3      0.335        0.099
 4      1.208        0.357
 5      0.492        0.146
 6      1.831        0.541
 7      0.472        0.140
 8      0.586        0.173
 9      0.827        0.245
10      4.016        1.188
11      0.551        0.163
12      0.817        0.242
```

```
    ∇ M55385
[1]  ⍝MOD 55.385 IS AN OLD ANTENNA THE PRG IS STRICTLY FOR DOCUMENTATION
[2]  ⍝ASSOCIATED WITH THE FIELD TESTS AFGL 81101/01369;19 OCT 83
[3]  ⍝THE VEHICLE IS A NOMINAL 38 INCH DIA. THE HARNESS LENGTH AND OTHER
[4]  ⍝DIMENSIONS WERE OBTAINED MEASUREING THE AMBERLITH. THE DIELECTIRIC
[5]  ⍝CONSTANT WAS CALCULATED BY ASSUMING THAT THE HARENESS LEG FROM THE
[6]  ⍝2 ELEMENT JCT. TO THE 4 ELEM. JCT. IS ONE WAVELENGTH IN THE DIEL.
[7]  ⍝THE MEASURED DIMENSIONS ARE IN CENTIMETERS.
[8]  ⍝
[9]  ⍝MEASURED DIMENSIONS
[10]  STL←5.8 ⍝SLOT LENGTH
[11]  STW←0.4 ⍝SLOT WIDTH
[12]  SAL←49.1 ⍝SUBARRAY LENGTH (NOT TRIM LENGTH)
[13]  SP←SAL÷8 ⍝ELEMENT SPACING
[14]  SPI←SP×2.54
[15]  LW←0.2 ⍝LINE WIDTH (54 OHM LINE)
[16]  L1←2.1
[17]  L2←STW
[18]  L3←0.85
[19]  L4←SP÷2
[20]  L5←1.25
[21]  L6←4.65
[22]  L7←1.2
[23]  L8←SP-L6
[24]  L9←2.1
[25]  L10←10.2
[26]  L11←1.4
[27]  L12←(2×SP)-L10
[28]  LC←L1,L2,L3,L4,L5,L6,L7,L8,L9,L10,L11,L12
[29] ⍝
[30]  F←2.25 ⍝FREQUENCY (GHZ)
[31]  EPS←2.407 ⍝ASSUMED DIELECTRIC CONSTANT
[32]  WA←11.803÷F ⍝WAVELENGTH IN AIR (INCHES)
[33]  WE←WA÷EPS*0.5 ⍝WAVELENGTH IN DIELECTRIC (INCHES)
[34]  LI←LC×2.54
[35]  LE←LI÷WE
[36]  LEG1←+/LE[3 4]
[37]  LEG2←+/LE[5 6 7 8]
[38]  LEG3←+/LE[9 10 11 12]
[39] ⍝
[40]  OM1← 4 1 ⍴(STL,STW,SAL,LW)×2.54
[41]  OM11←(⍳0) ROWNAMES '/SLOT LENGTH/SLOT WIDTH/SUBARRAY LENGTH/LINE WIDTH'
[42] ⍝
[43]  OM2← 3 1 ⍴SPI,(SPI×WA),(SPI×WE)
[44]  OM22←(⍳0) ROWNAMES '/ELEM. SPA.(INCH)/ELEM. SPA.(WAVEL.AIR)/ELEM. SPA. (WAVEL.DIELEC)'
[45] ⍝
[46]  OM3←⍉ 3 12 ⍴(⍳12),LI,LE
[47]  OM33← 1 23 ⍴'NO LENGTH(I) LENGTH(WE)'
[48] ⍝
[49]  OM4← 3 1 ⍴LEG1,LEG2,LEG3
[50]  OM44←(⍳0) ROWNAMES '/FROM SLOT TO 2 ELEM. JCT./FROM2 ELEM. JCT. TO 4 ELEM. JCT./FROM 4 ELEM. JCT TO 8 ELEM. JCT'
[51] ⍝
[52]  2⍴⎕TCNL
[53]  'OUTPUT'
[54]  'MOD 55.385; FIELD TEST; AFGL 81101/01369'
[55]  45⍴'*'
[56]  '15A1,F8.3' ⎕FMT(OM11;OM1)
[57]  ⎕TCNL
[58]  '25A1,F8.3' ⎕FMT(OM22;OM2)
[59]  ⎕TCNL
[60]  '32A1,F8.3' ⎕FMT(OM44;OM4)
[61]  ⎕TCNL
[62]  '2A1,X2,10A1,X2,10A1' ⎕FMT(OM33)
[63]  'I2,F10.3,F10.3' ⎕FMT(OM3)
[64]  2⍴⎕TCNL
```

END

FILMED